UNIVERSITA' DEGLI STUDI DI PADOVA

SCUOLA DI DOTTORATO DI RICERCA IN SCIENZE MEDICHE, CLINICHE E SPERIMENTALI

INDIRIZZO: SCIENZE CARDIOVASCOLARI

XXII CICLO

TESI DI DOTTORATO

PATHOPHYSIOLOGY OF THE MICROCIRCULATION AND ENDOTHELIAL FUNCTION: FROM MOLECULAR MECHANISMS TO CLINICAL EXPERIENCE

Coordinatore: Ch.mo Prof. Gaetano Thiene

Supervisore: Prof. Thomas F. Lüscher

Supervisore: Dr. Francesco Tona

Dottorando: Elena Osto, MD

DATA CONSEGNA TESI
15 Marzo 2010

Ai miei amati genitori

TABLE OF CONTENTS

Abstract

Endothelial dysfunction is an early feature of atherosclerotic vascular disease, characterized by a decrease in nitric oxide (NO) bioavailability and a concomitant increase in vascular superoxide (O_2^-) formation. Loss of NO bioavailability precedes the development of overt atherosclerosis and is an independent predictor of adverse cardiovascular events. Indeed, decreased NO and enhanced production of reactive oxygen species (ROS) have been recognized as major determinants of age-associated endothelial dysfunction.

Emerging evidence indicates a significant role played by the endothelium also in the onset and progression of the cardiac allograft vasculopathy (CAV), a peculiar type of coronary atherosclerosis which is considered nowadays the main limiting factor of long-term outcome after heart transplantation (HT). Furthermore, other quite common diseases, such as psoriasis and hyperparathyroidism, although proven to be at increased risk for cardiovascular mortality are poorly understood on a cardiovascular point of view. The exact pathogenesis of all these mentioned diseases remains not completely defined; however it is clear that immunologic mechanisms operating in the context of common cardiovascular risk factors lead to impaired endothelial function, mainly as a consequence of decreased NO bioavailability and excessive oxidative stress.

The work submitted in this thesis describes on one side studies aimed to investigate molecular mechanisms underlying endothelial dysfunction and vascular inflammation driven by oxidative stress in the context of aging, hypertension and atherosclerosis using in vitro and in vivo models. On the other side, we present clinical studies focused on the pathophysiology of coronary microcirculation as far as functional aspects are concerned in the immuno-inflammatory context of cardiac allograft vasculopathy.

Introduction

The first description of basic cardiovascular concepts can be traced back to the ancient Roman Age with Galeno (about 200 AD), "the father of experimental physiology", who first discovered that arteries contain blood instead of air. Later, important achievements were reached by other renowned anatomists such as Vesalio (1514-1564), after the Renaissance. But the foundation of the modern knowledge of the circulation and the role played by the heart, as a pump, have been established in the *Exercitatio Anatomica de Motu Cordis et Sanguinis in Animalibus*, written by William Harvey, in 1628, an English medical doctor who trained in Italy, at the University of Padua. For the first time, Harvey was able to integrate the single isolated discoveries of his predecessors, providing a comprehensive understanding of the cardiovascular system as we know it nowadays[1]

Later, Modern Age has witnessed major developments in cardiovascular physiology thanks to scientists like E.H. Starling in the 1920s, who described the "*foundamental properties of the heart muscle itself and then found out how these are modified, protected, and controlled under the influence of the mechanisms- nervous, chemical and mechanical- which under normal conditions play on the heart and blood vessels"*, quoting his remarkable studies. [1, 2] On the other side, the existence of pathological cardiovascular conditions have been recognized and described. The atherosclerotic vascular disease and its main clinical manifestation, angina pectoris have been firstly reported in the 18th century. In parallel, the earliest descriptions of some attempts for a pharmacological treatment appeared. Nitroglycerin, for example, has been initially prescribed by physicians in the late 19th century [3]. A number of new pharmacological agents found to be of benefit have followed, leading to the constitution of the currently established cardiovascular pharmacotherapy.

The atherosclerotic vascular disease was hypothesized to cause ischemia and infarction of the heart and other organs. Acute cardiovascular ischemic events, such as stroke, myocardial

infarction or sudden death, were frequently associated with localized arterial thrombus formation. However for many decades, these conditions remained totally mysterious and unpredictable events. Moreover, hypertension was recognized to damage large blood vessels and the microcirculation of different target organs, even if the specific mechanisms involved were unknown.

The revolutionary concepts of vascular biology

The Framingham Heart Study, a large-scale epidemiologic investigation began in the early 1950s, demonstrated a striking association between coronary artery disease (CAD), stroke, peripheral artery disease with diabetes mellitus (DM) and aging, forcing physicians to investigate the possible pathophysiological connections among those diverse clinical conditions[4].

Vascular biology, as the study of vascular cells under normal and pathological conditions, began in the 1970s. This novel research discipline, has since then enjoyed exponential growth, allowing the comprehension of common pathophysiologic processes of cardiovascular diseases (CVD), especially those linked to atherosclerosis and DM. Translation of this knowledge to clinical practice has profoundly influenced management strategies leading to an improvement of outcomes [5].

Traditionally, vascular smooth muscle cell (VSMC) was regarded as the site of control of the vascular tone in the resistance arteries of peripheral circulation. The same concept was translated to the regulation of the contractility in the coronary artery tree. In this view, a coronary spasm or a state of enhanced contractility was believed to elicit angina pectoris or to precipitate ischemia and myocardial infarction. For a long time, the endothelium was scarcely known and just mentioned as a simple, inert, selective barrier to the diffusion of macromolecules from the lumen of the vessel to the interstitial space.

This view completely changed in 1980, when it was described the obligatory role of endothelial cells in relaxation of arterial smooth muscle by acetylcholine (Ach) [6]. A seminal event in the field of vascular biology, which was later awarded with the Nobel Prize in 1998 to Robert Furchgott, Louis Ignarro and Ferid Murad. By means of in vitro experiments in organ chambers, preconstricted arterial rings were demonstrated to relax in response to the muscarinic cholinergic agonist only if endothelial cells were present. Removing the endothelium by any means abolished the vasorelaxation, which was mediated by an undefined endothelium-derived substance that was named endothelium derived relaxing factor (EDRF). EDRF, subsequently, was shown to be, in large part, nitric oxide[7]. During the last three decades, several studies have definitively proved that the endothelium is not only a cell monolayer covering the lumen surface of the vascular wall, but it is involved in many key regulatory functions for the homeostasis of cardiovascular system.

The endothelium and vascular homeostasis

Endothelial cells (ECs) actively regulate basal vascular tone and reactivity under both physiological and pathological conditions, by responding to mechanical forces (shear stress and pulsatile stretch) and neuro-hormonal mediators with the release of a variety of relaxing and contracting factors [8]. The endothelium has an endocrine/paracrine function and releases EDRFs, now known to be endothelial autacoids like NO, prostacyclin (PGI_2) and a still elusive endothelium derived hyperpolarizing factor (EDHF) The latter mediator is produced by the EDHF synthase cytochrome P450 2C [9] and together with PGI_2 might play an important role in the microcirculation. All these EDRFs can also inhibit platelet function and the proliferation of VSMCs. On the other hand, ECs may also produce vasoconstrictors and growth promoters, such as angiotensin II (Ang II), endothelin-1 (ET-1), thromboxane and prostaglandin H2 (PGH_2).

Thus, the activity of the endothelium extends far beyond the control of vascular tone and vasomotion. Indeed, the release of vasodilating mediators clearly reflects only one aspect of its homeostatic and protective role. In normal ECs, those mediators are synthesized and released to maintain vascular homeostasis, ensuring adequate blood flow, nutrient delivery and waste removal, while preventing thrombosis and leukocyte diapedesis [10]. The EC monolayer, because of its strategic anatomic position between the circulating blood and the vessel wall components is the crossroads of diverse signaling pathways affecting vascular function and structure, one of the most prominent being the L-arginine/NO pathway. NO is constitutively produced by endothelial NO synthase (eNOS, NOSIII), requiring tetrahydrobiopterin (BH4) as a cofactor, through a 5-electron oxidation of the guanidine-nitrogen terminal of L-arginine in response to receptor-dependent agonists (bradykinin, Ach, adenosine triphosphate (ATP) or haemodynamic forces [11]. The bioavailability of NO represents a key marker of vascular health. NO diffuses to the underlying VSMCs and stimulates the second-messenger cyclic guanosine monophosphate (cGMP) to cause relaxation. Many, if not most, vasodilator stimuli, such as flow and multiple G-protein–coupled receptors, including those for serotonin and muscarinic cholinergic agonists, act through such endothelium-dependent mechanism[11].

In addition, a functional endothelium is a major regulator of vascular inflammation and remodeling. NO finely modulates integrins and other surface signals expression. An intact endothelial layer is critical for preventing circulating blood cells from exposure to prothrombotic subendothelial matrix by mediating molecular signals that prevent platelet and leukocyte interaction with the vascular wall and by inhibiting VSMC proliferation and migration [12, 13]. Moreover, a healthy endothelium actively inhibits arterial thrombus formation. Indeed, endothelium-derived NO limits platelet activation, adhesion and aggregation, and inhibits the expression of prothrombotic protein plasminogen activator inhibitor-1 modulating the balance of profibrinolytic and prothrombotic activity [14]. Furthermore, platelets have been shown to express eNOS and to produce NO that likely limits recruitment and aggregation of

platelets. Endothelial prostacyclin production, largely dependent on cyclooxygenase 2 (COX-2), acts synergistically with NO to prevent platelet activation [15].

In 1997, the isolation of putative endothelial progenitor cells (EPCs) from human peripheral blood has been reported [16]. Subsequently, evidence has accumulated documenting the presence of a population of endothelial precursor cells and/or adult stem cells, derived from bone marrow, with a specific role in maintenance of endothelial integrity against vascular injury [17]. These cells are able to home areas of injury and ischemia-induced myocardial and peripheral neovascularization [18], healing endothelial integrity [19].

Endothelial dysfunction, atherosclerosis and vascular inflammation

Endothelial function has largely been investigated through the assessment of endothelium-dependent vasomotion. Indeed, an impaired endothelium-dependent relaxation reflects an extensive loss of endothelial function. The first published studies, confirming the utmost importance of the endothelium in the control of vasomotor tone, provided substantial evidence that endothelium-dependent responses are impaired in animal models and patients with vascular disease[20]. Is endothelial dysfunction associated with the development of coronary atherosclerosis? The results of a study evaluating this hypothesis were published by Ludmer et al. in 1986. The authors concluded that Ach causes a dose-dependent dilation of coronary arteries in healthy subjects, while a “paradoxical” vasoconstriction is observed in patients with coronary disease, indicating an impaired endothelium-dependent coronary vasomotion [21]. Later, Quyyumi et al. confirmed that the impaired response to Ach in patients with CAD or cardiovascular risk factor is largely due to reduced coronary availability of endothelium-derived NO [22]. Abnormalities of endothelial function in vasomotor control have been demonstrated both in large arteries and in the microvasculature in multiple settings besides atherosclerosis,

including congestive heart failure, systemic and pulmonary hypertension. Cardiovascular risk factors such as DM, smoking, dyslipidemia, hypertension, low-estrogen states, were also shown to have synergistic effect in determining endothelial function.

The emerging hypothesis following these observations was to assess whether common mechanisms may lead to impaired endothelial cell function in different conditions. Furthermore, it was important to characterize how endothelial dysfunction relates to the pathogenesis of atherosclerosis. Studies addressing these issues continue to provide remarkable evidence that the endothelial interface between the vascular wall and the circulation is the primary site for the triggering of cardiovascular events [23].

A prototypical pattern of vascular changes has been proposed in atherosclerosis and predisposing conditions that constitutes a sort of sick vessel syndrome, with the following hallmarks: endothelial dysfunction, preserved relaxation of VSMC, exaggerated vasoconstrictor responses and structural changes/vascular remodeling initially triggered as adaptive and protective mechanisms that turn out to be deleterious and self sustaining [24].

Under pathologic conditions the endothelium has a reduced availability of vasodilating factors, in particular NO, and an augmented production of vasoconstricting factors, leading to impaired endothelium-dependent vasodilation. Furthermore, endothelium derived NO has been demonstrated to exert a major anti-inflammatory effect and can therefore be considered the most important endogenous antiatherogenic molecule. Endothelial dysfunction promotes arterial inflammation and *vice versa*, chronic inflammation maintains a pro-inflammatory phenotype of the endothelium[25]. Therefore EC dysfunction seems to participate in atherosclerotic process from its inception onwards till ultimate complications with a complex and pleiotropic involvement of inflammation sustained by humoral and cellular inflammatory elements [26, 27].

For decades, the fundamental inflammatory nature of atherosclerosis has been known in principle, but not fully appreciated. Atherosclerosis has been clearly recognized as a chronic, systemic, and diffuse disease with focal complications in different vascular beds. The

mechanisms by which a specific site is rendered more prone to the development of symptomatic disease with cardiovascular events were not known. However, the observation that all stages of atherosclerosis may be at distant and multiple locations simultaneously but, at the same time, this process may spare entire vascular segments led to hypothesize that the interface and interactions between the vascular wall and the circulation blood is a primary site for the mechanisms underlying cardiovascular events [23]. The second seminal achievement has been to understand the importance of oxidation mechanisms in mediating physiological and pathophysiological responses in blood vessels. The intriguing observation that only after exposure of low density lipoprotein (LDL) to endothelial cells modified LDL were taken up by the macrophages to form foam cells led to extensive studies on lipoprotein metabolism [28]. The modification undergone by LDL was recognized to be of oxidative nature and the presence of oxidized LDL (oxLDL) have been shown to exert multiple proinflammatory activities, including transcription of proatherogenic genes, production of matrix metalloproteinases and tissue factor, inhibition of NO activity, and promotion of VSMC apoptosis [29]. Over the past years hypercholesterolaemia has been consistenly associated with endothelial dysfunction and has been established as a major risk factor for the development of atherosclerosis. OxLDLs antagonize the endothelial production of NO, reducing the expression of eNOS [30], decreasing the uptake of L-arginine and enhancing the level of asymmetric dimethylarginine (ADMA) [31].In both coronary and peripheral circulation, hypercholesterolaemia is associated with impaired endothelium-derived NO bioavailability, even when the coronary arteries are angiographically normal [32]. There is evidence that cholesterol levels even in the normal range may be inversely related to endothelium-dependent vasodilation, and this finding has important clinical implications. This suggests that lowering cholesterol levels even when it is within the normal range may improve the production and release of endothelium-dependent NO and hence improve endothelial function[33]. Indeed, lowering of cholesterol levels in patients with documented CAD leads to decreased rates of myocardial infarction, and this protective effect

may in part be due to improvement in endothelial function[34]. Recent evidence suggest that chronic exposure to increased plasma cholesterol levels might also impair the repair of lipoprotein-mediated endothelial injury, possibly by reducing the availability and function of circulating endothelial progenitors [35]

Endothelial dysfunction and cardiac allograft vasculopathy: a paradigmatic immuno-inflammatory vascular disease

Heart transplantation is the treatment of choice for patients with refractory end-stage heart disease. Numerous advances have been achieved in recipient selection, tissue preservation, surgical techniques as well as in post-transplant immunosuppression, improving short-term outcomes after HT[36, 37]. Although the procedure is nowadays considered effective in extending and improving quality of life, the onset of CAV remains the major limiting factor of long-term survival after HT. According to the 25th report of the Registry of the International Society for Heart and Lung Transplantation, CAV is the leading cause of death between 1 and 3 years after transplantation. After year 3, CAV accounts for 17% of deaths. Angiographic CAV occurs in 54% of all heart transplant patients 10 years after transplantation. Intravascular ultrasonography (IVUS), a more sensitive technique, detects CAV in 75% of patients at 3 years[36]. The presence of allograft vasculopathy, is not unique to cardiac transplantation, but it is a key feature of most chronic rejection syndromes, limiting long-term graft success of other solid organ transplants (e.g. kidney, liver and lung allografts)[38-41]. Recent evidence defines CAV as a peculiar accelerated and aggressive form of CAD, however its exact pathogenesis remains unclear[36]. Emerging data indicate that the endothelium plays a significant role in the onset, progression and complication of this multifactorial disease, with both immunologic and non-immunologic risk factors contributing to its development. Improving our understanding of the integral role of

the endothelium in CAV is of crucial clinical interest since it could provide further insights into the related pathophysiological mechanisms and possible new strategies for CAV prevention and therapy.

CAV is a fibroproliferative vascular disease resulting from "chronic rejection" of the cardiac allograft [36, 37, 42]. As transplanted patients increase in number and live longer, non-transplant physicians need to be familiar with the pathophysiology and clinical presentation of CAV. The disease is a wholly peculiar arteriosclerotic entity. Many features are similar to both traditional atherosclerosis and arteritis, but there are at the same time important differences in both pathology and distribution of the disease. CAV is caused by immunologic mechanisms that combine with non-immunologic factors leading to persistent endothelial injury[42, 43]. The result is intimal thickening and VSMC proliferation. Intimal hyperplasia progresses towards coronary obstruction, which ultimately ends up in graft failure.

The pathogenesis of the disease is complex, since it involves a peculiar, chronic, progressive immune-mediated insidious injury, refractory to conventional immunosuppression, intertwining with non-immunologic factors such as older donor age, sex, obesity, diabetes mellitus, hypertension, hyperhomocysteinemia (HHcy), cytomegalovirus (CMV) infection[44], ischemia/reperfusion (I/R) injury, brain death[45] and prothrombogenicity[46]. Along with hyperlipidemia and insulin resistance, which are the most significant non-immunologic risk factors, occurring in 50% to 80% of the HT population[36]. The recent evidence demonstrates that both the fibroproliferative disease resulting from chronic rejection and the classical atherosclerosis, arise secondary to endothelial dysfunction[47-49]. The endothelium seems to be initially a target, but lately an active player in the CAV process. The current accepted paradigm suggests that an initial specific immune-mediated injury trigger a following chronic non-specific inflammatory response due in part to conventional risk factors and in part to continuous repetitive immune damage. As a consequence of this multifactorial injury, the endothelium may become first activated and afterwards dysfunctional. Of note, once the injury has been

sufficiently strong and prolonged, the balance is definitively tipped towards stable endothelial damage and fibroproliferative modifications of the vessel wall. Then, the vicious circle becomes self-sustaining and autonomous, leading to CAV progression towards clinical complications[48, 50]. Understanding the exact role of endothelial dysfunction in the initiation and progression CAV is important in order to achieve insight into the occurrence of late heart failure after HT.

Evaluation of endothelial function

Since endothelium plays a central role in the pathogenesis of cardiovascular disease, to establish a reliable, accurate and easily reproducible assessment of endothelial function represents a cardinal goal for clinical cardiology. Endothelial function may be tested by 2 main methods. These tests are based on the concept that certain stimuli trigger the release of NO from the endothelium to mediate vascular relaxation. Endothelial vasomotor testing may be performed in the coronary circulation by use of quantitative angiography with measurement of coronary artery diameter, before and after infusion of vasoactive substances, i.e. acetylcholine. Whereas acetylcholine caused a dose-dependent dilation of coronary arteries in healthy subjects, a "paradoxical" vasoconstriction was observed in response to acetylcholine in patients with coronary disease, indicating an impaired endothelium-dependent vasomotion[21]. Later, Quyyumi *et al*. confirmed that the impaired response to acetylcholine in patients with coronary disease or cardiovascular risk factor was largely due to reduced coronary availability of endothelium-derived NO[32]. Although quantitative angiography is still considered the gold standard for the evaluation of endothelial function, it is an invasive and time consuming procedure. Hence, it is not suitable to detect early onset of endothelial alterations or to be repeated many times to monitor therapeutic interventions. Unfortunately, the recently introduced IVUS, which allows not only endothelial function evaluation, but also extremely promising measurement of atheroma burden beyond mere angiographical luminal narrowing, shares the same limitations

described for coronary angiography. The alternative endothelial vasomotor tests involve the peripheral circulation. Venous occlusion pletismography permits assessement of endothelial function measuring vasodilator capacity of the forearm resistance vessels when venous outflow is stopped by blood pression cuff inflation; vasoactive drugs can be administered directly through brachial artery cannulation. It is a procedure reproducible and accurate, but still moderately invasive and though, not suitable for large scale applications. Among recently alternative methods, the measurement of flow mediated dilation (FMD) of the brachial artery in response to increased shear stress during hyperemia, with high-resolution ultrasound was introduced in 1992 by Celermajer et al.[51] as a non-invasive endothelial function test. Accordingly, it was demonstrated that flow-dependent dilation of the radial and brachial arteries is largely sustained by NO synthase[52] and therefore provides a valuable "read-out" of vascular NO availability. This approach has now been used by numerous groups throughout the world to monitor endothelial function, with demonstration that the major cardiovascular risk factors impair FMD in a progressive manner, so that a more severe impairment of flow-dependent vasodilation is observed with increasing numbers of risk factors[53]. Several, but not all[54], studies, show a comparable predictive value of FMD and coronary endothelial function to detect the presence and extent of CAD[55, 56]. Furthermore, a recent study evidenced a correlation between results of FMD and cardiac stress single photon emission computed tomography imaging (SPECT), which is another well established and reliable method to assess flow-limiting CAD[57]. However, the presence of controversial observations on the possibility to correlate FMD findings with other endothelial vasomotor tests, not only in different vascular beds, but also in the same vascular district[58] and the evidence of some intrinsic methodological limitations, such as high variability, lack of standardized protocols, intra/interobservers variability, still prevent to validate FMD as a clinical established tool, although very promising[59].

Assessment of coronary flow reserve to investigate the pathophysiology of coronary microcirculation in heart transplantation

Early clinical diagnosis of CAV is difficult, owing to the denervation of the transplanted heart. Patients with CAV do not usually experience chest pain, but typically are asymptomatic until they present with sudden death or congestive heart failure, including fatigue, impaired exercise tolerance[60] and ventricular arrhythmias[61]. Several noninvasive screening methods such as dobutamine stress echocardiography[62], multi-slice computer tomography[63], magnetic resonance imaging [64] have not proved yet fully reliable even if encouraging results have been achieved[50, 65]. Therefore, periodic coronary angiography are performed for routine CAV diagnosis and surveillance in most transplant centers, however the sensitivity of this procedure, except for significant focal stenosis, is quite low. Coronary angiography frequently underestimates the extent and severity of the disease; by the common involvement of small intramyocardial vessels and by the occurrence of functional coronary alterations early before morphological changes are present[66]. IVUS technology is more sensitive than angiography[67]. IVUS, using an intracoronary catheter with a transducer at its tip, uniquely allows to visualize distinctively the 3 layers of the vessel wall, the intima, media, and adventitia. IVUS has been helpful in addressing the role of donor transmitted coronary artery disease *vs.* CAV arising *de novo*. Using this method, it has been shown that CAV (as coronary intimal thickening) can be demonstrated in almost all patients, being as high as 75% at 1 year after HT[68] and occurs most rapidly during the initial 2 years after transplant[69]. Usually only 1 of the major epicardial vessels is imaged, when imaging of all 3 vessels is performed the percentage of patients with CAV is even higher. The incidence of angiographically-diagnosed CAV is 42% at five years[70] while using multi-vessel IVUS, 58% of HT patients have CAV at 1 year, 71% at 2 years, and 74% at 3 years[71]. Intimal thickening

diagnosed by IVUS predicts later angiographic CAV, and is associated with impaired survival even in patients with normal angiography[69]. Progression of intimal thickening during the first year after heart transplantation detected with IVUS is a reliable surrogate marker for subsequent adverse events[67]. The widespread use of IVUS is limited by several problems. The cost is markedly more than angiography alone. The procedure is time-consuming and increases the complexity and risks of an invasive angiogram. Lack of extensive expertise is also a limiting factor. Finally, complete evaluation of the entire coronary tree is not feasible due to the physical size of the IVUS catheter, leaving the secondary or tertiary vessels unexplored.

Early CAV diagnosis remains the key for identification of recipients who are prone to develop the disease and suffering subsequent allograft failure. Growing interest is receiving the early assessment of the microcirculatory function in the coronary vascular bed, since at this level it is provided the primary control over myocardial tissue perfusion. Thus, the study of microvascular function may be more physiologically relevant than alterations in epicardial arteries. Most studies suggest that these 2 entities are distinct with different implications.

A body of literature demonstrating impaired endothelium-dependent vasomotor function and a derangement of the eNOS system in coronary arteries of HT patients[43, 48, 72] shows that endothelial dysfunction can be observed early after transplantation and predicts subsequent development of CAV[73] as well as adverse clinical outcomes[74]. Microcirculatory aberrations tend to be present across all coronary territories in cardiac transplant recipients and are associated with poor survival, suggesting a generalized microvascular involvement even in the presence of a normal angiogram[75]. Other investigators have found heterogeneous distribution in endothelial dysfunction according to the vessel section examined as well a as the drug used[76]. Predominant allograft microvascular dysfunction is detectable in around 15% of patients after HT[77]. Very recently, stenotic microvasculopathy (detected in biopsy samples) has been characterized as a prognostic factor for long-term survival after HT[78] even if not in all studies[79].

Coronary flow reserve (CFR) is an important functional parameter commonly used to investigate the pathophysiology of coronary circulation. The available methodologies in assessing CFR have been either invasive such as the intracoronary Doppler flow wire (IDFW), or expensive and scarcely available such as the positron emission tomography. In fact the evaluation of endothelial function in many studies have been investigated with an invasive Doppler flow wire[77] hence, not suitable to detect early onset of endothelial alterations or to be repeated many times to monitor therapeutic interventions. The ability to detect and distinguish changes in epicardial and microvascular function early and non invasively may aid in identifying modifiable factors that lead to CAV. Our group has focused on the use of contrast-enhanced transthoracic echocardiography (CE-TTE) in assessing CFR. We demonstrated that blood flow velocity and flow reserve recording of distal left anterior descending artery (LAD), having a superficial course close to the anterior chest wall, is possible during a transthoracic Doppler study and can be greatly improved using contrast and second harmonic Doppler technology[80]. CFR by CE-TTE is a noninvasive, reproducible, feasible and reliable method for the CFR assessment. It has been validated *vs.* an independent reference method such as IDFW showing close correlation in patients with and without CAD[81]. We [82] studied 73 patients a mean of 8 years after HT and found that using a CFR cutoff of 2 or less, the specificity for angiographic luminal irregularities or more significant disease was 100% (sensitivity of only 38%). Using a ROCderived cutoff of 2.7, the specificity and sensitivity were 87% and 82%, respectively. Later[83] we showed that a CFR of 2.6 or less was associated with a 3.1 relative risk of death, myocardial infarction, congestive heart failure, or need for percutaneous intervention at a mean of 19 months. This technique, however, is fairly new and further data are required.

Outline of the thesis

Based on the background presented above, the work submitted in this thesis describes on one side the studies aimed to investigate molecular mechanisms underlying endothelial dysfunction and vascular inflammation driven by oxidative stress in the context of hypertension and atherosclerosis using in vitro and in vivo models. These studies have been performed during the Fellowship I have spent in the Cardiovascular Research Division at the Department of Cardiology and Physiology at the University Hospital and at the University of Zürich, Switzerland.

On the other side I present clinical studies aimed to provide novel understanding of the pathophysiology of coronary microcirculation as far as functional aspects are concerned in conditions such as cardiac allograft vasculopathy or inflammatory disease i.e. psoriasis and hormon disorders, like primary hyperparathyroidism. These studies have been built up along with clinical and echocardiographic follow up of these patients, clinical data collection and database maintenance in parallel with the development and validation of new non invasive imaging techniques to provide functional assessment of the coronary microvasculature. These studies have been performed during my residency at the Department of Cardiac, Thoracic and Vascular Sciences, Cardiovascular Unit of the University of Padova, Italy.

PART 1. UNDERSTANDING MOLECULAR PATHWAYS OF ENDOTHELIAL DYSFUNCTION AND ATHEROSCLEROSIS

ORIGINAL DATA

Experimental studies

c-Jun N-Terminal Kinase 2 Deficiency Protects Against HypercholesterolemiaInduced Endothelial Dysfunction and Oxidative Stress

Atherosclerosis is a systemic immunoinflammatory disease that develops in response to endothelial injury.[1] Indeed, the endothelium is a key determinant of vascular integrity. Hypercholesterolemia, a well-known risk factor for cardiovascular disease, leads to accumulation and oxidation of low-density lipoprotein cholesterol within the intima of the vessel wall, triggering endothelial dysfunction and proinflammatory milieu as crucial steps in the early phase of the atherosclerotic process.[2] Oxidative stress, resulting from an imbalance between reactive oxygen species (ROS) and the antioxidant defense system, is a crucial mediator of hypercholesterolemia-induced endothelial dysfunction.[3,4] Indeed, ROS interact and inactivate nitric oxide (NO) and lead to protein nitration and lipid peroxidation. The c-Jun N-terminal kinases (JNKs), also known as stress-activated protein kinases, are serine/threonine protein kinases belonging to the mitogen-activated protein kinase superfamily.[5] JNKs play a fundamental role in stress responses, cell survival, and apoptosis. The JNK pathway is activated by stress factors such as ultraviolet radiation, reperfusion injury, ceramides, and inflammatory cytokines.[6] The dimerization of JNK leads to activation of other kinases, their nuclear translocation, and subsequent modulation of the activity of different transcription factors such as c-Jun, ATF-2, Elk-1, p-53, and c-myc.[7] Three distinct *JNK* genes have been described, *JNK1*, *JNK2*, and *JNK3*, encoding for different isoforms. *JNK3* expression is restricted to brain, heart, and testis, whereas *JNK1* and *JNK2* proteins are ubiquitously expressed.[8] Both *JNK1*- and *JNK2*-deficient mice are viable, indicating that neither *JNK1* nor *JNK2* plays an essential role in development and normal cellular functions; however, genetic disruption of both *JNK1* and *JNK2* is lethal.[9] Studies using gene targeting as well as JNK inhibitors demonstrated the involvement of *JNK1* and *JNK2* genes in several pathological conditions including cancer, immune diseases, and neurological diseases as well as metabolic disorders and inflammatory conditions such as arthritis and atherosclerosis.[10] JNKs are expressed in vascular smooth muscle cells and endothelial cells and activated by a wide range of stimuli such as oxidative stress, mechanical stretch, hypertension,[11–13] hyperglycemia, apoptosis,[14] and inflammation.[10] A recent study suggested a role of JNK in endothelial dysfunction: short-term exposure of coronary arterioles to tumor necrosis factor-α–induced endothelial dysfunction through activation of *JNK*

signal transduction pathway and generation of superoxide anion.[15] We recently reported a critical role of *JNK2* in atherogenesis showing that *JNK2* is required for foam cell formation within the atherosclerotic plaque by activating the scavenger receptor A.[16] The role of *JNK2* in the early stage of atherosclerosis related to endothelial dysfunction as it occurs under hypercholesterolemic conditions remains unknown. Thus, we compared *JNK2*-deficient with wild-type (WT) mice exposed to a high-cholesterol diet (HCD) or a normal diet (ND). We found that endogenous *JNK2* is critically involved in hypercholesterolemia-induced endothelial dysfunction and oxidative stress.

Methods

Animals and Diets

JNK2-/- and WT mice (both in a C57BL/6J background) were obtained from Jackson Laboratory (Bar Harbor, Maine) and kept on a regular diet. Mice were housed in temperature-controlled cages (20°C to 22°C), fed ad libitum, and maintained on a 12/12-hour light/dark cycle. At the age of 8 weeks, mice were fed a ND or a HCD (D12108 containing 1.25% cholesterol; Research Diets, New Brunswick, NJ) for 14 weeks, respectively. All animal experiments were approved by the local institutional animal care committee.

Plasma Lipid Measurements

At the time of tissue harvesting, 0.5 to 1 mL of blood was drawn from the right ventricle with heparinized syringes and immediately centrifuged at 4°C, and the plasma was stored at -80°C. Total cholesterol, triglycerides, and free fatty acids were analyzed with the reagents TR13421, TR22421 (both Thermo Electron Clinical Chemistry and Automation Systems, Thermo Fisher Scientific, Waltham, Mass), and 994-75409 (Wako Chemicals GmbH, Neuss, Germany), as recommended by the manufacturer. The lipid distribution in plasma lipoprotein fractions was assessed by fast-performance liquid chromatography gel filtration with a Superose 6 HR 10/30 column (Pharmacia, Basking Ridge, NJ).

Tissue Harvesting

Mice were euthanized by intraperitoneal administration of 50 mg/kg sodium pentobarbital. The entire aorta from the heart to the iliac bifurcation was excised and placed immediately in cold modified Krebs-Ringer bicarbonate solution (pH 7.4, 37°C, 95% O2, 5% CO2) of the following composition (mmol/L): NaCl (118.6), KCl (4.7), CaCl2 (2.5), KH2PO4 (1.2), MgSO4 (1.2), NaHCO3 (25.1), glucose (11.1), and calcium EDTA (0.026). The aorta was cleaned from

adhering connective tissue under a dissection microscope and either snap-frozen in liquid nitrogen and stored at -80°C or used immediately for organ chamber experiments.

Organ Chamber Experiments

For endothelial function experiments, aortas were cut into rings (2 to 3 mm long). Each ring was connected to an isometric force transducer (Multi-Myograph 610M, Danish Myo Technology A/S, Aarhus, Denmark), suspended in an organ chamber filled with 5 mL Krebs-Ringer bicarbonate solution (37°C, pH 7.4), and bubbled with 95% O2, 5% CO2. Isometric tension was recorded continuously. After a 30-minute equilibration period, rings were gradually stretched to the optimal point of their length-tension curve as determined by the contraction in response to potassium chloride (100 mmol). Concentration-response curves were obtained in a cumulative fashion. Several rings cut from the same artery were studied in parallel. Responses to acetylcholine (10^{-9} to 10^{-6} mol/L; Sigma-Aldrich, St Louis, Mo) in the presence or absence of polyethylene glycol–superoxide dismutase (PEG-SOD, 150 U/mL, Sigma-Aldrich) were recorded during submaximal contraction to norepinephrine (10^{-6} mol/L). The NO donor sodium nitroprusside (10^{-10} to 10^{-5} mol/L; Sigma-Aldrich) was added to test endothelium-independent relaxation. Relaxations were expressed as a percentage of the precontracted tension.

Measurements of NO, O2-, and ONOO-

Concurrent measurements of NO, O2-, and ONOO- were performed with 3 electrochemical nanosensors combined into 1 working unit with a total diameter of 2.0 to 2.5 um. Their design was based on previously developed and well-characterized chemically modified carbon-fiber technology.[4,17,18] Amperometry was performed with a computer-based Gamry VFP600 multichannel potentiostat. A current at the peak potential characteristic for NO (0.65 V) oxidation and ONOO- (-0.40 V) or O2- (-0.23 V) reduction was directly proportional to the local concentrations of these compounds in the immediate vicinity of the sensor. Linear calibration curves (current versus concentration) were constructed for each sensor from 10 nmol/L to 2 umol/L before and after measurements with aliquots of NO, O2-, and ONOO- standard solutions, respectively. At a constant distance of the sensors from the surface of the endothelial cell, the reproducibility of measurements is high (5% to 12%). The consumption of redox species by nanosensors depends on the area of the electrode (<0.12 umq) and the duration time of electrolysis (≈5 to 10 seconds). For the amperometric measurements used, it varied between 0.04% and 0.1% of the NO, O2-, and ONOO- peak concentration. This value is negligible compared with the experimental error. The position of nanosensors (*x*,*y*, *z*

coordinates) versus the endothelial cell was established with the help of a computercontrolled micromanipulator. To establish a constant distance from cells, the module of sensors was lowered until it reached the surface of the cell membrane. After that, the sensors were slowly raised 4±1 um (*z* coordinates) from the surface of cells. The sensors were then moved horizontally (*x*, *y* coordinates) and positioned above a surface of randomly chosen single endothelial cells in an aortic ring. Acetylcholine was then injected with a nanoinjector that was also positioned by a computer-controlled micromanipulator.

Western Blotting

Frozen samples of aortas were pulverized and dissolved in lysis buffer (120 mmol/L sodium chloride, 50 mmol/L Tris, 20 mmol/L sodium fluoride, 1 mmol/L benzamidine, 1 mmol/L dithiothreitol, 1 mmol/L EDTA, 6 mmol/L EGTA, 15 mmol/L sodium pyrophosphate, 0.8 ug/mL leupeptin, 30 mmol/L *p*-nitrophenyl phosphate, 0.1 mmol/L phenylmethylsulfonyl fluoride, and 1% NP-40) for immunoblotting. Cell debris was removed by centrifugation (12 000*g*) for 10 minutes at 4°C. The samples (20 ug) were treated with x5 Laemmli's SDS-PAGE sample buffer (0.35 mol/L Tris-Cl, pH 6.8, 15% SDS, 56.5% glycerol, 0.0075% bromophenol blue), followed by heating at 99°C for 5 minutes, and then subjected to 10% SDS-PAGE gel for electrophoresis. The proteins were then transferred onto Immobilon-P filter papers (Millipore AG, Bedford, Mass) with a semidry transfer unit (Hoefer Scientific, San Francisco, Calif). The membranes were then blocked by use of 5% skim milk in TBS-Tween buffer (0.1% Tween 20; pH 7.5) for 1 hour at room temperature and incubated with anti total JNK and p-JNK; (1:1000 dilution; Santa Cruz Biotechnology, Inc, Santa Cruz, Calif), anti-NOS3 rabbit polyclonal antibody (1:1000 dilution; Santa Cruz Biotechnology Inc), anti-phospho (Ser1177)– endothelial NO synthase (eNOS) rabbit polyclonal antibody (1:250; Cell Signaling), anti-Mn-SOD rabbit polyclonal antibody (1:2000; Upstate USA Inc, Charlottesville, Va), anti-Cu/Zn-SOD rabbit polyclonal antibody (1:2000; Upstate Biotechnology, Lake Placid, NY) and antiextracellular (EC)-SOD (1:1000; Upstate Biotechnology) for 1 hour at room temperature. Membranes were then incubated with the secondary antibody (horseradish peroxidase–conjugated anti-mouse/rabbit immunoglobulin antibody; Amersham Biosciences, Piscataway, NJ) at a dilution of 1:2000. Prestained markers (Bio-Rad Laboratories, Hercules, Calif) were used for molecular mass determinations. The immunoreactive bands were detected by an enhanced chemiluminescence kit (Amersham Biosciences). Anti-α-tubulin mouse monoclonal antibody (1:2000) or anti-α-actin (1:1000; Sigma-Aldrich) was employed as a loading control. Western blots were quantified densitometrically (National Institutes of Health Image 1.6, Bethesda, Md).

Immunohistochemistry and Superoxide Detection

Freshly isolated aortic segments were immediately embedded in OCT medium and snap-frozen in pentane/liquid nitrogen. Cryosections of 6-um thickness were mounted on SuperFrost glass slides and incubated at 37°C for 30 minutes with 1 umol/L dihydroethidium for superoxide detection. To stain for protein-bound nitrotyrosine or Mn-SOD, sections were fixed in 4% PBS-buffered formalin for 5 minutes, blocked with 10% BSA in PBS, and incubated with polyclonal anti-nitrotyrosine antibody (1:50; Upstate) and anti-Mn-SOD antibody (1:250; StressGen, Victoria, Canada) at 4°C overnight, respectively. For visualization, the secondary antibody (Alexa568 anti-rabbit IgG; 1:300; Molecular Probes, Carlsbad, Calif) was incubated for 1 hour at room temperature. Slides were then rinsed, embedded in glycerin-PBS, and examined under a fluorescent microscope (DM-IRB; Leica, Heerbrugg, Switzerland) connected to a digital imaging system (Spot-RT; Diagnostic Instruments/Visitron Systems, Puchheim, Germany). Pictures were obtained with identical camera and microscope settings. Dihydroethidium-stained specimens were background-corrected for autofluorescence of elastic fibers and the basal lamina with the use of ImageJ/ National Institutes of Health (rsb.info.nih.gov/ij/).

Thiobarbituric Acid Reactive Substances Assay

In vitro assessment of aortic levels of lipid peroxidation was performed with the use of the thiobarbituric acid reactive substances (TBARS) assay kit (OXItek, ZeptoMetrix Corp, Buffalo, NY), according to the manufacturer's instructions. Briefly, snap-frozen tissue was crushed in a prechilled mortar and pestle and resuspended at a concentration of 50 mg/mL in PBS. Then 100 uL of homogenate was added to SDS solution and mixed thoroughly. After TBA/buffer reagent addition, samples were incubated at 95°C for 60 minutes and centrifuged at 3000 rpm at room temperature for 15 minutes. Absorbance was read at 532 nm.

Statistical Analysis

Results are expressed as mean±SEM, and n indicates number of experiments. Statistical analysis was performed with Student *t* test for simple comparisons between 2 values. For multiple comparisons, results were analyzed by ANOVA followed by Bonferroni post hoc correction. A value of $P<0.05$ was considered statistically significant. The authors had full access to and take full responsibility for the integrity of the data. All authors have read and agree to the manuscript as written.

Results

Lipid Profiles

We determined plasma cholesterol, triglycerides, and free fatty acids in *JNK2-/-* and WT mice fed either a HCD or a ND (Table). Both *JNK2-/-* and WT mice developed significant hypercholesterolemia after 14 weeks of HCD. Interestingly, *JNK2-/-* mice had slight but significantly increased levels of total plasma cholesterol compared with WT mice on either ND or HCD (Table). No difference in plasma triglycerides or free fatty acids was observed between the groups (Table).

Hypercholesterolemia Activates Aortic JNK

To determine the effect of hypercholesterolemia on JNK activation, we compared Western blot analyses of aortic lysates from normocholesterolemic and hypercholesterolemic WT mice using a phosphospecific JNK antibody. Aortas from WT mice on HCD showed increased JNK phosphorylation compared with vessels from WT on ND (Figure 1).

JNK2 Deletion Protects From Hypercholesterolemia-Induced Endothelial Dysfunction

Isometric tension studies demonstrated no difference in vascular contractions to norepinephrine between aortas obtained from WT or $^{-/-}$ mice fed either a HCD or ND (data not shown). Endothelium-dependent relaxations to acetylcholine were impaired in WT mice on HCD compared with WT mice on ND. Interestingly, endothelium-dependent relaxations remained normal in *JNK2-/-* HCD mice, suggesting a preserved NO bioavailability favored by the lack of *JNK2* (Figure 2A). Concurrent with this notion, addition of the free radical scavenger PEG-SOD (150 U/mL) significantly improved endothelium-dependent relaxations in HCD WT mice (Figure 2B). Endothelium-independent relaxations to sodium nitroprusside were similar in all groups (data not shown).

Preserved Endothelial NO Release in Hypercholesterolemic *JNK2-/-* Mice

For assessing NO bioavailability at the level of endothelial cells, we determined NO in single endothelial cells using nanosensors. After stimulation with acetylcholine (10^{-7} mol/L), maximal NO levels were 242±10 nmol/L in WT mice on ND and decreased ≈50% in WT mice on HCD (Figure 3A). In contrast, similar levels of NO release were found in *JNK2-/-* mice on ND or HCD (Figure 3A).

Decreased Oxidative Stress in Hypercholesterolemic *JNK2-/-* Mice

To determine the effect of hypercholesterolemia on oxidative stress in endothelial cells, we measured superoxide anion (O2-) and peroxynitrite (ONOO-) production in single aortic endothelial cells. A significant increase in O2- concentration was observed in WT mice exposed to HCD compared with WT mice on ND, whereas no significant hypercholesterolemia-induced changes were observed in *JNK2-/-* mice (Figure 3B and 3C). In agreement with preserved NO bioavailability and O2- findings, ONOO- concentrations were increased only in WT but not in *JNK2-/-* mice fed a HCD (Figure 4A). Because ONOO- leads to increased 3-nitrotyrosine–containing proteins, we performed in situ immunohistochemistry with a polyclonal antibody against 3-nitrotyrosine in aortic cross sections. *JNK2-/-* HCD mice showed a markedly reduced immunoreactivity both in the endotheliumand in the media compared with diet-matched WT mice (Figure 4B). This favorable redox profile was confirmed by measuring aortic TBARS levels. After HCD exposure, *JNK2-/-* mice did not exhibit an increase in lipid peroxidation compared with WT mice (Figure 4C).

Free Radical Scavenger Expression and Activity

Protein expression of 3 pivotal free radical scavengers was assessed to determine whether an upregulation of antioxidant defense mechanisms might explain the preserved NO bioavailability in hypercholesterolemic *JNK2-/-* mice. Cu/Zn-SOD was similar in all experimental groups (data not shown), whereas aortic expression of Mn-SOD and EC-SOD was significantly decreased in WT mice fed a HCD compared with WT mice on a ND (Figure 5A and 5B). By contrast, levels of Mn-SOD and EC-SOD in *JNK2-/-* HCD were similar to WT ND mice (Figure 5A and 5B). Unexpectedly, *JNK2-/-* ND mice exhibited a reduced expression of both SOD isoforms compared with diet-matched WT mice (Figure 5A and 5B). Accordingly, immunofluorescent stainings for Mn-SOD showed similar results in aortic cross sections (Figure 5C).

Increased eNOS Expression in *JNK2-/-* Mice

To obtain more insight into the mechanisms of preserved NO bioavailability in *JNK2-/-* mice with hypercholesterolemia, we quantified eNOS expression in aortic lysates. ENOS expression was not affected by HCD in WT mice, whereas *JNK2-/-* HCD mice showed a significantly increased expression of eNOS (Figure 6A). Furthermore, to determine whether NO production was also regulated by eNOS activity, we performed additional blotting of phosphorylated Ser1177-eNOS in pooled samples. pS1177-eNOS protein levels were similar in aortic lysates

from *JNK2-/-* on either diet and WT mice on ND. In contrast, we found reduced eNOS phosphorylation in WT mice on HCD (Figure 6B).

Discussion

The present study demonstrates for the first time that genetic deletion of *JNK2* protects against hypercholesterolemiainduced and ROS-mediated endothelial dysfunction. The following findings support our conclusion:[1] Long-term exposure of WT mice to a HCD induces aortic JNK phosphorylation[2]. In contrast to WT mice, long-term exposure of *JNK2-/-* to HCD did not impair endothelium-dependent relaxation to acetylcholine[3]. Lower ONOO- levels in hypercholesterolemic *JNK2-/-* mice were associated with decreased protein nitration and lipid peroxidation. Accordingly, [4] expression of the antioxidant enzymes Mn-SOD and EC-SOD was increased in *JNK2-/-* mice. In contrast, we observed a downregulation of these enzymes after 14 weeks of HCD in WT mice. Genetic deletion of JNK2 did not affect severity of hypercholesterolemia, although *JNK2-/-* mice had slightly but significantly increased levels of total cholesterol compared with WT mice fed with either ND or HCD. Thus, we could rule out that differences observed among the 2 groups were caused by different experimental conditions. In contrast to our findings, a recent study showed similar total plasma cholesterol levels in *JNK2-/-* and WT controls[19]. Preserved bioavailability of NO is a key marker of vascular integrity. In vivo, activity of the L-arginine/NO pathway is determined by a balance between synthesis and breakdown of NO for its reaction with O2-. This balance is impaired in hypercholesterolemia and atherosclerosis[20,21]. Endothelial dysfunction, reflected by impaired endothelium-dependent relaxation, occurs in experimental models of hypercholesterolemia, as was confirmed in WT mice of this study[22,23]. Similarly, many clinical studies reported abnormal endothelium-dependent vasodilation in hypercholesterolemic patients[24]. Hypercholesterolemia induces a series of molecular events that increase the production of ROS and inactivate NO to form ONOO-[25]. In this study, acetylcholine-induced relaxation did not differ between *JNK2-/-* and WT mice in control conditions of normocholesterolemia following ND. However, on chronic hypercholesterolemia induced by 14 weeks of HCD, WT mice but not *JNK2-/-* mice developed endothelial dysfunction. The finding that addition of the free radical scavenger PEG-SOD restored endothelium-dependent relaxation in WT mice on HCD suggests an important role of ROS in this context. Hypercholesterolemia-induced oxidative stress has been attributed to activation of oxidases in the vasculature and in infiltrating leukocytes.[22] Moreover, hypercholesterolemia has been shown to impair antioxidant defense mechanisms against

ONOO- formation.[25] To investigate whether preserved endothelial function in hypercholesterolemic *JNK2-/-* mice was associated with increased bioavailability of NO, we assessed NO release from single endothelial cells after stimulation with acetylcholine. In hypercholesterolemic control mice, NO levels decreased by ≈50%, whereas they remained unchanged in *JNK2-/-* mice. Because O2- is the main inactivator of NO, we tested whether decreased endothelial production of O2- contributes to increased NO bioavailability in *JNK2-/-* mice. We found enhanced O2- production in hypercholesterolemic WT mice compared with mice on ND, whereas no significant dietinduced changes were detected in *JNK2-/-* mice. Dihydroethidium stainings of aortic segments confirmed these findings.In aortas exposed to chronic hypercholesterolemia, the reaction of NO and O2- leads to enhanced ONOO- formation and, in turn, increased nitrotyrosine residues, which are typical end products of the reaction of ONOO- with biological compounds. [26] Tyrosine nitration is responsible for inactivation of several enzymes.[27] Our group has shown that nitration of Mn-SOD and prostacyclin synthase occurs in aged and diabetic mice, respectively.[28,29] In agreement with the notion that *JNK2* deficiency induces preserved NO bioavailability but reduced O2- production, we found that ONOO- concentrations were increased in WT but not in *JNK2-/-* mice fed a HCD. In parallel, nitrotyrosine immunoreactivity was detected in both endothelium and smooth muscle cells of hypercholesterolemic mice, as shown previously by our group.[30] However, aortas from hypercholesterolemic WT mice exhibited enhanced immunostaining compared with diet-matched *JNK2-/-* mice. ONOO- contributes to atherogenesis by promoting lipid peroxidation.[31] In contrast to hypercholesterolemic WT mice, *JNK2-/-* mice were protected against lipid peroxidation, as determined by TBARS in aortic lysates. To investigate whether antioxidant defense mechanisms contribute to the preserved endothelial function in hypercholesterolemic *JNK2-/-* mice, we assessed protein expression of 3 pivotal O2- scavengers. Aortic expression of Mn-SOD and EC-SOD was decreased in hypercholesterolemic WT mice compared with normocholesterolemic controls. By contrast, both Mn-SOD and EC-SOD were induced after 14 weeks of hypercholesterolemia in *JNK2-/-* mice. Furthermore, in situ immunohistochemistry showed that changes in Mn-SOD expression occur throughout the aortic vascular wall. These findings suggest that the ability of the SOD scavenging system to respond to oxidative stress remains intact in *JNK2-/-* mice. Unexpectedly, normocholesterolemic *JNK2-/-* mice exhibited a reduced expression of Mn-SOD and EC-SOD compared with diet-matched WT mice. However, these changes did not translate into differences in endothelium-dependent, NO-mediated responses, as shown by organ chamber experiments and in situ measurements of NO release. At low concentrations, O2- diffusion is slow, and O2- is scavenged by highly diffusible NO.

Therefore, at low O2- in *JNK2-/-* mice on ND, SOD may be less competitive for O2- than NO. This process may change under high O2 and low NO levels, as found in the context of hypercholesterolemia, in which the role of SOD becomes more substantial. Accordingly, the reduced expression of Mn-SOD and EC-SOD in *JNK2-/-* mice on ND did not translate into changes of NO, O2-, and ONOO- production. To obtain more insight into the mechanisms of preserved NO bioavailability in hypercholesterolemic *JNK2-/-* mice, we assessed eNOS expression in aortic lysates. Western blot analysis revealed higher eNOS expression in hypercholesterolemic *JNK2-/-* compared with WT mice. Conflicting data have been reported related to the regulation of eNOS during hypercholesterolemia. Evidence exists of reduced transcription and enhanced breakdown of eNOS transcripts on increasing concentrations of oxidized lowdensity lipoprotein. Long-term stimulation with oxidized lowdensity lipoprotein may also lead to a decrease in the amount of NOS protein through induction of cytokines.[32] Experimental atherosclerosis is associated with an increased eNOS expression and NO production, whereas decreased eNOS expression and NO release are found in advanced human atherosclerosis.[33] To determine whether NO production was also regulated by eNOS activity, we determined eNOS phosphorylation. Interestingly, the observed upregulation of eNOS protein in *JNK2-/-* on HCD did not translate into increased eNOS phosphorylation, justifying unchanged NO concentrations and endothelium-dependent relaxations in *JNK2-/-* mice. On the other hand, decreased eNOS phosphorylation in WT HCD mice matched reduced NO levels found in this group. Because deletion of *JNK2* in hypercholesterolemic mice was associated with upregulation of SOD, it is likely that this antioxidant defense system contributes to protect against hypercholesterolemia-mediated oxidative stress in *JNK2-/-* mice. Thus, our findings suggest that *JNK2* is involved in the pathways regulating vascular endothelial ROS production and antioxidant defense systems under hypercholesterolemic conditions. Our results are in accordance with previous studies that associate JNK activation with increased levels of oxidative stress and ROS-mediated cell death.[34] In particular, JNK is known to play a major role in cardiovascular disease and is activated on mechanical stress, hypertension,[11–13] and ischemia/reperfusion.[35] JNK has also been reported to be activated in advanced atherosclerotic plaques in rabbits as well as in humans[34] and to activate matrix proteases involved in disease progression of abdominal aortic aneurysm in mice and humans.[36] Along this line, *JNK2* is necessary for scavenger receptor A– or CD36-mediated foam cell formation in atherogenesis.[16,37,38] *JNK2* has also been demonstrated to be involved in insulitis of type I diabetes mellitus.[39] Pharmacological JNK inhibition is a promising strategy given its beneficial effects in mouse models of atherogenesis,[16] abdominal aneurysm,[37] and cerebral ischemia.[40]

JNK inhibition may even be more rewarding considering its critical role in obesity and insulin resistance.[41] Thus, JNK inhibition could represent a attractive therapeutic target to prevent progression of atherosclerosis and metabolic disease. Our findings suggest that JNK may also be a promising target for preventing atherosclerosis at its early stage of endothelial dysfunction.

Acknowledgments

We would like to thank Alexander Akhmedov, PhD, for genotyping *JNK2-/-* mice and Elisabeth Muessig for Mn-SOD immunostaining.

Sources of Funding

This work was supported in part by Swiss National Research Foundation grants 310000108463 (Dr Cosentino), 3100-068118 (Dr Luescher), and 31-114094/1 (Dr Matter) and the Swiss Heart Foundation (Drs Cosentino and Matter) as well as US Public Health grant 0418061 (Dr Malinski). The University Research Priority Program "Integrative Human Physiology" at the University of Zurich (Drs Cosentino, Luescher, and Matter) and European Vascular Genomic Network, Mercator Foundation (Dr Luescher), also supported this study.

Disclosures

None.

References

1. Hansson GK. Inflammation, atherosclerosis and coronary artery disease. *N Engl J Med*. 2005;352:1685–1695.

2. Libby P, Ridker PM. Inflammation and atherothrombosis: from population biology and bench research to clinical practice. *J Am Coll Cardiol*.2006;48:A33–A46.

3. Vergnani L, Hatrik S, Ricci F, Passaro A, Manzoli N, Zuliani G, Brovkovych V, Fellin R, Malinski T. Effect of native and oxidized low-density lipoprotein on endothelial nitric oxide and superoxide production: key role of L-arginine availability. *Circulation*. 2000;101:1261–1266.

4. Erdei N, Toth A, Pasztor ET, Papp Z, Edes I, Koller A, Bagi Z. High-fat diet-induced reduction in nitric oxide-dependent arteriolar dilation in rats: role of xanthine oxidase-derived superoxide anion. *Am J Physiol*. 2006;291:H2107–H2115.

5. Ichjio H. From receptors to stress-activated MAP kinases. *Oncogene*.1999;18:6087– 6093.

6. Kyriakis JM, Avruch J. Mammalian mitogen-activated protein kinase signal transduction pathways activated by stress and inflammation. *Physiol Rev*. 2001;81:807– 869.
7. Jaeschke A, Karasarides M, Ventura JJ, Ehrhardt A, Zhang C, Flavell RA, Shokat KM, Davis RJ. JNK2 is a positive regulator of the cJun transcription factor. *Mol Cell*. 2006;23:899 –911.
8. Davis RJ. Signal transduction by the JNK group of MAP kinases. *Cell*.2000;103:239 –252.
9. Kuan CY, Yang DD, Samanta Roy DR, Davis RJ, Rakic P, Flavell RA. The Jnk1 and Jnk2 protein kinases are required for regional specific apoptosis during early brain development. *Neuron*. 1999;22:667– 676.
10. Bogoyevitch MA. The isoform-specific functions of the c-Jun N-terminal Kinases (JNKs): differences revealed by gene targeting. *BioEssays*. 2006;28:923–934.
11. Xu Q, Liu Y, Gorospe M, Udelsman R, Holbrook NJ. Acute hypertension activates mitogen-activated protein kinases in arterial wall. *J Clin Invest*.1996;97:508 –514.
12. Touyz RM, Yao G. Up-regulation of vascular and renal mitogen-activated protein kinases in hypertensive rats is normalized by inhibitors of the Na_/Mg2_ exchanger. *Clin Sci*. 2003;105:235–242.
13. Touyz RM, Yao G, Viel E, Amiri F,. Schiffrin EL. Angiotensin II and endothelin-1 regulate MAP kinases through different redox-dependent mechanisms in human vascular smooth muscle cells. *J Hypertens*. 2004;22:1141–1149.
14. Ho FM, Lin WW, Chen BC, Chao CM, Yang C, Lin LY, Lai CC, Liu SH, Liau CS. High glucose-induced apoptosis in human vascular endothelial cell is mediated trough NF-kB and c-Jun NH2-terminal kinase pathway and prevented by PI3K/Akt/eNOS pathway. *Cell Sign*. 2006;18:391–399.
15. Zhang C, Hein T, Wang W, Ren y, Shipley RD, Kuo L. Activation of JNK and xanthine oxidase by TNF-_ impairs nitric oxide-mediated dilation of coronary arterioles. *J Moll Cell Cardiol*. 2006;40:247–257.
16. Ricci R, Sumara G, Sumara I, Rozemberg I, Kurrer M, Akhmedov A, Hersberger M, Eriksson U, Eberli F, Becher B, Boren J, Chen M, Cybulsky MI, Moore KJ, Freeman MV, Wagner EF, Matter CM, Luescher TF. Requirement of JNK2 for scavenger receptor A-mediated foam cell
formation in atherogenesis. *Science*. 2004;306:1558 –1561.
17. Malinski T, Taha Z. Nitric oxide release from a single cell measured *in situ* by a porphyrinic-based microsensor. *Nature*. 1992;358:676–678.

18. Mason RP, Kalinowshki L, Jacob RF, Jacoby AM, Malinski T. Nebivolol reduces nitroxidative stress and restores nitric oxide bioavailability in endothelium of African Americans. *Circulation*. 2005;112:3795–3801.

19. Tuncman G, Hirosumi J, Solinas G, Chang L, Karin M, Hotamisligil G. Functional in vivo interactions between JNK1 and JNK2 isoforms in obesity and insulin resistance. *Proc Natl Acad Sci U S A*. 2006;103:10741–10746.

20. Lerman A, Zeiher AM. Endothelial function: cardiac events. *Circulation*.2005;111:63– 68.

21. Osto E, Coppolino G, Volpe M, Cosentino F. Restoring the dysfunctional endothelium. *Curr Pharm Des*. 2007;13:1053–1068.

22. White CR, Darley-Usmar V, Berrington WR, McAdams M, Gore JZ, Thompson JA, Parks DA, Tarpey MM, Freeman BA. Circulating plasma xanthine oxidase contributes to vascular dysfunction in hypercholesterolemic rabbits. *Proc Natl Acad Sci U S A*. 1996;93:8745– 8749.

23. Ohara Y, Peterson TE, Harrison DG. Hypercholesterolemia increases endothelial superoxide anion production. *J Clin Invest*. 1993;91:2546–2551.

24. Stroes E, Kastelein J, Cosentino F, Erkelens W, Wever R, Koomans H, Luescher T, Rabelink T. Tetrahydrobiopterin restores endothelial function in hypercholesterolemia. *J Clin invest*.1997;99:41– 46.

25. Ma XL, Lopez BL, Liu GL, Christopher TA, Gao F, Guo YP, Feuerstein GZ, Ruffolo RR Jr, Barone FC, Yue TL. Hypercholesterolemia impairs a detoxification mechanism against peroxynitrite and renders the vascular tissue more susceptible to oxidative injury. *Circ Res*. 1997;80:894 –901.

26. Beckam JS, Koppenol WH. Nitric oxide, superoxide and peroxynitrite: the good, the bad and the ugly. *Am J Physiol*. 1996;271:C1424–C1437.

27. Zou MH, Leist M, Ullrich V. Selective nitration of prostacyclin synthase and defective vasorelaxation in atherosclerotic bovine coronary arteries. *Am J Pathol*. 1999;154:1359 –1365.

28. van der Loo B, Labugger R, Skepper JN, Bachschmid M, Kilo J, Powell JM, Palacios-Callender M, Erusalimsky JD, Quaschning T, Malinski T, Gygi D, Ulrich V, Luascher TF. Enhanced peroxynitrite formation is associated with vascular aging. *J Exp Med*. 2000;192:1731–1744.

29. Cosentino F, Eto M, De Paolis P, van der Loo B, Bachschmid M, Ullrich V, Kouroedov A, Delli Gatti C, Joch H, Volpe M, Lüscher TF. High glucose causes upregulation of cyclooxygenase-2 and alters prostanoid profile in human endothelial cells: role of protein kinase C and reactive oxygen species. *Circulation*. 2003;25;107:1017–1023.

30. Camici GG, Schiavoni M, Francia P, Bachschmid M, Martin-Padura I, Hersberger M, Tanner FC, Pelicci P, Volpe M, Anversa P, Lüscher TF, Cosentino F. Genetic deletion of p66(Shc) adaptor protein prevents hyperglycemia-induced endothelial dysfunction and oxidative stress.*Proc Natl Acad Sci U S A*. 2007;104:5217–5222.

31. Kurosawa T, Itoh F, Nozaki A, Nakano Y, Katsuda S, Osakabe N, Tsubone H, Kondo K, Itakura H. Suppressive effects of cacao liquor polyphenols (CLP) on LDL oxidation and the development of atherosclerosis in Kurosawa and Kusanagi-hypercholesterolemic rabbits. *Atherosclerosis*.2005;179:237–246.

32. Jessup W. Oxidized lipoproteins and nitric oxide. *Curr Opin Lipidol*. 1996;7:274 –280.

33. Oemar BS, Tschudi MR, Godoy N, Brovkovich V, Malinski T, Luescher TF. Reduced endothelial nitric oxide synthase expression and production in human atherosclerosis. *Circulation*. 1998;97:2494 –2498.

34. Metzler B, Hu Y, Dietrich H, Xu Q. Increased expression and activation of stress-activated protein kinases/c-Jun NH(2)-terminal protein kinases in atherosclerotic lesions coincide with p53. *Am J Pathol*. 2000;156:1875–1886.

35. Milano G, Morel S, Bonny C, Samaja M, von Segesser LK, Nicod P, Vassalli G. A peptide inhibitor of c-Jun NH2-terminal kinase reduces myocardial ischemia-reperfusion injury and infarct size in vivo. *Am J Physiol*. 2007;292:H1828–H1835.

36. Yoshimura K, Aoki H, Ikeda Y, Fujii K, Akiyama N, Furutani A, Hoshii Y, Tanaka N, Ricci R, Ishihara T, Esato K, Hamano K, Matsuzaki M. Regression of abdominal aortic aneurysm by inhibition of c-Jun N-terminal kinase. *Nat Med*. 2005;11:1330 –1338.

37. Yoshimura K, Aoki H, Ikeda Y, Furutani A, Hamano K, Matsuzaki M. Identification of c-Jun N-terminal kinase as a therapeutic target for abdominal aortic aneurysm. *Ann N Y Acad Sci*. 2006;1085:403– 406.

38. Rahaman SO, Lennon DJ, Febbraio M, Podrez EA, Hazen SL, Silverstein RL. A CD36-dependent signaling cascade is necessary for macrophage foam cell formation. *Cell Metab*. 2006;4211– 4221.

39. Jaeschke A, Rincon M, Doran B, Reilly J, Neuberg D, Greiner DL, Shultz LD, Rossini AA, Flavell RA, Davis RJ. Disruption of the Jnk2 (Mapk9) gene reduces destructive insulitis and diabetes in a mouse model of type I diabetes. *Proc Natl Acac Sci U S A*. 2005;102:6931– 6935.

40. Borsello T, Clarke PG, Hirt L, Vercelli A, Repici M, Schorderet DF, Bogousslavsky J, Bonny C. A peptide inhibitor of c-Jun N-terminal kinase protects against excitotoxicity and cerebral ischemia. *Nat Med*. 2003;9:1180 –1186.

41. Hirosumi J, Tuncman G, Chang L, Görgün CZ, Uysal KT, Maeda K, Karin M, Hotamisligil GS. A central role for JNK in obesity and insulin resistance. *Nature*. 2002;420:333–336.

Figures and table

Table. Plasma Lipids From *JNK2*$^{-/-}$ and WT Littermates After 14 Weeks of ND or HCD

	WT		*JNK2*$^{-/-}$	
	ND	HCD	ND	HCD
Total cholesterol, mmol/L	3.3±0.2	7.1±2.4*	3.9±0.3†	9.6±1.2*‡
Triglycerides, mmol/L	1.34±0.45	0.79±0.18	1.40±0.6	1.35±0.27
Free fatty acid, mmol/L	0.54±0.34	0.33±0.07	0.35±0.05	0.34±0.09

Values are mean±SEM. n=4 to 6 in each group.
*P<0.05 vs ND WT and *JNK2*$^{-/-}$ mice, respectively; †P<0.05 vs diet-matched WT mice; ‡P<0.05 vs HCD WT mice.

Figure 1

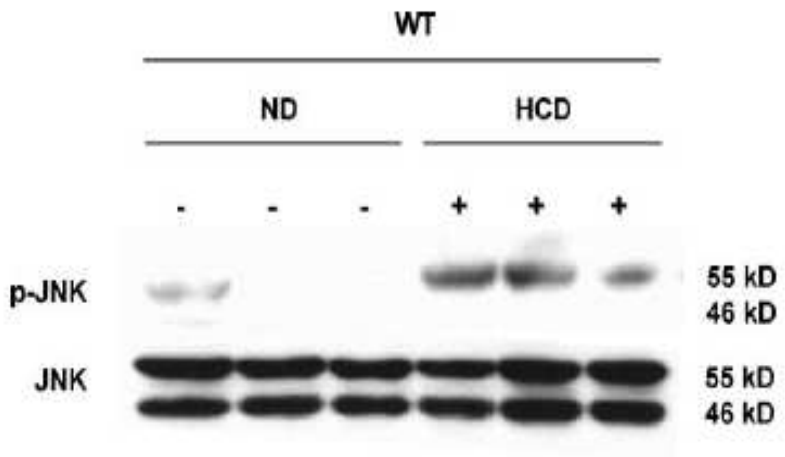

Figure 1. Representative Western blots show phosphorylated JNK (p-JNK) protein expression in aortic lysates from WT mice after 14 weeks of ND or HCD. Expression of total JNK was used as a loading control.

Figure 2

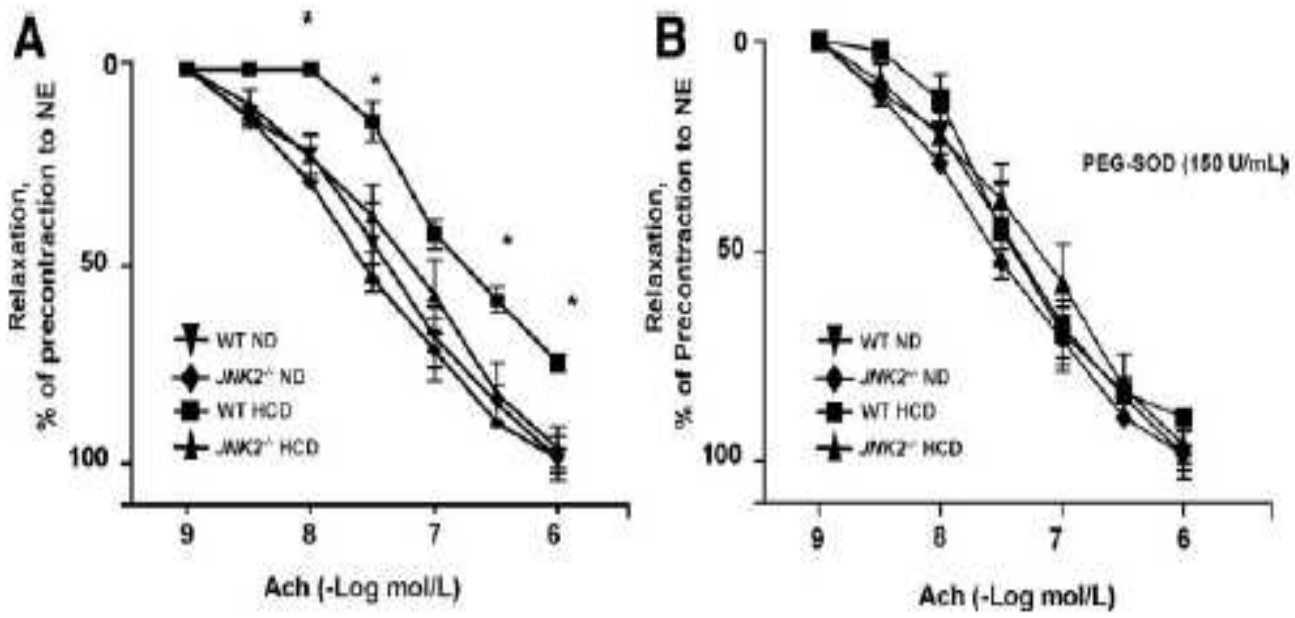

Figure 2. A, Hypercholesterolemiainduced changes in endotheliumdependent relaxation of aortas isolated from WT and *JNK2*-deficient (*JNK2-/-*) mice after 14 weeks of ND or HCD. Line graphs show concentration-response curves to acetylcholine (Ach) during submaximal contraction to norepinephrine (NE) (10^{-6} mol/L). B, Effect of PEG-SOD on the endothelium-dependent relaxation to acetylcholine in all experimental groups. Results are presented as mea±SEM; n=4 to 6 in each group. *P<0.05 for WT HCD vs all other groups.

Figure 3

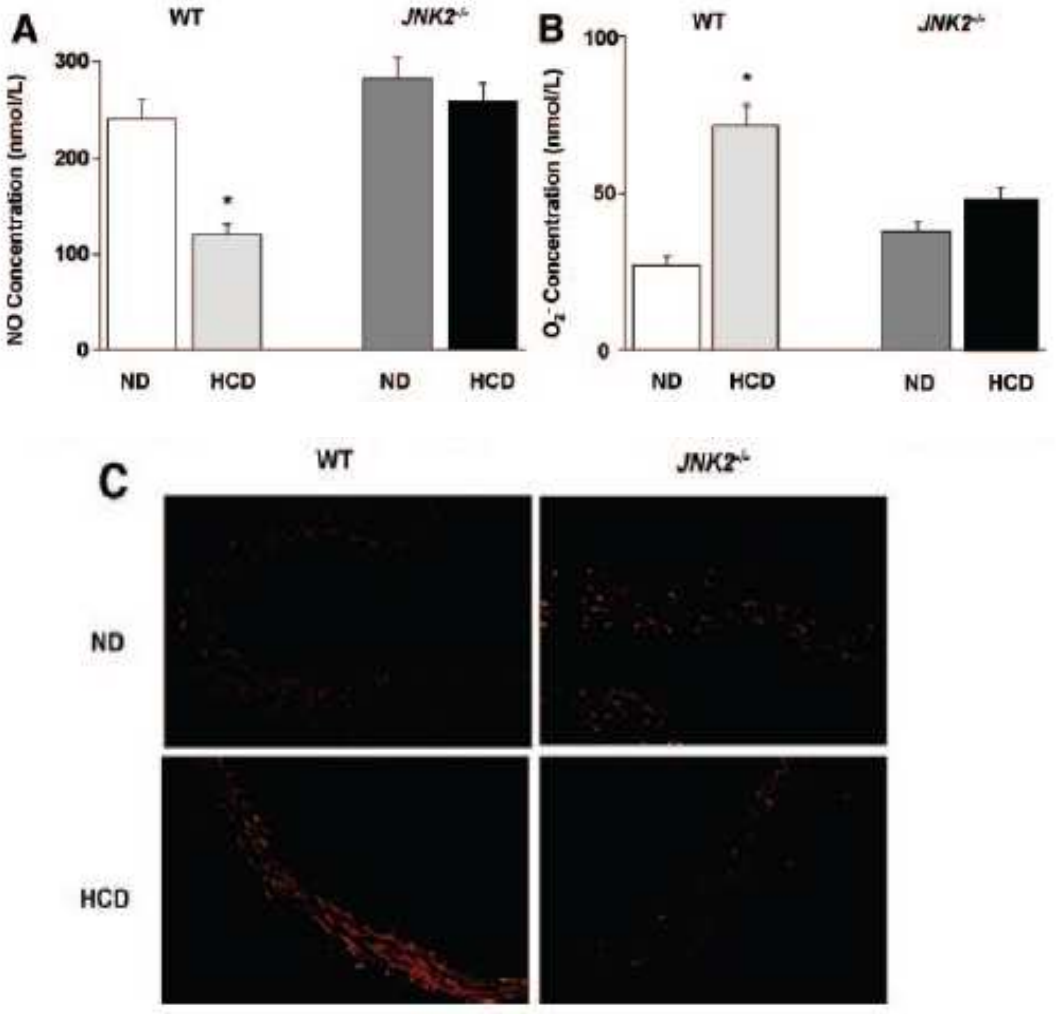

Figure 3. Bar graphs show the concentration of NO (A) and superoxide (O2-) (B) produced by a single aortic endothelial cell of WT and *JNK2-/-* mice after 14 weeks of ND or HCD. Peak concentrations were measured after stimulation with acetylcholine (10^{-7} mol/L). Results are presented as mean±SEM; n=4 to 6 in each group. **P*<0.05 vs WT ND. C, Similar results were obtained by fluorescence detection of O2- (red dihydroethidium staining) in freshly isolated aortic segments of WT and *JNK2-/-* mice after ND or HCD, respectively.

Figure 4

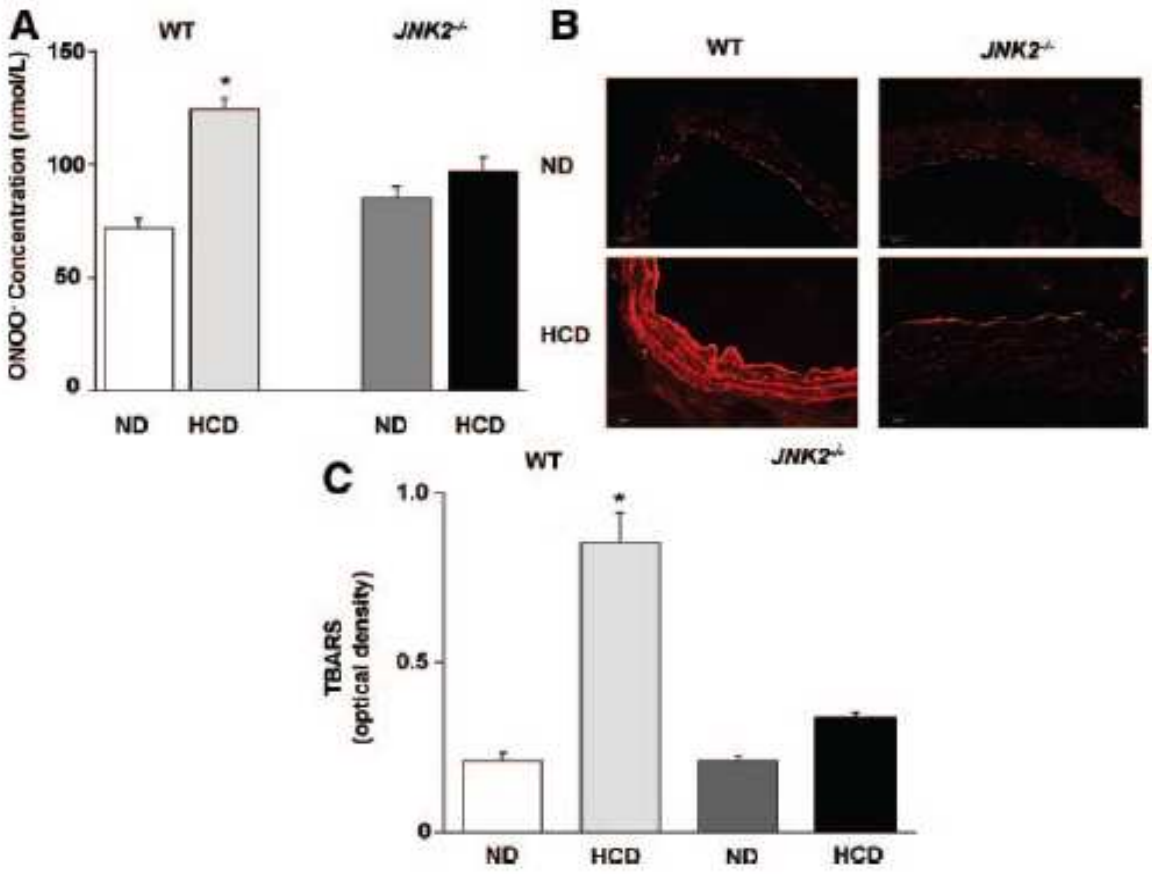

Figure 4. A, Bar graphs show peroxynitrite (ONOO-) concentration produced by a single aortic endothelial cell of WT and *JNK2-/-* mice after 14 weeks of ND or HCD. ONOO- was measured simultaneously with NO and O2- after stimulation with acetylcholine (10^{-7} mol/L). B, In aortas of WT and *JNK2-/-* mice after ND or HCD, immunostaining for nitrotyrosine (red staining) was detected in both the endothelium and in the media. C, Bar graphs show TBARS levels in aortas of WT and *JNK2-/-* mice after ND or HCD, respectively. Results are presented as mean±SEM; n=4 to 6 in each group. **P*<0.05 vs WT ND.

Figure 5

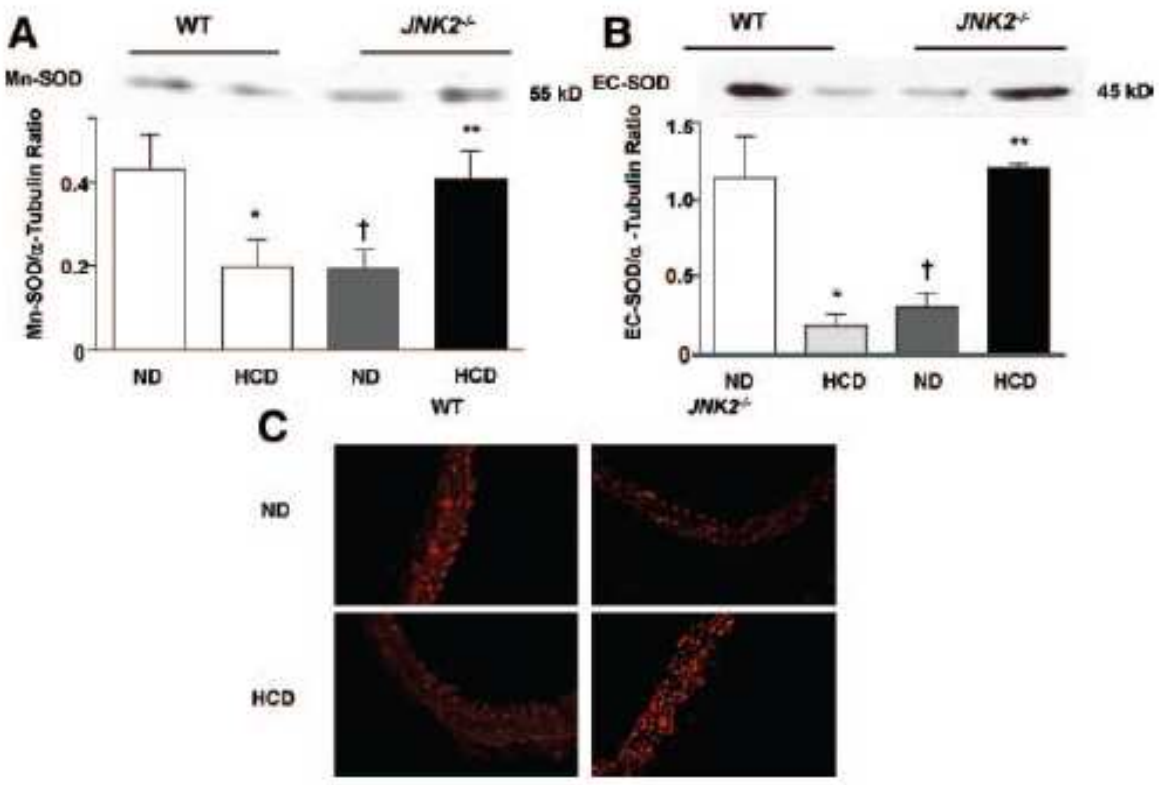

Figure 5. Mn-SOD (A) and EC-SOD (B)protein expression from aortas of WT and *JNK2-/-* mice after 14 weeks of ND or HCD. Representative Western blots and densitometric quantification are shown. Results are presented as mean±SEM of Mn-SOD and EC-SOD/α-tubulin expression ratio; n=4 to 6 in each group. **P*<0.05 vs ND WT; ***P*<0.05 vs *JNK2-/-* ND; †*P*<0.05 vs diet-matched WT. C, In aortas of WT and *JNK2-/-* mice after ND or HCD, immunostaining for Mn-SOD (red staining) was detected in both the endothelium and the media.

Figure 6

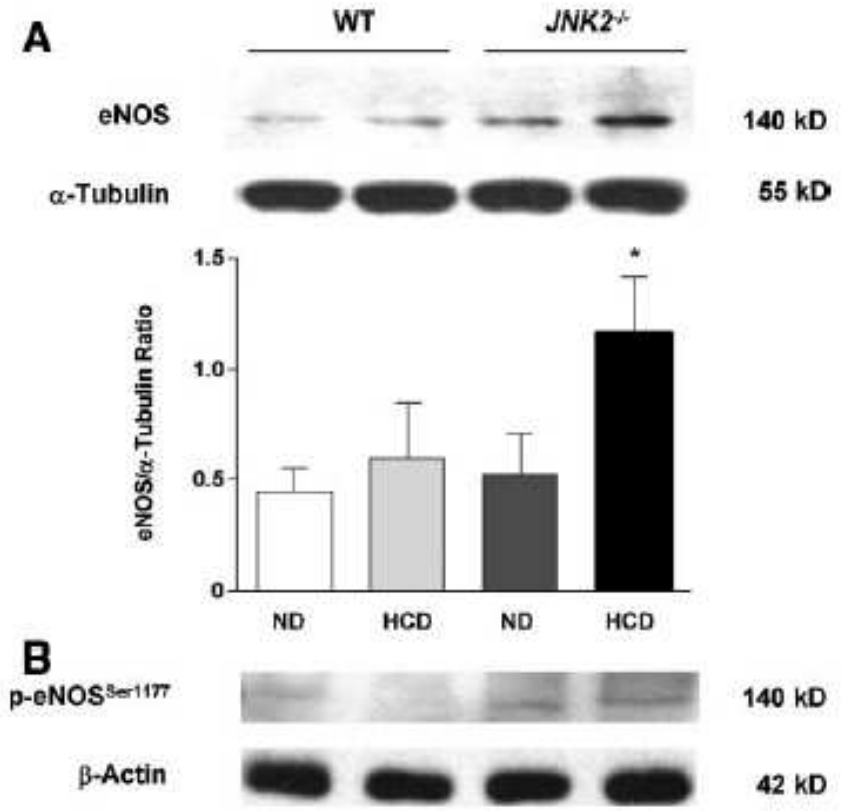

Figure 6. eNOS protein expression and phosphorylation in aortic lysates from WT and *JNK2-/-* mice after 14 weeks of ND or HCD. A, Representative Western blot and densitometric quantifications are shown for eNOS expression. Results are presented as mean±SEM of eNOS/α-tubulin expression ratio; n=4 to 6 in each group. **P*<0.05 for *JNK2-/-* HCD vs all other groups. B, Western blot of eNOS phosphorylation (pooled samples of n=3 mice in each group) with α-actin used as a loading control.

Inhibition of Protein Kinase Cβ Prevents Foam Cell Formation by Reducing Scavenger Receptor A Expression in Human Macrophages

Protein kinase C (PKC) comprises several structurally related serine/threonine kinases classified into 3 groups. The conventional or classic PKCs include PKCα, PKCβ1, PKCβ2, and PKCγ. These isoforms can be activated by Ca2+ and/or diacylglycerol, as well as by phorbol esters. The novel PKCδ, PKCε, and PKCθ also are activated by diacylglycerol and phorbol esters but are Ca2+ independent. The atypical PKCs, which include PKCζ and PKCι, are unresponsive to Ca2+/diacylglycerol and phorbol esters.[1] Particularly interesting is the modulation of PKC activity by phosphorylation of serine and threonine amino acid residues within its catalytic and regulatory domains.[2] Both conventional and novel PKC isoforms can translocate to the membranous compartment of the cell to elicit biological actions in the presence of diacylglycerol, the de novo synthesis of which is increased by hyperglycemia.[3] Indeed, the activation of PKC pathway, especially the PKCβ isoform, has been shown extensively to cause diabetic vascular dysfunction.[4–7] Because nonselective PKC inhibition is associated with lethal side effects, isoformspecific inhibitors have been developed. The macrocyclic bis (indolyl) maleimides like ruboxistaurin (LY333531), LY379196, LY317615, and LY290181 are competitive inhibitors of ATP binding sites within the PKC molecule.[8,9] The advantage of macrocyclic bis (indolyl) maleimides is their high selectivity for PKCβ compared with other isoforms of PKC.[10] Treatment of diabetic patients for 3 months with PKC412, a multitarget kinase inhibitor that also acts as a nonselective PKC inhibitor, resulted in significant gastrointestinal side effects such as nausea, vomiting, and diarrhea, as well as liver toxicity.[11] On the contrary, a multicenter, randomized clinical trial with the selective PKCβ inhibitor ruboxistaurin in patients with diabetic retinopathy revealed that its oral administration was well tolerated and did not cause any adverse events in patients with diabetes at doses up to 16 mg twice daily for 28 days.[12] Furthermore, in patients with type 1 and 2 diabetes and minimal retinopathy, retinal blood flow was increased by the PKCβ inhibitor in a dose-dependent fashion.[13] Treatment for >1 year with ruboxistaurin has shown beneficial effects in delaying the progression of diabetic nephropathy.[14] These studies provided the first demonstration that a PKCβ isoform–selective inhibitor can be used for long-term clinical treatment of diabetic microangiopathy with minimal side effects.[15] However, increasing evidence suggests that activation of PKCβ is involved in many mechanisms promoting atherosclerosis.[16] Interestingly,

phorbol 12-myristate 13-acetate (PMA), a structural analogue of diacylglycerol, which is a natural activator of PKC, can trigger transformation of monocytes to macrophages.[17] The accelerated atherosclerosis[18] and chronic activation of PKCβ in vascular tissues of diabetic patients, including the retina, heart, aorta, and circulating monocytes, [4,19,20] prompted us to hypothesize that, among all PKC isoforms, PKCβ could be involved in foam cell formation.

The present study was designed to investigate whether selective pharmacological inhibition of PKCβ prevents modified LDL uptake and hence foam cell formation. Our findings unmask an antiatherosclerotic effect of PKCβ inhibitors, extending their application far beyond diabetic vascular complications.

Methods

Cell Culture

Peripheral blood mononuclear cells were isolated from healthy control subjects by density centrifugation in BD Vacutainer cell preparation tubes with sodium heparin (Becton Dickinson, Franklin Lakes, NJ) and further purified by magnetic-activated cell separation sorting with anti–human CD14 antibody (Miltenyi Biotec, Cologne, Germany) conjugated with magnetic beads. After density centrifugation, highly purified monocytes were recovered. Human monocyte purity was assessed by flow cytometry (FACSCanto, BD, Heidelberg, Germany) using FITC-conjugated anti–human CD14 antibody (Miltenyi Biotec). The human monocytic THP-1 cell line was obtained from the American Type Culture Collection (Rockville, Md). Monocytes were cultured in RPMI 1640 medium containing 25 mmol/L HEPES buffer (supplemented with 10% FCS, 1% L-glutamine 200 mmol/L, penicillin 100 U/mL, and streptomycin 100 ug/mL) in humidified air, 5% CO2 at 37°C. Freshly isolated human monocytes and THP-1 monocytes were differentiated into monocyte-derived macrophages (MDMs) in vitro by treatment with 0.1 umol/L PMA (Calbiochem, Darmstadt, Germany) overnight in starvation medium, 0.5% FCS RPMI 1640. During starvation, the cells were exposed to LY379196 (10^{-6} mol/L), a nonselective inhibitor of both PKCβ isoforms, and CGP53353 (10^{-6} mol/L), a PKCβ2-selective inhibitor, and then incubated for another 24 hours in the presence of 10 ug/mL DiI-labeled acetylated low-density lipoprotein (DiI-acLDL) and DiI-labeled oxidized LDL (DiI-oxLDL) (Intracel, Frederick, Md). Human MDMs also were pretreated with myristoylated cell-permeable myr-PKC peptide (10^{-4} mol/L) based on the pseudosubstrate motif of PKCβ, which keeps the enzyme in an inactive state by interacting with the substrate binding site of PKCβ catalytic domain.[21] In another set of experiments, MDMs were pretreated with the 2 PKCβ inhibitors or myr-PKC and stimulated for 24 hours with 100 ng/mL lipopolysaccharide (Sigma,

Buchs, Switzerland). Afterward, tumor necrosis factor-α (TNFα) levels were measured in cell supernatant by ELISA (R&D Systems, Minneapolis, Minn). To exclude cytotoxicity, a colorimetric assay for detection of lactate dehydrogenase in cell supernatant was performed according to the manufacturer's recommendations (Roche, Basel, Switzerland).

siRNA Transfection

Transfections were performed with INTERFERin (Polyplus Transfection, Basel, Switzerland) according to the manufacturer's instructions in human MDMs (THP-1 cell line). Commercially available human PKCβ- and GAPDH- (Santa Cruz, Heidelberg, Germany) specific siRNAs were used for transfecting. The MDMs were transfected after 24 hours of seeding. INTERFERin transfection reagent (8 uL) was added to 100 uL OptiMEM serum-free medium containing 80 nmol/L of each siRNA oligo, incubated for 10 minutes, and added to the 3-cm plate containing 2 mL medium. GAPDH siRNA was used as a negative control. The FITC-labeled (Santa Cruz) control siRNA A was used as a marker for transfection efficiency. Gene silencing was measured after 48 hours by Western blotting. The transfected cells were incubated for an additional 24 hours in the presence of 10 ug/mL DiI-acLDL (Intracel), and acLDL uptake was measured by flow cytometry. Another set of transfected MDMs were used for Western blotting.

Real-Time Polymerase Chain Reaction

Total RNA was extracted from MDMs (THP-1 cell line) with Trizol reagent (Invitrogen, Basel, Switzerland) according to the manufacturer's recommendations. The total cellular RNA was converted to cDNA with Moloney murine leukemia virus reverse transcriptase and random hexamers (Amersham Bioscience, Otelfingen, Switzerland) in a final volume of 35 uL, using 4 ug cDNA according to the manufacturer's recommendations. Real-time polymerase chain reaction (PCR) was performed in a MX3000P PCR cycler (Stratagene, La Jolla, Calif). All PCR experiments were performed in triplicate using the SYBR Green JumpStart kit provided by Sigma. Each reaction (25 uL) contained 2 uL cDNA, 1 pmol of each primer, 0.25 uL internal reference dye, and 12.5 uL JumpStart Taq ReadyMix (containing buffer, dNTPs, stabilizers, SYBR Green, Taq polymerase, and JumpStart Taq antibody). The following primers were used: for scavenger receptor A (SR-A): sense primer, 5'-CCAGGGACATGGGAATGCAA–3'; antisense primer, 5'CAGTGGGACCTCGATCTCC–3'; and for human L28: sense primer, 5'GCATCTGCAATGGATGGT-3'; antisense primer, 5'–TGTTCTTGCGGATCATGTGT-3'. The amplification program consisted of 1 cycle at 95°C for 10 minutes, followed by 40 cycles

with a denaturing phase at 95°C for 30 seconds, an annealing phase of 1 minute at 60°C, and an elongation phase at 72°C for 1 minute. A melting curve analysis was performed after amplification to verify the accuracy of the amplicon. For verification of the correct amplification, PCR products were analyzed on an ethidium bromide–stained 1% agarose gel. In each real-time PCR run for F3 and L28, a calibration curve was included that was generated from serial dilutions ($2x10^7$, $2x10^6$, $2x10^5$, $2x10^4$, $2x10^3$, and $2x10^3$ copies per reaction for SR-A; $2x10^7$, $2x10^6$, $2x10^5$, $2x10^4$, $2x10^3$, and $2x10^3$ copies per reaction for L28) of purified amplicons for SR-A and L28.

Western Blotting

Human MDMs, THP-1 cell line, and freshly isolated blood monocytes (when indicated) were washed twice with PBS and harvested in the extraction buffer (120 mmol/L sodium chloride, 50 mmol/L Tris, 20 mmol/L sodium fluoride, 1 mmol/L benzamidine, 1 mmol/L DTT, 1 mmol/L EDTA, 6 mmol/L EGTA, 15 mmol/L sodium pyrophosphate, 0.8 ug/mL leupeptin, 30 mmol/L p-nitrophenyl phosphate, 0.1 mmol/L phenyl-methane-sulfonyl fluoride, and 1% NP-40) for immunoblotting. All cell debris was removed by centrifugation (12 000*g*) for 10 minutes at 4°C. The protein extracts (20 ug) were treated with 5x Laemmli's SDS-PAGE sample buffer (0.35 mol/L Tris-Cl, pH 6.8, 15% SDS, 56.5% glycerol, 0.0075% bromophenol blue), followed by heating at 99°C for 5 minutes, and then applied to 10% SDS–polyacrylamide gel for electrophoresis. The proteins were then transferred onto Immobilon-P filter papers (Millipore AG, Bedford, Mass) with a semidry transfer unit (Hoefer Scientific, San Francisco, Calif). The membranes were then blocked by use of 5% skim milk in TBS-Tween buffer (0.1% Tween 20, pH 7.5) for 1 hour and incubated overnight with anti–human SR-A (1:500, TransGenic, Kobe, Japan), anti–human lectin-like oxLDL receptor 1 (LOX-1; 1:4000, R&D Systems, Bad Nauheim, Germany), anti–phospho-Thr-642 PKCβ1 (1:1000, Biosource, Nivelles, Belgium), anti-PKCβ1 (1:1000, Santa Cruz), and anti-CD14 (1:1000, Dako Cytomation, Baar, Switzerland) antibodies in 0.5% BSA PBS. Antigen detection was performed with an enhanced chemiluminescence detection system (Amersham Biosciences, Otelfingen, Switzerland).

LDL Uptake Measurement by Flow Cytometry

After incubation with DiI-acLDL (10 ug/mL) and DiI-oxLDL (10ug/mL), human MDMs both freshly isolated and from the THP-1 cell line were subjected to flow cytometry to measure the amount of internalized LDL. Adherent and nonadherent cells were harvested by gentle scraping.

Cells were then washed twice with PBS and resuspended in 0.2% BSA in PBS. Samples were analyzed with the FACScanto II flow cytometer and Flowjo software.

Measurements of Superoxide Anion Production

Superoxide production in MDMs, both freshly isolated and from the THP-1 cell line, treated with LY379196 (10^{-6} mol/L) and silencing of PKCβ was determined by electron spin resonance spectroscopy analysis using the spin trap CM-H (1-hydroxy-3-methoxycarbonyl-2,2,5,5-tetramethylpyrrolidine, Noxygen, Elzach, Germany) as described previously.22 In brief, MDMs were centrifuged (380*g* for 5 minutes) and resuspended in Krebs-HEPES buffer (pH 7.35) containing diethyldithiocarbamate (5 umol/L) and deferoxamine (25 umol/L). Electron spin resonance spectra were recorded using a Bruker e-scan electron spin resonance spectrometer (Bruker Corp, Faellenden, Switzerland) after the addition of the spin trap CM-H (200 umol/L) under stable temperature conditions (37°C; temperature-controlled system). The electron spin resonance instrumental settings were as follows: center field, 3495 G; field sweep width, 10.000 G; microwave frequency, 9.75 GHz; microwave power, 19.91 mW; magnetic field modulation frequency, 86.00 kHz; modulation amplitude, 2.60 G; conversion time, 10.24 ms; detector time constant, 328 ms; and number of x scans, 10.

Confocal Fluorescent Microscopy

Human MDMs were washed once with PBS, fixed in 4% paraformaldehyde for 10 minutes, washed again with PBS, blocked with 0.1 mol/L glycine for 5 minutes, permeabilized with 0.2% Triton 100 for 7 minutes, and incubated overnight with anti–human SR-A (Trans-Genic), anti-PKCβ1 (Biosource), anti-PKCβ2 (Biosource), or anti-CD68 (Dako Cytomation) antibody in 0.2% BSA. Afterward, the cells were washed 3 times with PBS and incubated with secondary Alexa Fluor 488–labeled antibody (Molecular Probes, Eugene, Ore) in 0.2% BSA for 1 hour. Cells were counterstained with 4', 6 diamidino-2-phenylindol (DAPI; Vector Laboratories, Burlingame, Calif) and analyzed with a Leica confocal laser microscope.

Drugs

LY379196 was provided by Eli Lilly (Indianapolis, Ind). CGP53353 was kindly provided by Dr Doriano Fabbro (Novartis Pharma AG, Basel, Switzerland). Calphostin C, PMA, and myr-PKC were purchased from Calbiochem. Lipopolysaccharide was obtained from Sigma.

Statistical Analysis

Results are expressed as mean±SEM, and n indicates the number of experiments. Statistical evaluation of the data was performed with Student's *t* test for simple comparisons between 2 values when appropriate. For multiple comparisons, results were analyzed by ANOVA followed by Fisher's exact test. A value of $P<0.05$ was considered statistically significant. The authors had full access to and take full responsibility for the integrity of the data. All authors have read and agree to the manuscript as written.

Results

Role of PKCβ in Mediating Human MDM Foam Cell Formation

The differentiation of human primary monocytes and monocytic THP-1 cell line into macrophages (MDMs) was induced by PMA (0.1 umol/L). Incubation of human MDMs with DiI-acLDL (10 ug/mL) led to binding of acLDL to the plasma membrane and accumulation of lipoproteins into the cytoplasm as assessed by fluorescence microscopy (Figure 1A). The nonselective inhibitor of both PKCβ isoforms, LY379196 (10^{-6} mol/L), abolished acLDL uptake in MDMs as shown in Figure 1B. To identify the isoform of PKCβinvolved, human MDMs were exposed to selective antibodies against PKCβ1 and PKCβ2. PKCβ isoforms were localized in the nucleus and in the cytoplasm of MDMs, showing an activated state of the enzyme. The PKCβ1 isoform was distributed homogeneously within the cytoplasm and plasma membrane (Figure 1C), whereas PKCβ2 was present in the perinuclear patch and plasma membrane (Figure 1D). Accordingly, LY379196 showed a dose-dependent decrease in both acLDL and oxLDL uptake in MDMs by flow cytometry (Figure 2A and 2B). In contrast, the selective inhibitor of PKCβ2, CGP53353, did not exert any significant effect (data not shown).

Effect of PKCβ Inhibition on SR-A Expression

To delineate the molecular mechanism by which LY379196 blunted modified LDL uptake, MDM gene and protein expression of SR-A was determined. Quiescent cells did not express SR-A mRNA; stimulation with PMA (0.1 umol/L) increased SR-A expression (Figure 3). A more pronounced upregulation of SR-A expression was achieved by the addition of acLDL (10 ug/mL) to the medium. SR-A mRNA expression was abolished by treatment with LY379196 (10^{-6} mol/L), whereas CGP53353 (10^{-6} mol/L) did not exert any inhibitory effect on PMA/acLDL-induced SR-A expression in human MDMs (Figure 3). In agreement with these results, SR-A protein expression was increased after exposure to acLDL as and oxLDL (Figure

4A and 4B). Treatment with LY379196, but not with CGP53353, totally abrogated PMA/acLDL-induced macrophage SR-A expression (Figure 4A). MDMs exposed to oxLDL in the presence of LY379196 (10^{-6} mol/L) showed similar results (Figure 4B). A myristoylated cellpermeable myr-PKC inhibitory peptide was used to confirm the modulatory role of PKCβ on SR-A expression. Like LY379196, the inhibitory peptide myr-PKC (10^{-4} mol/L) significantly blunted SR-A protein expression in human MDMs (Figure 4C). In contrast to SR-A, LOX-1 protein expression did not change after exposure of MDMs to modified LDL. Furthermore, LY379196 (10^{-6} mol/L) did not exert any significant effect on LOX-1 expression (Figure 4D).

SR-A Expression

The transfection of PKCβ siRNA into MDMs resulted in reduced expression of the protein, whereas the GAPDH and mock controls did not exert any significant effect (Figure 5A). Using flow cytometry, we examined the DI-acLDL uptake by the transfected cells. PKCβ silencing reduced the uptake and blunted SR-A protein expression, reproducing the same effect as the pharmacological inhibitor LY379196 (Figure 5B and 5C).

Role of Thr-642 Phosphorylation in PKCβ1-Mediated SR-A Expression

Western blotting with an antibody against phosphorylated PKCβ1 at a specific amino residue revealed that incubation of the cells with PMA/acLDL increased Thr-642 phosphorylation within the catalytic domain of this molecule (Figure 6). The inhibitor of both PKCβ isoforms, LY379196 (10^{-6} mol/L), and the inhibitory peptide myr-PKC (10^{-4} mol/L) blunted PMA/acLDL-induced Thr-642 phosphorylation (Figure 6), suggesting that phosphorylation of PKCβ1 at Thr-642 may thus represent a selective regulatory mechanism for SR-A upregulation. Accordingly, the selective PKCβ2 inhibitor, CGP53353 (10^{-6} mol/L), did not affect Thr-642 phosphorylation (Figure 6).

Effect of PKCβ Inhibition on Macrophage Activation and Functioning

As shown by confocal microscopy, high levels of SR-A expression in MDMs stimulated with acLDL were blunted in the presence of LY379196 (Figure 7A and 7B). However, LY379196 did not exert any effect on the expression of CD68, a marker of macrophage activation (Figure 7C and 7D). In addition, human MDMs were exposed to lipopolysaccharide (100 ng/mL) to rule out an effect of PKCβ inhibition on macrophage functioning in innate immunity.

Lipopolysaccharide elicited degradation of CD14 and secretion of TNFα, crucial steps in the activation of innate immunity (Figure 8A and 8B). Interestingly enough, increasing concentrations of LY379196 did not inhibit either lipopolysaccharide-induced CD14 degradation (Figure 8A) or TNFα release (Figure 8B). Treatment with LY379196 did not elicit any release of lactate dehydrogenase (data not shown), ruling out that its effects on human MDMs were due to cellular toxicity. In agreement with this finding, no apoptotic nuclei by DAPI staining were observed (Figure 7). Furthermore, the effect of LY379196 (10^{-6} mol/L) on the ability of macrophages to produce superoxide anion (O2-) was measured. No significant changes in O2- production were observed (Figure 8C). In addition, silencing of PKCβ did not affect O2- production (data not shown).

Discussion

Accumulation of cholesterol-loaded foam cells in the arterial intima is a hallmark and key event of early atherogenesis.[23] Circulating monocytes adhere to activated endothelial cells and transmigrate into the subintima to become tissue macrophages. On exposure to modified lipoproteins such as the oxLDL and acLDL, these macrophages become foam cells.[24] Two receptors appear to be essential in foam cell formation and receptor-mediated binding/uptake of modified lipoproteins: CD36 and SR-A.[25] Despite increasing evidence supporting that PKC is involved in many mechanisms promoting atherosclerosis,[16] only a few studies have examined the role of PKC signaling in foam cell formation.[20,26] In this study, we demonstrated that inhibition of PKCβprevents uptake of modified LDL by reducing human MDM SR-A expression. Several lines of evidence support this conclusion. First, fluorescent-activated cell sorter analysis revealed that the nonselective inhibitor of PKCβ isoforms blunted modified LDL uptake of human MDMs. Second, silencing of PKCβ by siRNA transfection also reduced LDL uptake. Third, we observed a selective Thr-642 phosphorylation within the catalytic domain of PKCβ1 and an increase in SR-A mRNA and protein expression in human MDMs exposed to modified LDL. Fourth, both LY379196 and the inhibitory peptide myr-PKC blunted phosphorylation of Thr-642 and upregulation of SR-A. In contrast, CGP53353, the selective inhibitor of PKCβ2,7 did not exert any significant effect. Expression and function of macrophage SR-A play a crucial role in the pathogenesis of atherosclerosis.[27,28] Accordingly, SR-A gene– deficient mice bred with atherosclerosis-prone *ApoE -/-* or *LDLrec-/-* mice have been found to develop less atherosclerosis.[29] We recently showed that *ApoE-/-* mice simultaneously lacking c-Jun N-terminal kinase 2 (*ApoE-/-/JNK2-/-* mice) developed less

atherosclerosis than *ApoE-/-* mice.[30] Macrophages lacking c-Jun N-terminal kinase 2 displayed markedly decreased phosphorylation of SR-A and hence suppressed foam cell formation.[30] Thus, upstream signaling molecules that regulate the expression and function of SR-A may represent potential targets for therapeutic interventions.[24] The present findings clearly indicate that SR-A expression in human MDMs is regulated by PKCβ. In contrast to SR-A, LOX-1 expression did not change after stimulation of MDMs with modified LDL. Furthermore, LY379196 did not exert any significant effect on LOX-1. Because SR-A expression was enhanced on modified LDL stimulation and not LOX-1, we conclude that SR-A might be the primary receptor for modified LDL uptake. Several studies have strongly implicated activation of PKCβ in the pathogenesis of the vascular complications of diabetes.[31] The synthesis of isoform-specific inhibitors for PKCβ has provided not only important insights into diabetic cardiovascular disease but also effective drugs against diabetic microvascular complications.[15,32,33] Glucose-induced activation of PKCβ may lead to endothelial dysfunction by causing activation of vascular NADPH oxidase, endothelial nitric oxide synthase uncoupling, and reactive oxygen species production.[6,34] Furthermore, high glucose enhances human macrophage LOX-1 expression via PKCβ activation.[20] Treatment with a PKCβ inhibitor prevents impaired endotheliumdependent vasodilation caused by hyperglycemia.[5] We demonstrated that selective inhibition of PKCβ2 inhibits glucose-induced vascular cellular adhesion molecule-1 expression in human endothelial cells.[7] Interestingly enough, our data unmask an antiatherosclerotic effect of PKCβ inhibitors even in the nondiabetic condition of hypercholesterolemia. Specific siRNA-mediated knockdown of PKCβ further supports our conclusion. Indeed, on silencing of PKCβ, LDL uptake was blunted, SR-A expression was reduced, and hence foam cell formation was prevented. The molecular link between the PKCβ signaling pathway, SR-A upregulation, and uptake of modified LDL might involve Thr-642 phosphorylation within the catalytic domain of PKCβ1. Indeed, inhibition of PKCβ by either LY379196 or the inhibitory peptide myr-PKC blunting PMA/acLDLinduced Thr-642 phosphorylation abolished upregulation of SR-A and LDL uptake of human MDMs. In contrast, the selective inhibitor of PKCβ2, CGP53353, did not affect any of these events. According to our results, phosphorylation of PKCβ1 at Thr-642 represents a selective regulatory mechanism for SR-A upregulation and foam cell formation. Of particular interest is the fact that in our study LY379196, as a drug targeting macrophages, prevented only foam cell formation without affecting macrophage host defense activity. Indeed, LY379196 blunted modified LDL uptake but did not affect the expression of CD68, a marker of macrophage activation.[35] We also

demonstrated that LY379196 did not inhibit lipopolysaccharide-induced CD14 degradation or TNFα release in human MDMs. Moreover, PKCβ knockdown or inhibition did not affect superoxide anion production. These findings rule out any effect of PKCβinhibition on macrophage functioning in innate immunity. In agreement with our results, PKCβ-deficient mice have not been reported to present any impairment in macrophage activity.[36] Although these mice show a reduced peritoneal population of B-1 lymphocytes, the absolute number of splenic B cells is similar to wild-type animals. Furthermore, the thymuses of PKCβ-deficient mice were of normal size and cellularity and contained CD4+CD8+ double-positive cells and CD4+ or CD8+ single-positive cells at normal ratios.[36] Earlier studies of the role of vascular PKCβ activation in diabetes were focused primarily on microvascular dysfunction. [37,38] Indeed, PKCβ inhibitors are currently being tested in clinical trials with microvascular end points.[12–14]

Conclusions

The results of our study suggest a role for PKCβ in atherogenesis even in the nondiabetic condition and anticipate the application of PKCβ inhibitors as putative antiatherosclerotic drugs. However, before deciding whether PKCβ inhibitors deserve to be tested in clinical trials of atherosclerosis, animal models will help evolve our current suggestive in vitro evidence concerning a proatherosclerotic role of PKCβ signaling.

Acknowledgment

We would like to thank Dr Anna Bogdanova for helping with superoxide anion measurements.

Sources of Funding

This work was supported in part by Swiss National Research Foundation grants 310000108463 (to Dr Cosentino) and 3100068118.02 (to Dr Lüscher) and a grant from the Swiss Heart Foundation (to Dr Kouroedov).

Disclosures

None.

References

1. Ron D, Kazanietz MG. New insights into the regulation of protein kinase C and novel phorbol ester receptors. *FASEB J*. 1999;13:1658 –1676.

2. Edwards AS, Faux MC, Scott JD, Newton AC. Carboxyl-terminal phosphorylation regulates the function and subcellular localization of protein kinase C betaII. *J Biol Chem*. 1999;274:6461– 6468.

3. Sheetz MJ, King GL. Molecular understanding of hyperglycemia's adverse effects for diabetic complications. *JAMA*. 2002;288:2579 –2588.

4. Inoguchi T, Battan R, Handler E, Sportsman JR, Heath W, King GL. Preferential elevation of protein kinase C isoform beta II and diacylglycerol levels in the aorta and heart of diabetic rats: differential reversibility to glycemic control by islet cell transplantation. *Proc Natl Acad Sci U S A*. 1992;89:11059 –11063.

5. Beckman JA, Goldfine AB, Gordon MB, Garrett LA, Creager MA. Inhibition of protein kinase Cbeta prevents impaired endotheliumdependent vasodilation caused by hyperglycemia in humans. *Circ Res*. 2002;90:107–111.

6. Cosentino F, Eto M, De Paolis P, van der Loo B, Bachschmid M, Ullrich V, Kouroedov A, Delli Gatti C, Joch H, Volpe M, Luscher TF. High glucose causes upregulation of cyclooxygenase-2 and alters prostanoid profile in human endothelial cells: role of protein kinase C and reactive oxygen species. *Circulation*. 2003;107:1017–1023.

7. Kouroedov A, Eto M, Joch H, Volpe M, Luscher TF, Cosentino F. Selective inhibition of protein kinase Cbeta2 prevents acute effects of high glucose on vascular cell adhesion molecule-1 expression in human endothelial cells. *Circulation*. 2004;110:91–96.

8. Birch KA, Heath WF, Hermeling RN, Johnston CM, Stramm L, Dell C, Smith C, Williamson JR, Reifel-Miller A. LY290181, an inhibitor of diabetes-induced vascular dysfunction, blocks protein kinase C-stimulated transcriptional activation through inhibition of transcription factor binding to a phorbol response element. *Diabetes*. 1996;45:642–650.

9. Faul MM, Gillig JR, Jirousek MR, Ballas LM, Schotten T, Kahl A, Mohr M. Acyclic N-(azacycloalkyl)bisindolylmaleimides: isozyme selective inhibitors of PKCbeta. *Bioorg Med Chem Lett*. 2003;13:1857–1859.

10. Jirousek MR, Gillig JR, Gonzalez CM, Heath WF, McDonald JH 3rd, Neel DA, Rito CJ, Singh U, Stramm LE, Melikian-Badalian A, Baevsky M, Ballas LM, Hall SE, Winneroski LL, Faul MM. (S)-13-[(dimethylamino) methyl]-10,11,14,15-tetrahydro-4,9:16, 21-dimetheno-1H,13Hdibenzo[e,k]pyrrolo[3,4-h][1,4,13]oxadiazacyclohexadecene-1,3(2H)-dione (LY333531) and related analogues: isozyme selective inhibitors of protein kinase C beta. *J Med Chem*. 1996;39:2664 –2671.

11. Campochiaro PA, for the C99-PKC412–003 Study Group. Reduction of diabetic macular edema by oral administration of the kinase inhibitor PKC412. *Invest Ophthalmol Vis Sci*. 2004;45:922–931.

12. PKC-DRS Study Group. The effect of ruboxistaurin on visual loss in patients with moderately severe to very severe nonproliferative diabetic retinopathy: initial results of the Protein Kinase C Beta Inhibitor Diabetic Retinopathy Study (PKC-DRS) multicenter randomized clinical trial. *Diabetes*. 2005;54:2188 –2197.

13. Aiello LP, Clermont A, Arora V, Davis MD, Sheetz MJ, Bursell SE. Inhibition of PKC beta by oral administration of ruboxistaurin is well tolerated and ameliorates diabetes-induced retinal hemodynamic abnormalities in patients. *Invest Ophthalmol Vis Sci*. 2006;47:86 –92.

14. Tuttle KR, Bakris GL, Toto RD, McGill JB, Hu K, Anderson PW. The effect of ruboxistaurin on nephropathy in type 2 diabetes. *Diabetes Care*. 2005;28:2686 –2690. 15. Vinik A. The protein kinase C-beta inhibitor, ruboxistaurin, for the treatment of diabetic microvascular complications. *Expert Opin Investig Drugs*. 2005;14:1547–1559.

16. Rask-Madsen C, King GL. Proatherosclerotic mechanisms involving protein kinase C in diabetes and insulin resistance. *Arterioscler Thromb Vasc Biol*. 2005;25:487– 496.

17. Llaverias G, Noe V, Penuelas S, Vazquez-Carrera M, Sanchez RM, Laguna JC, Ciudad CJ, Alegret M. Atorvastatin reduces CD68, FABP4, and HBP expression in oxLDL-treated human macrophages. *Biochem Biophys Res Commun*. 2004;318:265–274.

18. Beckman JA, Creager MA, Libby P. Diabetes and atherosclerosis: epidemiology, pathophysiology, and management. *JAMA*. 2002;287:2570–2581.

19. Idris I, Gray S, Donnelly R. Protein kinase C activation: isozyme-specific effects on metabolism and cardiovascular complications in diabetes. *Diabetologia*. 2001;44:659–673.

20. Li L, Sawamura T, Renier G. Glucose enhances human macrophage LOX-1 expression: role for LOX-1 in glucose-induced macrophage foam cell formation. *Circ Res*. 2004;94:892–901.

21. Ward NE, O'Brian CA. Inhibition of protein kinase C by N-myristoylated peptide substrate analogs. *Biochemistry*. 1993;32:11903–11909.

22. Spiekermann S, Landmesser U, Dikalov S, Gamez G, Tatge H, Hornig B, Drexler H, Harrison DG. Electron spin resonance characterization of vascular NAD(P)H- and xanthine-oxidase-activity in patients with coronary artery disease: relation to endothelium-dependent vasodilation. *Circulation*. 2003;107:1383–1389.

23. Osterud B, Bjorklid E. Role of monocytes in atherogenesis. *Physiol Rev*. 2003;83:1069 –1112.

24. Li AC, Glass CK. The macrophage foam cell as a target for therapeutic intervention. *Nat Med*. 2002;8:1235–1242.

25. Kunjathoor VV, Febbraio M, Podrez EA, Moore KJ, Andersson L, Koehn S, Rhee JS, Silverstein R, Hoff HF, Freeman MW. Scavenger receptors class A-I/II and CD36 are the principal receptors responsible for the uptake of modified low density lipoprotein leading to lipid loading in macrophages. *J Biol Chem*. 2002;277:49982– 49988.

26. Feng J, Han J, Pearce SF, Silverstein RL, Gotto AM Jr, Hajjar DP, Nicholson AC. Induction of CD36 expression by oxidized LDL and IL-4 by a common signaling pathway dependent on protein kinase C and PPAR-gamma. *J Lipid Res*. 2000;41:688–696.

27. Steinberg D, Parthasarathy S, Carew TE, Khoo JC, Witztum JL. Beyond cholesterol: modifications of low-density lipoprotein that increase its atherogenicity. *N Engl J Med*. 1989;320:915–924.

28. Kosswig N, Rice S, Daugherty A, Post SR. Class A scavenger receptormediated adhesion and internalization require distinct cytoplasmic domains. *J Biol Chem*. 2003;278:34219 –34225.

29. Lessner SM, Prado HL, Waller EK, Galis ZS. Atherosclerotic lesions grow through recruitment and proliferation of circulating monocytes in a murine model. *Am J Pathol*. 2002;160:2145–2155.

30. Ricci R, Sumara G, Sumara I, Rozenberg I, Kurrer M, Akhmedov A, Hersberger M, Eriksson U, Eberli FR, Becher B, Boren J, Chen M, Cybulsky MI, Moore KJ, Freeman MW, Wagner EF, Matter CM, Luscher TF. Requirement of JNK2 for scavenger receptor A-mediated foam cell formation in atherogenesis. *Science*. 2004;306:1558 –1561.

31. Creager MA, Luscher TF, Cosentino F, Beckman JA. Diabetes and vascular disease: pathophysiology, clinical consequences, and medical therapy, part I. *Circulation*. 2003;108:1527–1532.

32. Koya D, Haneda M, Nakagawa H, Isshiki K, Sato H, Maeda S, Sugimoto T, Yasuda H, Kashiwagi A, Ways DK, King GL, Kikkawa R. Amelioration of accelerated diabetic mesangial expansion by treatment with a PKC beta inhibitor in diabetic db/db mice, a rodent model for type 2 diabetes. *FASEB J*. 2000;14:439–447.

33. Avignon A, Sultan A. PKC-B inhibition: a new therapeutic approach for diabetic complications? *Diabetes Metab*. 2006;32:205–213.

34. Inoguchi T, Li P, Umeda F, Yu HY, Kakimoto M, Imamura M, Aoki T, Etoh T, Hashimoto T, Naruse M, Sano H, Utsumi H, Nawata H. High glucose level and free fatty acid stimulate reactive oxygen species production through protein kinase C–dependent activation of NAD(P)H oxidase in cultured vascular cells. *Diabetes*. 2000;49:1939 –1945.

35. Gordon S. Macrophage-restricted molecules: role in differentiation and activation. *Immunol Lett*. 1999;65:5– 8.

36. Leitges M, Schmedt C, Guinamard R, Davoust J, Schaal S, Stabel S, Tarakhovsky A. Immunodeficiency in protein kinase Cbeta-deficient mice. *Science*. 1996;273:788 –791.

37. Ishii H, Jirousek MR, Koya D, Takagi C, Xia P, Clermont A, Bursell SE, Kern TS, Ballas LM, Heath WF, Stramm LE, Feener EP, King GL. Amelioration of vascular dysfunctions in diabetic rats by an oral PKC beta inhibitor. *Science*. 1996;272:728 –731.

38. Idris I, Gray S, Donnelly R. Protein kinase C-beta inhibition and diabetic microangiopathy: effects on endothelial permeability responses in vitro. *Eur J Pharmacol*. 2004;485:141–144.

Figures and table

Figure 1

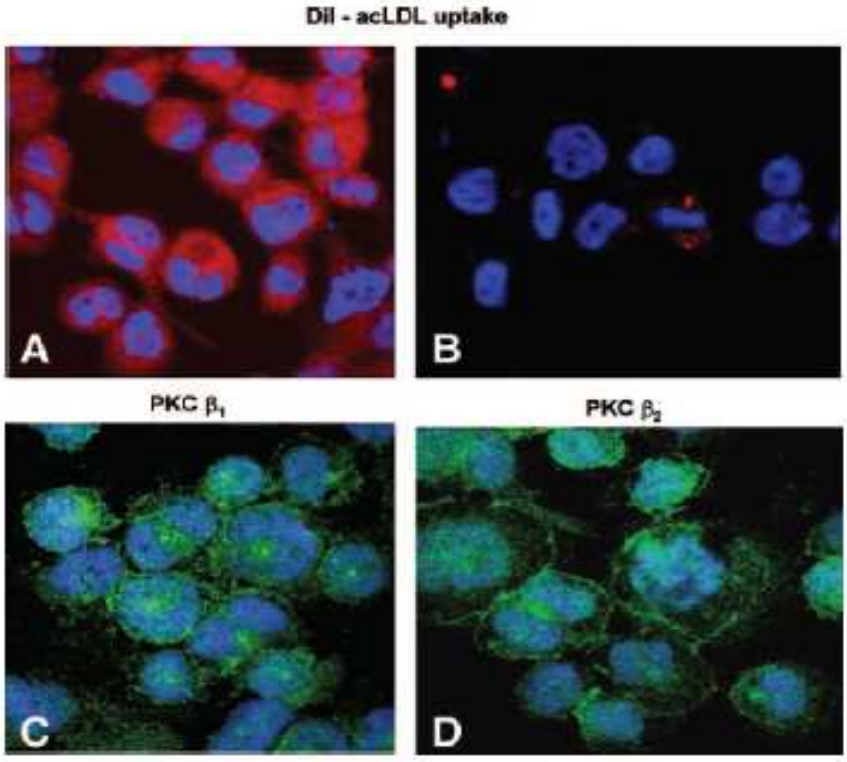

Figure 1. A, Fluorescent confocal microscopy of human MDMs after incubation with DiI-acLDL. Red particles in the cytoplasm represent internalized DiI-acLDL. B, LY379196 ($5x10^{-6}$ mol/L) abolished modified LDL uptake. In human MDMs, green staining shows intracellular distribution of PKCβ1 (C) and PKCβ2 (D). Nuclei stained blue with DAPI.

Figure 2

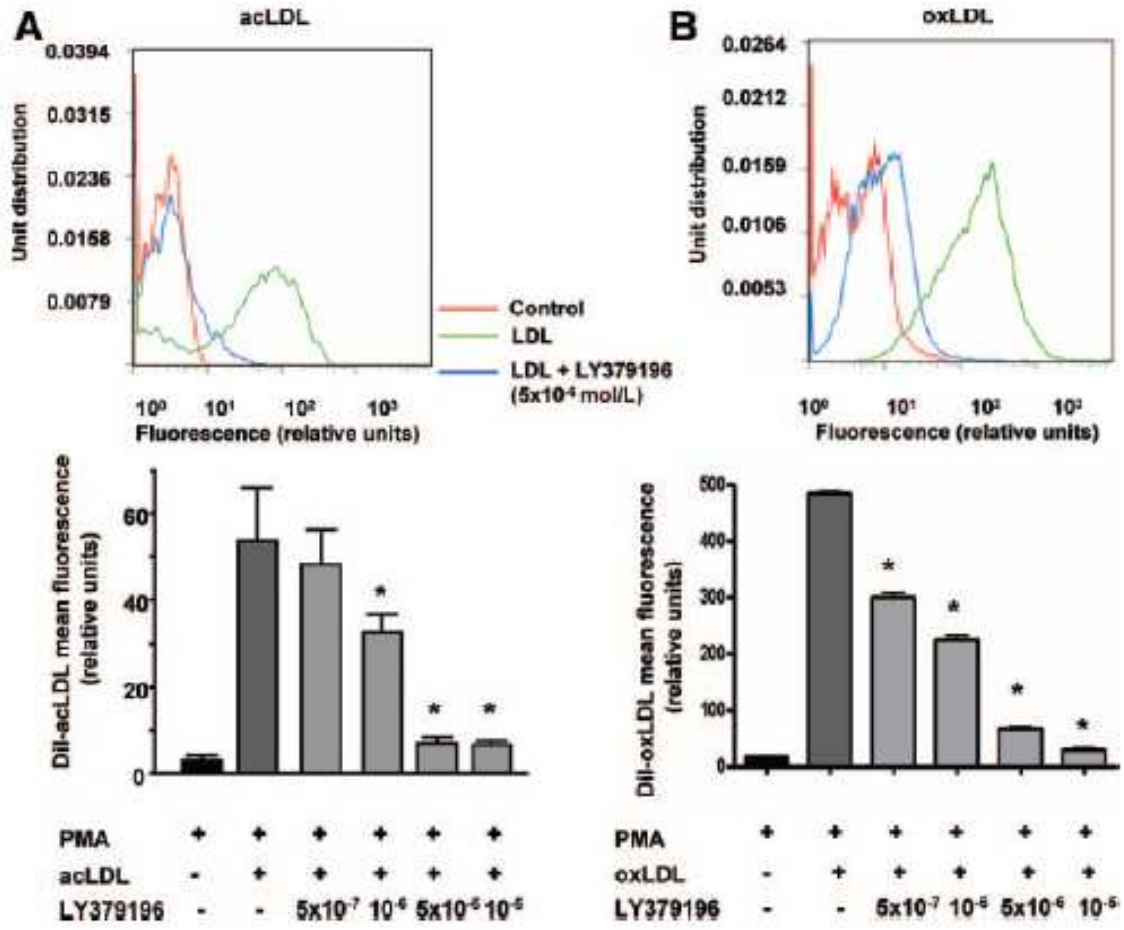

Figure 2. Fluorescent-activated cell sorter analysis of human MDMs in the presence or absence of LY379196 after 24 hours of incubation with DiI-acLDL (A) and DiIoxLDL (B). LY379196 ($5x10^{-6}$ mol/L) blunted modified LDL uptake (blue). CGP53353 did not show any significant effect (data not shown). LY379196 exerted a dose-dependent inhibition of acLDL (A) and oxLDL (B) uptake. Results are presented as mean±SEM; n=4 in each group. **P*<0.05 vs PMA plus acLDL or oxLDL.

Figure 3

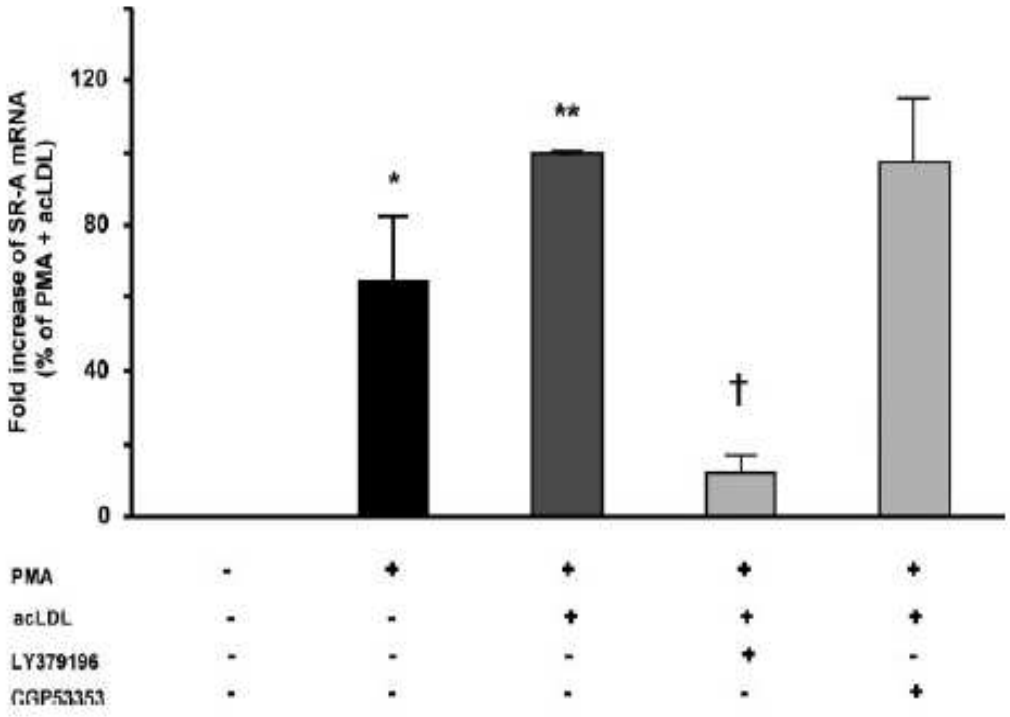

Figure 3. Expression of SR-A in PMA-induced human MDMs and after incubation with acLDL in the presence and absence of LY379196 (10^{-6} mol/L) or CGP53353 (10^{-6} mol/L). SR-A mRNA expression assessed by real-time PCR is normalized to L28 mRNA. Results are presented as mean±SEM; n=3 in each group. *P<0.05 vs control; **P<0.05 vs PMA alone; †P<0.05 vs PMA plus acLDL.

Figure 4

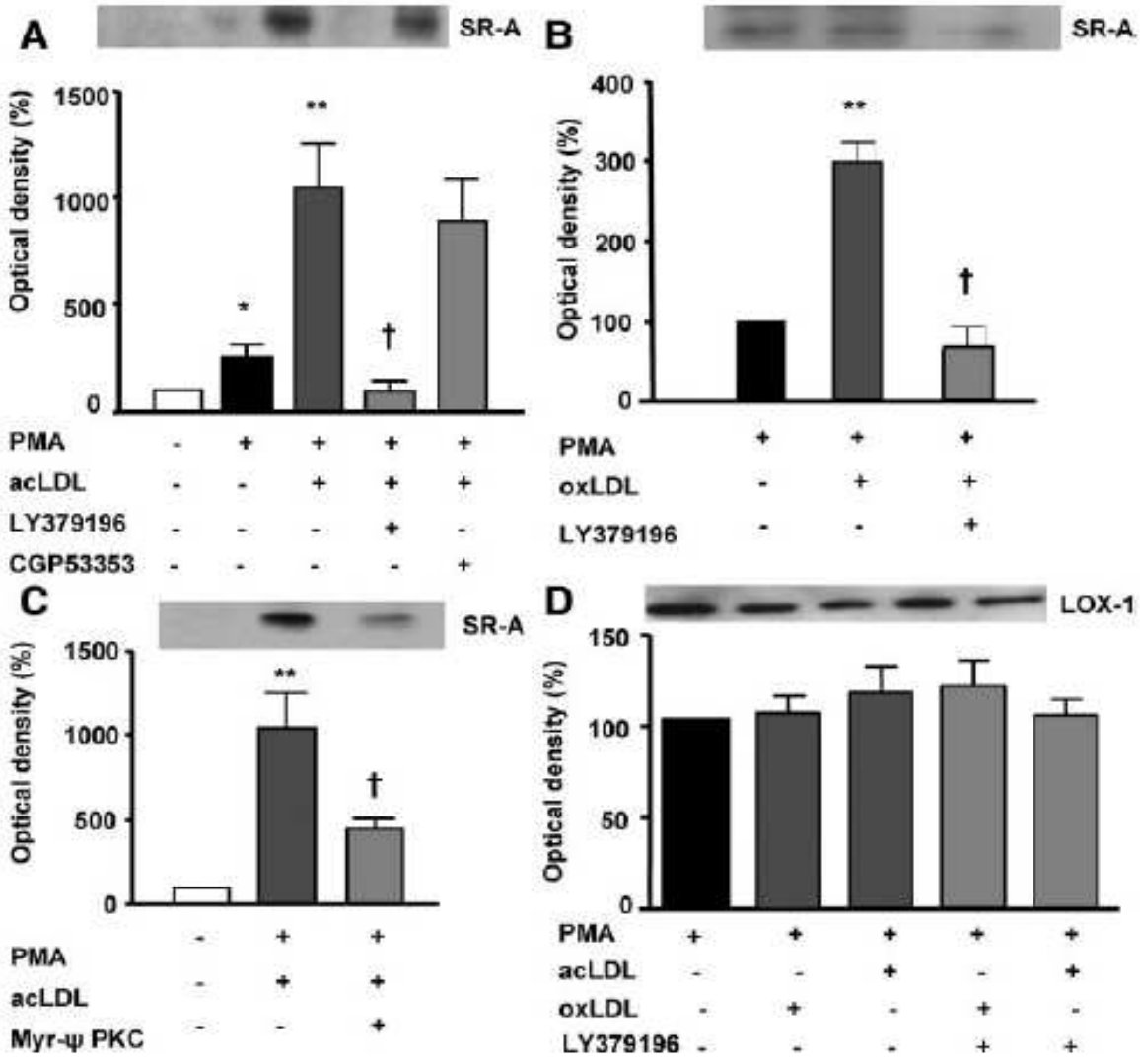

Figure 4. Representative Western blot and densitometric quantification of SR-A protein expression in PMA-induced human MDMs and after incubation with acLDL (A) and oxLDL (B) in the presence and absence of LY379196 (10^{-6} mol/L) or CGP53353 (10^{-6} mol/L). C, The inhibitory effect of myristoylated cell-permeable peptide, myr-PKC, on SR-A protein expression in PMA-induced human MDMs after incubation with acLDL. D, LOX-1 protein expression in PMA-induced human MDMs and after incubation with acLDL and oxLDL in the presence and absence of LY379196. Results are presented as mean±SEM; n=4 in each group. **P*<0.05 vs control; ***P*<0.05 vs PMA alone; †*P*<0.05 vs PMA plus acLDL or oxLDL.

Figure 5

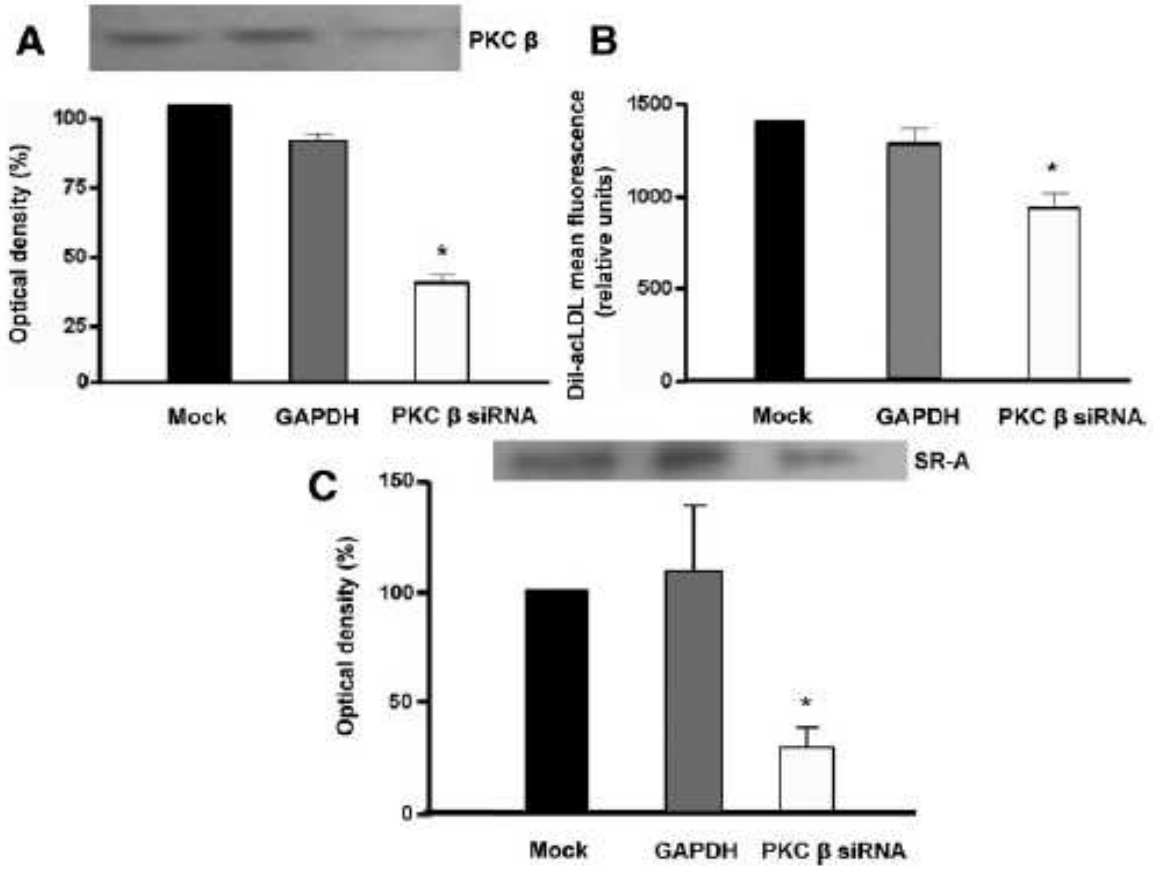

Figure 5. Representative Western blot and densitometric quantification of PKCβ(A) and SR-A (C) protein expression after transfection of selective PKCβ siRNA into MDMs. B, Fluorescent-activated cell sorter analysis of transfected human MDMs after 24 hours of incubation with DiI-acLDL. On silencing of PKCβ, the uptake of modified LDL and SR-A expression is reduced. GAPDH and mock served as controls. Results are presented as mean±SEM; n=4 in each group. **P*<0.05 vs mock and GAPDH.

Figure 6

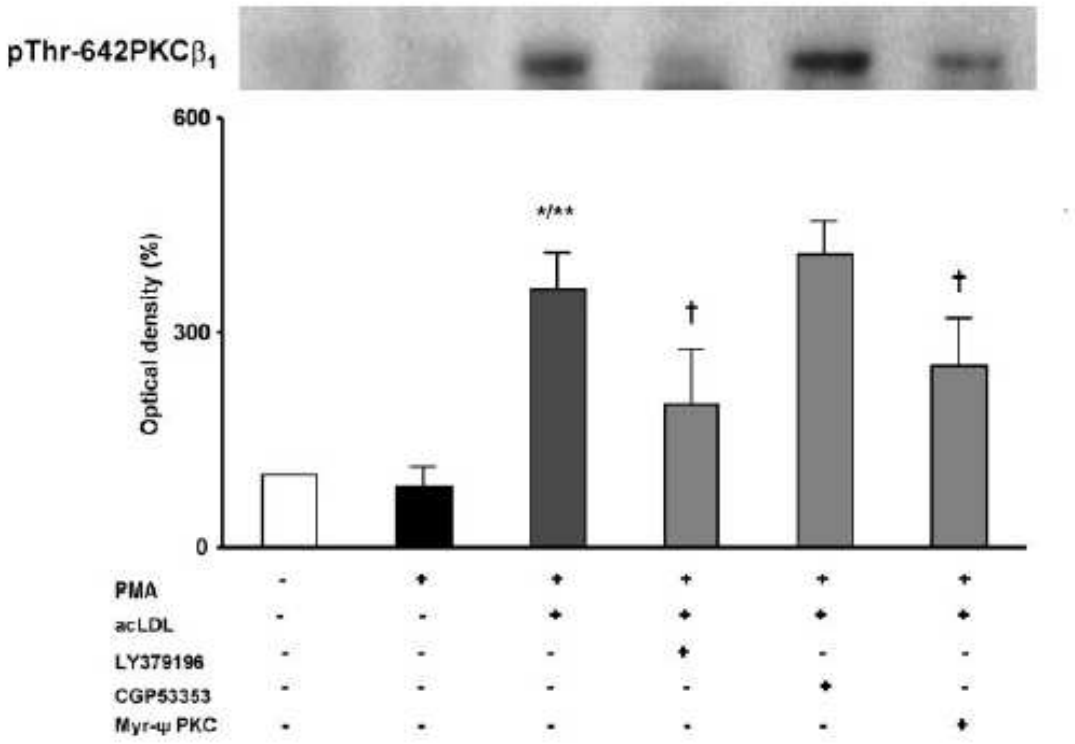

Figure 6. Representative Western blot and densitometric quantification of PKCβ1 phosphorylation at the Thr-642 residue in PMA-induced human MDMs after incubation with acLDL in the presence and absence of LY379196 (10^{-6} mol/L), CGP53353 (10^{-6} mol/L), or myr-PKC (10^{-4} mol/L). Results are presented as mean±SEM; n=4 in each group. **P*<0.05 vs control; ***P*<0.05 vs PMA alone; †*P*<0.05 vs PMA plus acLDL.

Figure 7

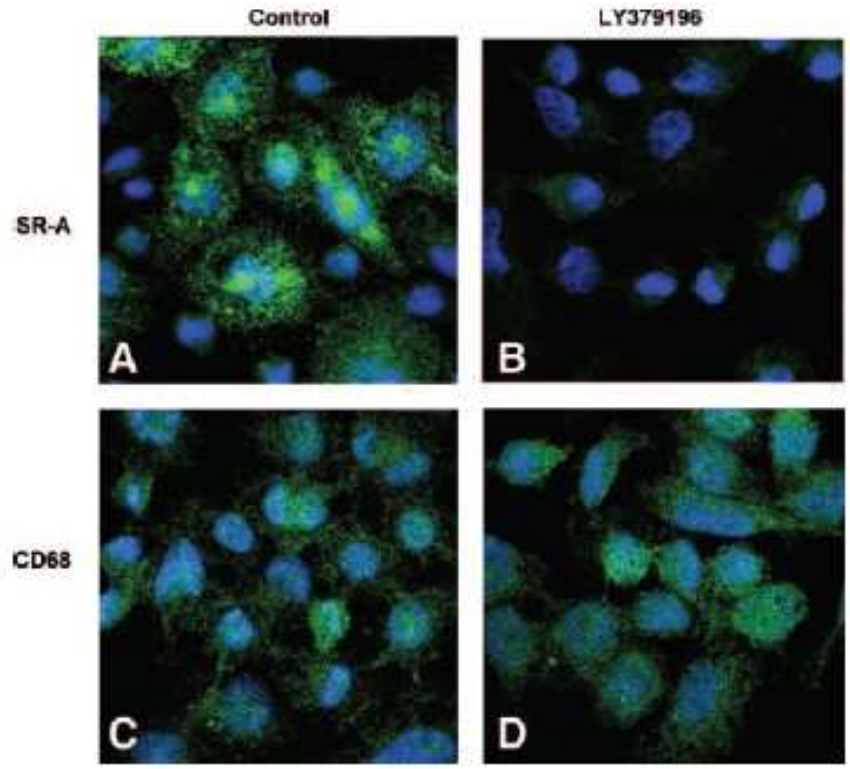

Figure 7. Treatment with LY379196 (10^{-6} mol/L) affects SR-A expression but not activation of human MDMs stimulated with acLDL. SR-A (A, B) and CD68, a marker of macrophage activation (C, D), are shown by fluorescent confocal microscopy. The nuclei stained with DAPI are blue; SR-A and CD68 stainings are both green.

Figure 8

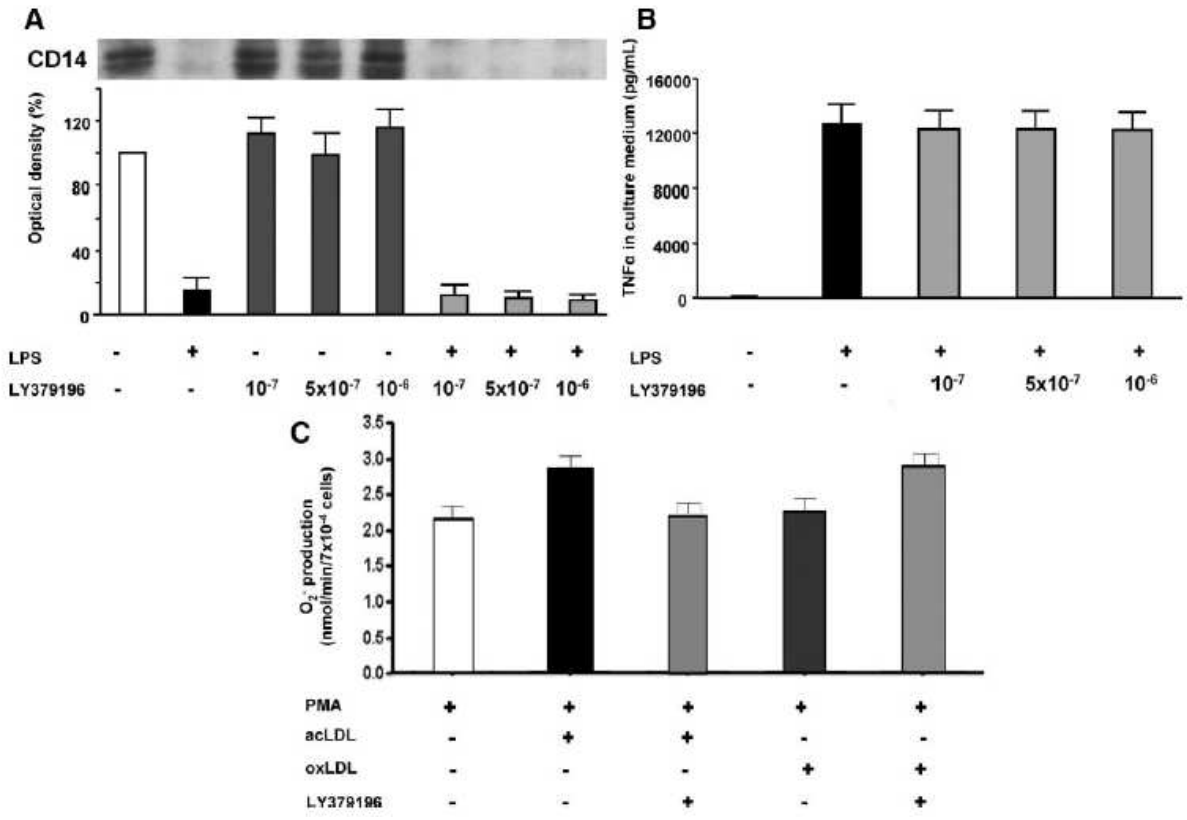

Figure 8. LY379196 did not inhibit lipopolysaccharide-induced CD14 degradation, TNFα release, or O2-) production in human MDMs. Representative Western blot and densitometric quantification of CD14 expression (A) and TNFα levels in supernatant (B) after 24 hours of stimulation with lipopolysaccharide (100 ng/mL). O2- production after incubation with acLDL and oxLDL (10 ug/mL; C). Results are presented as mean±SEM; n=3 to 5 in each group.

Pulsatile Stretch Induces Release of Angiotensin II and Oxidative Stress in Human Endothelial Cells Effects of ACE Inhibition and AT_1Receptor Antagonism

Under homeostatic conditions, endothelial-derived nitric oxide (NO) mantains vascular structure and function, regulating vasomotor tone, blood fluidity and vascular cell growth. Impaired NO bioavailability, resulting in endothelial dysfunction, intertwines with other conditions, such as chronic inflammation, increased oxidative stress and impaired blood flow to determine atherosclerotic vascular disease [(1).] The activity of endothelial NO depends on the balance between synthesis of NO and its breakdown by superoxide anion ($O_2^{\bullet-}$). Increased production of reactive oxygen species (ROS) is regarded as major determinant of reduced level of NO [(1).]

A whole body of evidence shows a great impact of the interplay between altered mechanical forces and activation of renin-angiotensin system (RAS) to determine endothelial dysfunction in the context of cardiovascular risk factors, such as hypertension, as well as overt atherosclerotic disease [(2,3)]. Moreover, nowadays it is becoming clear that induction of oxidative stress is the unifying mechanism that links both mechanical stress and RAS activation to endothelial dysfunction [(2,3)]. In pathological conditions, angiotensin II (Ang II), via AT_1 receptor-activated signaling, appears to be the most important factor influencing structural and functional changes leading to inflammation, vasoconstriction, vascular remodeling and prothrombotic state. Different angiotensin II-signaling pathways are involved, but growing evidence indicates a prominent role for the NADPH oxidase-driven generation of ROS, namely $O_2^{\bullet-}$ [(4,5)]. Moreover Ang II via NADPH oxidase-derived $O_2^{\bullet-}$ and hydrogen peroxide (H_2O_2) damaging effect, can lead to uncoupling of eNOS resulting in reduced NO production and NOS-dependent $O_2^{\bullet-}$ formation [(6)]. Accordingly, some of the beneficial long-term effects of RAS blockade with angiotensin I-converting enzyme (ACE) inhibitors [(7)] or angiotensin type 1 (AT_1) receptor antagonists [(8)] have been correlated to the favourable influence exerted on $NO/O_2^{\bullet-}$ balance [(9-12)]. However, little is known about the specific link between RAS and the regulation of $NO/O_2^{\bullet-}$ balance in endothelial cells exposed to mechanical stress.

Plenty of data provided over recent years indicate that mechanical forces due to blood pressure and blood flow—namely, stretch and shear stress—can become crucial players of pathological structural and functional modifications of endothelial cells when disturbed flow profiles occur and persist [13]. Cyclic stretch applied to endothelial cells and vascular smooth muscle cells induces oxidative stress with and H2O2 production [14,15]; the influence on NADPH oxidase

activity exerted by stretch is considered to be of crucial importance [13,16]. Interestingly, pulsatile stretch enhanced the release of angiotensin II by cardiac myocytes [17]. Although we previously reported that in human aortic endothelial cells (HAEC), pulsatile stretch increases production as well as eNOS mRNA and protein expression [14,15], the contribution of cyclic strain to the regulation of balance in human endothelial cells has not been fully defined. We investigate the role of RAS blockade, comparing the effect of ACE inhibitor quinaprilat and AT1-receptor antagonist losartan on production and NO bioavailability in HAEC exposed to pulsatile stretch.

Materials and Methods

Cell Culture

Human aortic endothelial cells were obtained from Clonetics (San Diego, Ca) and grown in gelatin-coated flasks in optimized endothelial growth medium (Clonetics) supplemented with 10% fetal calf serum (Hyclone). Cells were detached by exposure to trypsin/EDTA for about 120 sec in Hepes buffer saline, reseeded in type I collagen–coated plates for stretch experiments (Flex I). Cells were grown to confluency in humidified air (5% CO_2 at 37°C). Cells between passages 2 and 6 were used for experiments.

Application of Pulsatile Stretch on Cultured Cells

Pulsatile stretch was applied to HAEC as previously described [20,21]. Briefly, HAEC were seeded onto type I collagen-coated Flex I (Flexcell International Corp) culture plates at an initial density of 10^5 cells/mL. Flex I culture plates were placed on a computerized Flexcell Strain Unit gasketed base plate in the incubator. The membranes were subjected to a deformation with -20 kPa of vacuum, respectively, at a frequency of 50 cycles/min. A vacuum of -20 kPa causes a deformation pattern of the membrane ranging from 0% at the center to 24% at the periphery (10% average strain). In parallel, other Flex I culture plates not subjected to stretch served as controls. The cell viability with and without stretch, as assessed with trypan blue exclusion test, was >90% throughout the experiments. Previous studies from our laboratory demonstrated a time-dependent increase of $O_2^{\bullet-}$ production up to 60 min from HAEC exposed to pulsatile stretch (10% average elongation at a frequency of 50 cycles/min) [22]. Indeed, after exposure of endothelial cells to different concentration of angiotensin II, $O_2^{\bullet-}$ production reaches a maximal level after 1 h stimulation [26]. Accordingly, a 60-minute interval was choosen for all our experiments.

Measurement of Angiotensin II

Aliquots of culture medium were collected from stretch and control culture plates. All samples were purified with Sep-Pak column (Sep-Pak Light, Waters) as described [27]. Levels of angiotensin II were determined by radioimmunoassay (RIA), using a specific antibody, according to the instruction of the manufacturer (Peninsula).

NO Measurements

Direct in situ measurements of NO were carried out as described [28]. Immediately before NO measurements, the active tip of the L-shaped porphyrinic NO microsensor was placed directly on the surface of the endothelial cell monolayer. For maximal stimulation of eNOS calcium ionophore A23187 was injected into the cell culture dish to yield a final concentration of 1 umol/L in all our experiments, as previously established [28].

Measurement of $O_2^{\bullet-}$ Production

$O_2^{\bullet-}$ production was measured as the SOD-inhibitable reduction of cytochrome *c* [22]. Briefly, HAECs were preincubated in DMEM without phenol red for 30 minutes at 37°C, and then cytochrome *c* (final concentration, 1 mg/mL) with or without SOD (final concentration, 500 U/mL) was added in a CO_2 incubator. After 60 min, the medium was removed from the cells, and the absorbance was read at 550 nm against a distilled water blank. Reduction of cytochrome *c* in the presence of SOD was subtracted from the values without SOD. The portion of $O_2^{\bullet-}$ specific reduction of cytochrome *c*- was between 20% and 35% according to the experiments. The optical density difference between comparable wells with or without SOD was converted to equivalent $O_2^{\bullet-}$ production by use of the molar extinction coefficient for cytochrome *c* [21.0×10^3 $(mol/L)^{-1} \cdot cm^{-1}$] [29].

Expression of eNOS by Western blot

eNOS protein was analyzed by Western blotting using an anti-human endothelial NOS antibody (Transduction Laboratory). The antibody was used at 250x dilution. After the stretch experiments, HAECs were detached by trypsin-EDTA, and the cell number was determined by Coulter counter (Coulter Electronics). Then, 100 µL of lysis solution containing 10% glycerol, 2.3% SDS, Tris-HCl, pH 6.8, 62.5 mmol/L, 0.01% bromophenol blue, and 5% mercaptoethanol was added to 10^5 cells. The lysate was then heated at 95°C to 100°C at 5 minutes. Next, 30 µL of cell lysates containing 3.3×10^4 cells was subjected to 7.5% single percentages gel (Ready Gel, BIO RAD). The separated proteins were electrophoretically transferred to Immunobilon-P

membranes and then incubated with anti-human NOS III antibody for 1 hour as previously described [30]. The membranes were finally visualized by the ECL kit (Amersham Life Sciences). Densitometric measurements were performed by Fotodyne Visionary documentation system (Fotodyne, Bio Cell Consulting Research).

Statistical Analysis

Results are expressed as mean ± SEM and n indicates number of experiments. Statistical evaluation of the data was performed with Student's *t* tests for simple comparison between two values when appropriate. For multiple comparison, results were analyzed by ANOVA followed by Fisher's test. $P \leq 0.05$ was considered statistically significant.

Results

Pulsatile Stretch and Release of Angiotensin II

Levels of angiotensin II were determined in culture medium collected from the stretch plates after 60 min. Interestingly, pulsatile stretch increased angiotensin II immunoreactivity (Ang II-ir) (**Figure 1**). The mean concentrations of the Ang II-ir in the media were 0.29± 0.01 and 0.42±0.03 ng/mL for control and stretched cells, respectively (n=6; $P<0.05$). Accordingly, stretch-induced increase of Ang II-ir was blunted by ACE inhibitor quinaprilat, whereas AT_1-receptor antagonist losartan did not exert any significant effect (Figure 1).

RAS Blockade and Stretch-Induced Superoxide Production

To clarify the relationship between RAS and stretch-induced $O_2^{\bullet-}$ production, we studied whether inhibition of angiotensin II system at different levels may modulate stretch-induced $O_2^{\bullet-}$ production. We measured $O_2^{\bullet-}$ in cells exposed to pulsatile stretch with and without quinaprilat or losartan (10^{-8}-10^{-6} mol/L). Stretch-induced production of $O_2^{\bullet-}$ was blunted by both drugs (Figure 2).

RAS Blockade and Stretch-Induced Modulation of NO Pathway

Because eNOS can be influenced by mechanical forces, we determined the effect of pulsatile stretch on eNOS protein expression in the absence and presence of quinaprilat or losartan. Densitometric analysis showed a significant upregulation of eNOS in cells exposed to mechanical stress (Figure 3). Both drugs abolished stretch-induced upregulation of eNOS expression (Figure 3). Neither quinaprilat nor losartan affected eNOS expression in non-stretched control cells (data not shown).

Despite pulsatile stretch-induced increase of eNOS protein levels, NO release after stimulation with calcium ionophore A23187 (10 umol/L) was reduced in endothelial cells exposed to mechanical stress (n= 10; $P<0.05$; Figure 4). As expected, N^G-nitro-L-arginine methyl ester (L-NAME; 10^{-5}mol/L) abolished A23187-induced NO production (n=8; $P<0.05$; Figure 4).

Interestingly, quinaprilat and losartan blunted the inhibitory effect of pulsatile stretch on NO release in a concentration-dependent manner (n=10; $P<0.05$; Figure 4). However, an higher concentration of losartan was necessary to inhibit stretch-induced eNOS upregulation and restore NO production (Figure 3 and 4). Both quinaprilat and losartan did not affect NO production in non-stretched control cells (data not shown). These findings indicate a close link between stretch-induced increase in $O_2^{\bullet-}$ production and upregulation of eNOS.

RAS Blockade and NO/$O_2^{\bullet-}$ Balance

Furthermore, we characterized the role of bradykinin (B_2) and angiotensin type 2 (AT_2) receptor activation on NO/O_2^- balance in this context. As expected, the protective role of quinaprilat on NO release was abolished by the B_2-receptor antagonist Hoe140 (Figure 5). Interestingly enough, the preservation of NO release exerted by losartan was blunted not only by the AT_2-receptor antagonist (PD123319) but also by Hoe 140, suggesting that kinins, acting through AT_2 receptors, also contribute to the vascular protective effects of AT_1-receptor antagonists. The inhibitory effect of quinaprilat and losartan on stretch-induced $O_2^{\bullet-}$ production was blunted by Hoe140 and PD123319 in a similar fashion (data not shown). However, PD 123319 and Hoe 140 alone did not affect NO release in cells exposed to pulsatile stretch (Figure 5).

Discussion

The present study demonstrates for the first time that mechanical stretch of human endothelial cells triggers the autocrine release of Ang II, which in turn unfavourably alters the balance of NO and $O_2^{\bullet-}$. The novelty of this work is the simultaneous measurement of $O_2^{\bullet-}$ and NO, with the evidence that in cells exposed to pulsatile stretch, in spite of eNOS upregulation, NO release was significantly reduced by increased O_2^- production. Under these conditions we evaluated the effects of the ACE inhibitor quinaprilat and AT_1-receptor antagonist losartan.

Both quinaprilat and losartan abolished stretch-induced $O_2^{\bullet-}$ production and upregulation of eNOS. Accordingly, quinaprilat and losartan blunted the inhibitory effect of pulsatile stretch on NO release. These findings indicate a close relationship between stretch-induced increase in $O_2^{\bullet-}$ production, via angiotensin II, and upregulation of eNOS, the latter may represent a

compensatory mechanism attempting to counterbalance the angiotensin II-induced depletion of endothelial NO, through enhanced oxidative stress [26,31,32].

The restoring effects of quinaprilat and losartan on the balance of NO and $O_2^{\bullet-}$ were abolished by B_2- or AT_2-receptor antagonists, respectively. In particular, the effect of losartan on NO release was blunted not only by PD 123319 but also by the B_2-receptor antagonist Hoe 140, suggesting that kinins, via AT_2 receptors, may participate in the vascular protective effect of AT_1-receptor antagonists (Figure 6).

Although it is well established that mechanical forces cause a variety of effects on the structure and function of cells, little is known about how mechanical stimuli regulate cell function and gene expression [22,23]. This is particularly relevant for endothelial cells directly exposed to shear stress and pulsatility for their strategic anatomical position between the circulating blood and vascular smooth muscle [33]. Pulsatile stretch is involved in the development of atherosclerosis that primarily affects the aorta and its branches where this force is prominent. Indeed, cyclic strain increasing the production of endothelium-derived vasoactive substances, including endothelin-1 and growth factors [14-17], leads to smooth muscle cell proliferation [19,20]. In vitro models, replicating the major geometric features of blood vessels, have shown a 5-6% wall excursion at peak systole under control conditions, which can increase to 10% under pathological conditions such as hypertension [34].

Previous studies from our laboratory demonstrated that pulsatile stretch increases $O_2^{\bullet-}$ production via NADPH oxidase and upregulates eNOS expression as a scavenger mechanism for $O_2^{\bullet-}$ [22,23]. In the present study, we report that mechanical stretch induces the release of Ang II in human endothelial cells as shown in cardiac myocytes [25]. Such an activation of local RAS, tipping the balance of NO and $O_2^{\bullet-}$ in favour of the latter, exerts oxidative and nitrosative stress, contributing to endothelial dysfunction, the initial step in developing of atherosclerosis [35].

The inhibition of RAS either with quinaprilat or losartan, restores NO bioavailability by reducing $O_2^{\bullet-}$ production and stimulating bradykinin-mediated NO release. The reduction of stretch-induced production of $O_2^{\bullet}$ below control levels elicited by micromolar concentrations of both quinaprilat and losartan can be attributed to the blunting of angiotensin II-sensitive, NAD(P)H-dependent $O_2^{\bullet-}$producing enzymes. However, recent studies indicate that both treatment strategies not only inhibit AT_1-dependent activation of NAD(P)H oxidase but also increase antioxidant activity of superoxide dismutase [36-38].

Our present findings may provide the molecular basis to explain the improvement of endothelial function observed with these drugs. Quinaprilat is an ACE inhibitor with high affinity to tissue ACE, whose vasodilator effects in the human forearm arterial circulation have been shown to be

largely mediated by NO [39,40]. Furthermore, it has also been reported that quinaprilat increases flow-mediated dilation of the brachial artery in patients with essential hypertension [41]. In addition the Trial on Reversing Endothelial Dysfunction (TREND) has shown that quinaprilat improves coronary endothelium-dependent vasomotor function in patients with coronary disease[42].

Most vascular effects of ACE inhibitors have been attributed to the reduced generation of angiotensin II [43]. However, an inhibition of the breakdown of bradykinin by kininase II, which is synonymous with ACE, plays a role in the beneficial response to ACE inhibitors, since bradykinin stimulates the endothelial production of NO [44,45]. This raised the possibility that ACE inhibition might have a superior effect on endothelial function compared with AT_1 receptor antagonists. However, recent experimental data seem to weaken this hypotesis showing that AT_1 receptor antagonism may reverse endothelial dysfunction in humans not only through improvement of NO availability by reducing AT_1-induced oxidative stress, but also via an AT_2-mediated increase in NO synthesis [46-48]. Losartan and its metabolites have been recently demonstrated to possess AT_1 receptor-independent actions [49]. The AT_2 receptor exerts a tonic negative influence on ACE activity, suggesting that AT_1 receptors blockers may reduce ACE activity by stimulation of AT_2 receptors [48]. Our findings indicate that, in the presence of losartan, pulsatile stretch-induced autocrine release of Ang II stimulates AT_2 receptors and activation of the bradykinin/NO cascade. Indeed, the restoring effects of AT_1 receptor blockade on NO release are abolished by B_2-receptor antagonist Hoe 140.

According to the dose-dependent responses observed in our experimental setting, the restoring effect on NO release was obtained by using a higher concentration of losartan as compared with quinaprilat. The pro-drug nature of this compound, with marked lower AT1 receptor affinity compared to its active metabolite (E3174) may likely explain such a difference [50].

In conclusion, the modulation of RAS either by ACE inibition or angiotensin II receptor antagonism affects the crucial balance between NO and $O_2^{\bullet-}$. Quinaprilat improves NO bioavailability by blunting stretch-induced, Ang II-dependent $O_2^{\bullet-}$production as well as bradykinin degradation. Losartan exerts comparable effects involving AT_2 receptors with subsequent B_2 receptors activation.

These results define the link between mechanical forces, Ang II and redox state in endothelial cells, but also provide the molecular basis to understand the vascular protective effects of ACE inhibition and AT_1-receptor antagonism.

Acknowledgements

This work is supported by grants from Swiss National Research Foundation (310000108463 to F.C. and 3100-068118 to T.F.L.), Swiss Heart Foundation and by an MSD medical school grant and educational grant of Pfizer Pharmaceuticals. The University Research Priority Program "Integrative Human Physiology" at the University of Zurich (F.C., T.F.L.) also supported this study.

References

1. Wever RMF, Lüscher TF, Cosentino F, Rabelink TJ. Atherosclerosis and the two faces of endothelial nitric oxide synthase. Circulation. 1998;97:108–112.

2. Madamanchi NR, Vendrov A, Runge MS. Oxidative stress and vascular disease. Arterioscler Thromb Vasc Biol. 2005;25:29–38.

3. Paravicini TM, Touyz RM. Redox signaling in hypertension. Cardiovasc Res. 2006;71:247–258.

4. Griendling KK, Sorescu D, Ushio-Fukai M. NAD(P)H oxidase: Role in cardiovascular biology and disease. Circ Res. 2000;86:494–501.

5. Virdis A, Neves MF, Amiri F, Touyz RM, Schiffrin EL. Role of NAD(P)H oxidase on vascular alterations in angiotensin II-infused mice. J Hypertens. 2004; 22:535–542.

6. Chalupsky K, Cai H. Endothelial dihydrofolate reductase: Critical for nitric oxide bioavailability and role in angiotensin II uncoupling of endothelial nitric oxide synthase. Proc Natl Acad Sci USA. 2005;102:9056–9061.

7. Pitt B. ACE inhibitors for patients with vascular disease without left ventricular dysfunction—may they rest in PEACE? N Engl J Med. 2004;351:2115–2117.

8. Mancia G, Weber M. A new dawn in cardiovascular protection: Blood pressure lowering through AT1 blockade. J Hypertens. 2003;21 (Suppl. 6):S1–S2.

9. Prasad A, Tupas-Habib T, Schenke WH, Mincemoyer R, Panza JA, Wachawin MA, et al. Acute and chronic angiotensin-1 receptor antagonism reverses endothelial dysfunction in athersclerosis. Circulation. 2000;101:2349–2354.

10. Hornig B, Landmesser U, Kohler C, Ahlersmann D, Spiekermann S, Christoph A et al. Comparative effect of ACE inhibition and angiotensin II type 1 receptor antagonism on bioavailability of nitric oxide in patients with coronary artery disease. Role of superoxide dismutase. Circulation. 2001;103:799–805.

11. Ghiadoni L, Magagna A, Versari D, Kardasz I, Huang Y, Taddei S, et al. Different effect of antihypertensive drugs on conduit artery endothelial function. Hypertension. 2003;41:1281–1286.

12. Yoshida J, Yamamoto K, Mano T, Sakata Y, Nishikawa N, Nishio M, et al. AT1 receptor blocker added to ACE inhibitor provides benefits at advanced stage of hypertensive diastolic heart failure. Hypertension. 2004;43:686–691.

13. Lehoux S. Redox signalling in vascular responses to shear and stretch. Cardiovasc Res. 2006;71:269–279.

14. Hishikawa K, Lüscher TF. Pulsatile stretch stimulates superoxide production in human aortic endothelial cells. Circulation. 1997;96:935–941.

15. Hishikawa K, Oemar BS, Yang Z, Luscher TF. Pulsatile stretch stimulates superoxide production and activates nuclear factor-kB in human coronary smooth muscle. Circ Res. 1997;81:797–803.

16. Howard AB, Alexander RW, Nerem RM, Griendling KK, Taylor WR. Cyclic strain induces an oxidative stress in endothelial cells. Am J Physiol. 1997;272:C421–C427.

17. Sadoshima J-I, Xu Y, Slayter HS, Izumo S. Autocrine release of angiotensin II mediates stretchinduced hypertrophy of cardiac myocytes in vitro. Cell. 1993;75:977–984.

18. Predel H-G, Yang Z, Von Segesser L, Turina M, Buhler FR, Luscher TF. Implications of pulsatile stretch on growth of saphenous vein and mammary artery smooth muscle. Lancet. 1992;340:878–879.

19. Yang Z, Noll G, Lüscher TF. Calcium antagonists differently inhibit proliferation of human coronary smooth muscle cells in response to pulsatile stretch and platelet-derived growth factor. Circulation. 1993;88:832–836.

20. Zhang H, Schmeisser A, Garlichs, Plotze K, Damme U, Mugge A et al. Angiotensin II-induced superoxide generation in human vascular endothelial cells:role of membrane-bound NADH/NADPH–oxidases. Cardiovasc Res 1999;44:215–222.

21. DeSilva PE, Husain A, Smeby RR, Khairallah PA. Measurement of immunoreactive angiotensin in rat tissues: some pitfalls in angiotensin II analysis. Anal Biochem 1988;174:80–87.

22. Cosentino F, Eto M, De Paolis P, van der Loo B, Bachschmid M, Ullrich V, et al. High glucose causes upregulation of cyclooxygenase-2 and alters prostanoid profile in human endothelial cells. Role of protein kinase C and reactive oxygen species. Circulation. 2003;107:1017–1023.

23. Massey V. The microestimation of succinate and extinction coefficient of cytochrome c. Biochem Biophys Acta. 1959;34:255–257.
24. Miller VM, Burnett JJ. Modulation of NO and endothelin by chronic increases in blood flow in canine femoral arteries. Am J Physiol. 1992;248:H423–H437.
25. Pagano PJ, Clarck JK, Cifuentes-Pagano ME. Localization of a constitutively active, phagocytelike NADPH oxidase in rabbit aortic adventitia: Enhancement by angiotensin II. Proc Natl Acad Sci USA. 1997;94:14483–14488.
26. Lang D, Mosfer SI, Shakesby A, Donaldson F, Lewis MJ. Coronary microvascular endothelial cell redox state in left ventricular hypertrophy: The role of angiotensin II. Circ Res.2000;86:463–469.
27. Davies PF, Tripathi SC. Mechanical stress mechanism and the cell: An endothelial paradigm. Circ Res. 1993;72:239–245.
28. Ballermann BJ, Dardik A, Eng E, Liu A.Shear stress and the endothelium. Kidney Int Suppl.1998;67:S100–S108.
29. Hishikawa K, Nakaki T, Marumo T, Suzuki H, Kato R, Saruta T. Pressure enhances endothelin-1 release from cultured human endothelial cells. Hypertension. 1995;25:449–452.
30. Sumpio BE, Banes AJ. Prostacyclin synthetic activity in cultured aortic endothelial cells undergoing cyclic mechanical deformation. Surgery. 1988;104:383–389.
31. Wilson E, Mai Q, Sudhir K. Mechanical strain induces growth of vascular smooth muscle cells via autocrine action of PDGF. J Biol Cell. 1993;123:741–747.
32. Cheng GC, Libby P, Grodzinsky AJ, Lee RT. Induction of DNA synthesis by a single transient mechanical stimulus of human vascular smooth muscle cells. Circulation. 1996;93:99–105.
33. Rubanyi GM, Freay AD, Kause K. Mechanoreception by the endothelium: Mediators and mechanisms of pressure- and flow-induced vascular responses. Blood Vessels. 1990;27:246–257.
34. Sumpio BE, ed. Hemodynamic forces and vascular cell biology. Austin, Texas: RG Landes Co., 1993, 1–119.
35. Warnholtz A, Nickenig G, Schulz E, Macharzina R, Brasen JH, Skatchkov M, et al. Increased NADH-oxidase-mediated superoxide production in the early stages of atherosclerosis: Evidence for the involvement of the renin-angiotensin system. Circulation. 1999;99:2027–2033.
36. Khan BV, Sola S, Lauten WB, Natarajan R, Hooper WC, Menon RG. Quinapril, an ACE inhibitor, reduces markers of oxidative stress in the metabolic sindrome. Diabetes Care. 2004;27:1712–1715.

37. Lazaro A, Gallego-Delgado J, Justo P, Esteban V, Osende J, Mezzano S, et al. Long-term blood pressure control prevents oxidative renal injury. Antioxid Redox Signal. 2005;7:1285–1293.

38. Landmesser U, Drexler H. Effect of angiotensin II type 1 receptor antagonism on endothelial function: Role of bradykinin and nitric oxide. Hypertens Suppl. 2006;24:S39–S43.

39. Major TC, Overhiser RW, Taylor DJ Jr, Panek RL. Effects of quinapril, a new angiotensinconverting enzyme inhibitor, on vasocostrictor activity in the isolated perfused mesenteric vasculature of hypertensive rats. J Pharm Exp Ther. 1993;265:187–193.

40. Haefeli WE, Linder L, Lüscher TF. Quinaprilat induces arterial vasodilation mediated by nitric oxide in humans. Hypertension. 1997;30:912–917.

41. Uehata A, Takase B, Nishioka T, Isojima K, Satomura K, Ohsura F, et al. Effect of quinapril versus nitrendipine on endothelial dysfunction in patients with systemic hypertension. Am J Cardiol. 2001;87:1414–1416.

42. Mancini GBJ, Henry GC, Macaya C, O'Neill BJ, Pupillo AL, Carere RG, et al. Angiotensin converting enzyme inhibition with quinapril improves endothelial vasomotor dysfunction in patients with coronary artery disease. The TREND (Trial on Reversing ENdothelial Dysfunction) study. Circulation. 1996;94:258–265.

43. Griendling KK, Lassegue B, Alexander RW. Angiotensin receptors and their therapeutic implications. Annual Review of Pharmacology & Toxicology. 1996;36:281–306.

44. Hornig B, Kohler C, Drexler H. Role of bradykinin in mediating vascular effects of ACEinhibitors in humans. Circulation. 1997;95:1115–1118.

45. Benzing T, Fleming I, Blaukat A, Muller-Esterl W, Busse R. Angiotensin converting enzyme inhibitor ramiprilat interferes with the sequestration of the B2 kinin receptor within the plasma membrane of native endothelial cells. Circulation. 1999;99:2034–2040.

46. Gohlke P, Pees C, Unger T. AT2 receptor stimulation increases aortic cyclic GMP in SHRSP by a kinin-dependent mechanism. Hypertension. 1998;31:349–355.

47. Tsutsumi Y, Matsubara H, Kurihara H, Murosawa S, Takai S, Miyazaki M. Angiotensin II type 2 overexpression activates the vascular kinin system and causes vasodilation. J Clin Invest.1999;104:925–935.

48. Campbell DJ, Krum H, Esler MD. Losartan increases bradykinin levels in hypertensive humans. Circulation. 2005;111:315–320.

49. Sadoshima J. Novel AT1 receptor-independent functions of losartan. Circ Res. 2002;90:754–756.

50. Dickstein K, Timmermans P, Segal R. Losartan: A selective angiotensin II type 1 (AT1) receptor antagonist for the treatment of heart failure. Expert Opin Investig Drugs. 1998;7:1897–1914.

Figures

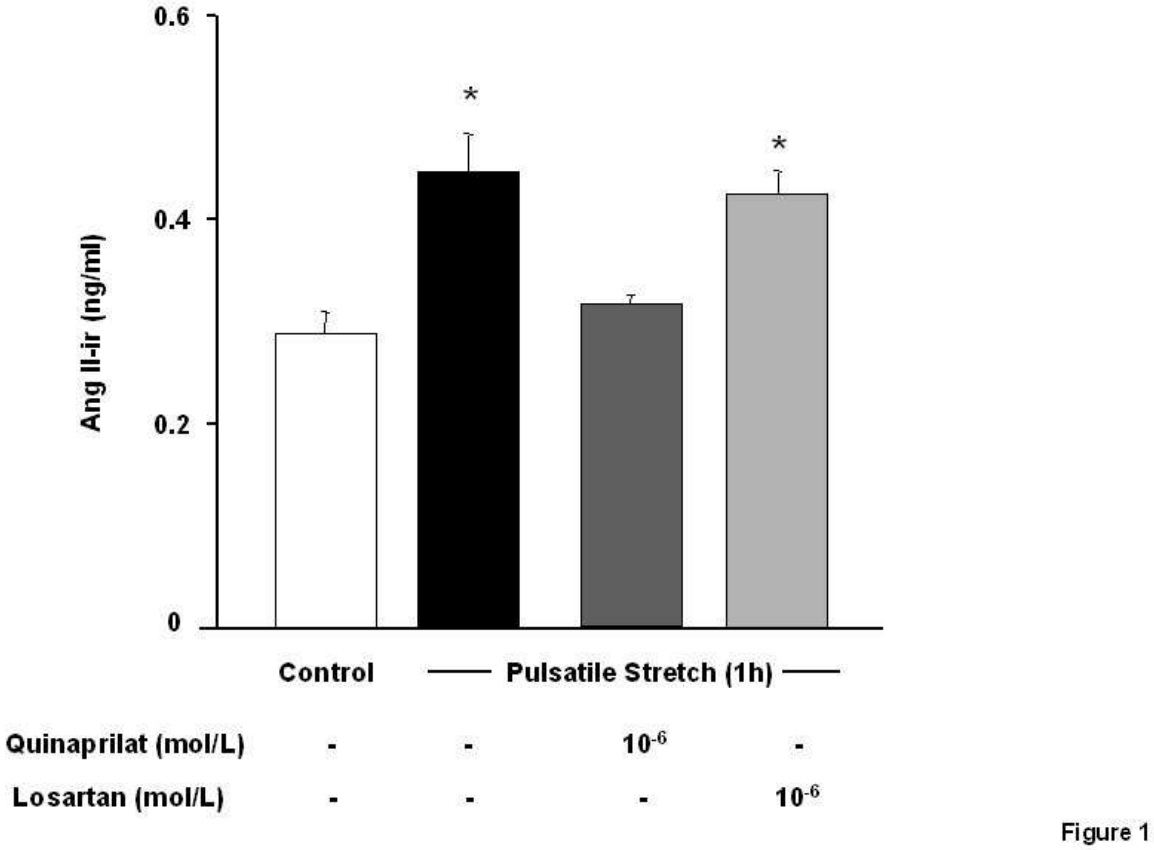

Figure 1. Stretch-induced increase in angiotensin II in human aortic endothelial cells. Culture media were obtained after 60 min of pulsatile stretch or at the same time point from nonstretched endothelial cells (control). Data are mean±SEM; (n=6); *$p<0.05$ vs control.

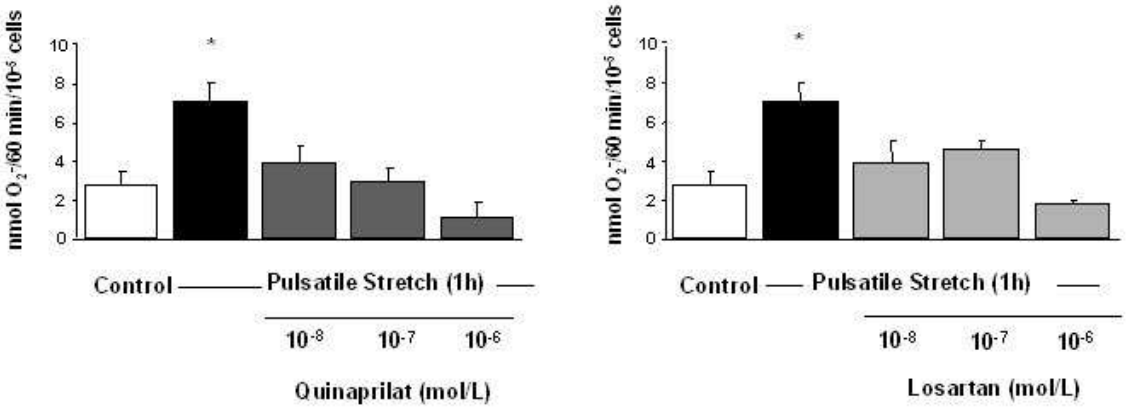

Figure 2

Figure 2. Bar graphs showing stretch-induced production of O_2^- in human aortic endothelial cells in the absence and in the presence of quinaprilat or losartan, respectively. Data are mean ± SE; (n= 6). *P<0.05 vs control.

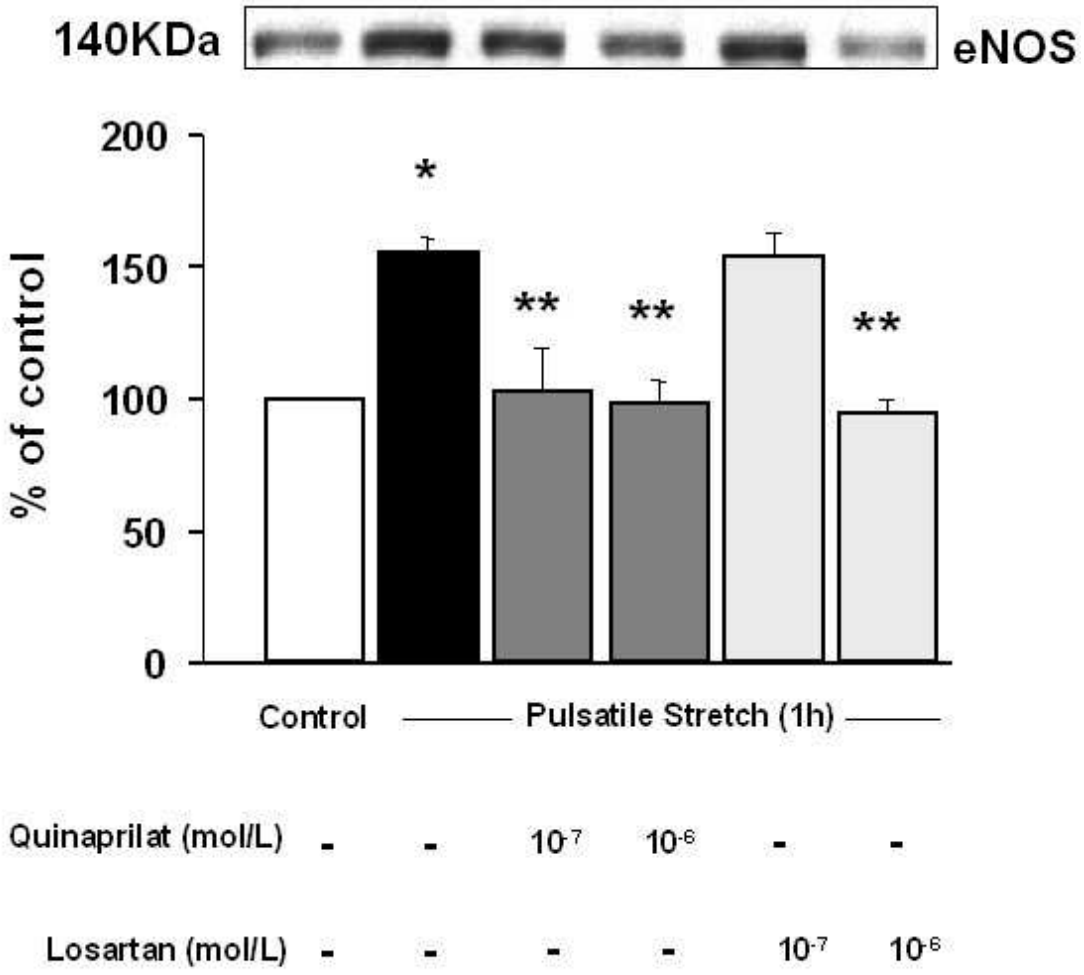

Figure 3

Figure 3. Effect of pulsatile stretch on eNOS protein expression in human aortic endothelial cells in the absence and in the presence of quinaprilat or losartan, respectively. HAEC were stimulated by pulsatile stretch (10% average, 50 cycles/min) up to 1 h. On the top representative Western blot result. On the bottom densitometric quantification of eNOS in protein homogenates, from the left each lane means control (static), control with pulsatile stretch and stretch in the presence of quinaprilat (10^{-7} and 10^{-6}) and losartan (10^{-7} and 10^{-6}), respectively . Data are mean ± SEM (n=4-6). *P<0.05 vs control cells, **P<0.05 vs stretch alone.

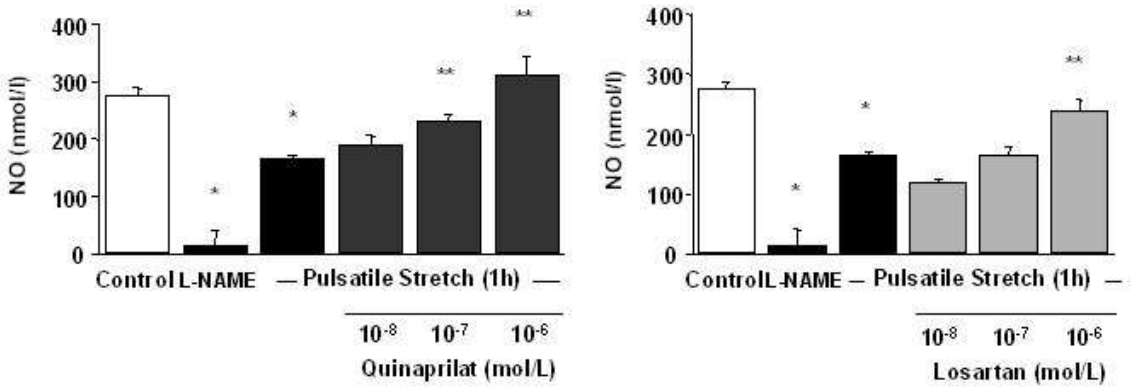

Figure 4

Figure 4. Bar graphs showing NO release following stimulation with calcium ionophore A23187 (1 μmol/L) in control nonstretched, L-NAME-treated, and endothelial cells exposed to pulsatile stretch in the absence and in the presence of quinaprilat or losartan, respectively. Data are mean ± SEM (n=8). *P<0.05 vs control, **P<0.05 vs stretch alone.

Figure 5

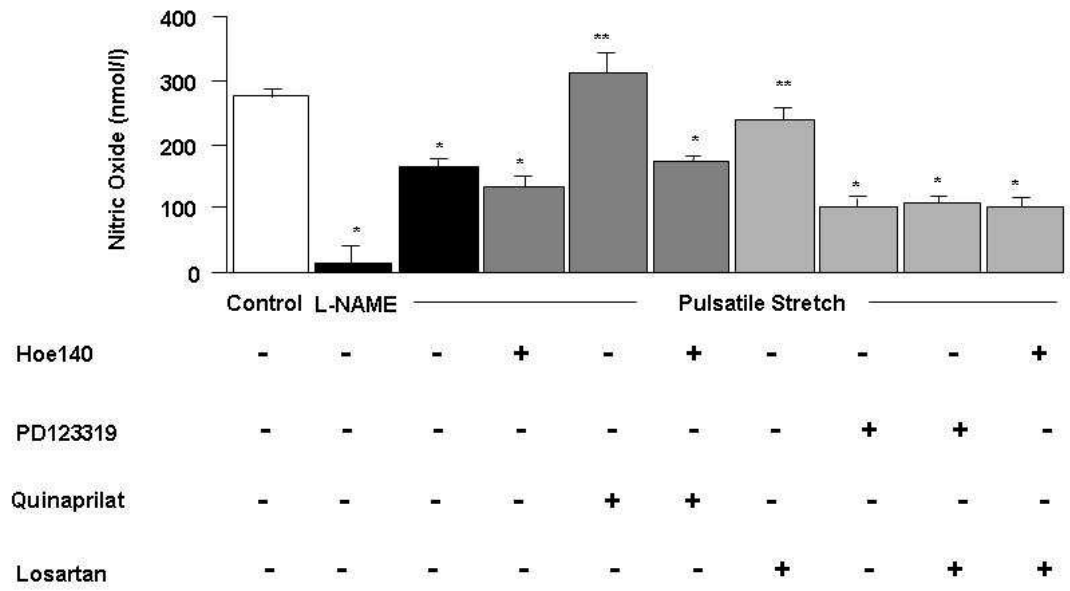

Figure 5. Bar graphs showing the effects of B_2–receptor antagonist (Hoe140; 10^{-7}mol/L) and AT_2-receptor antagonist (PD123319; 10^{-7}mol/L) on the restoration of NO release in the absence and in the presence of quinaprilat or losartan (10^{-6}mol/L) in HAEC exposed to pulsatile stretch. Data are mean ± SEM (n=8). *P<0.05 vs control, **P<0.05 vs stretch alone.

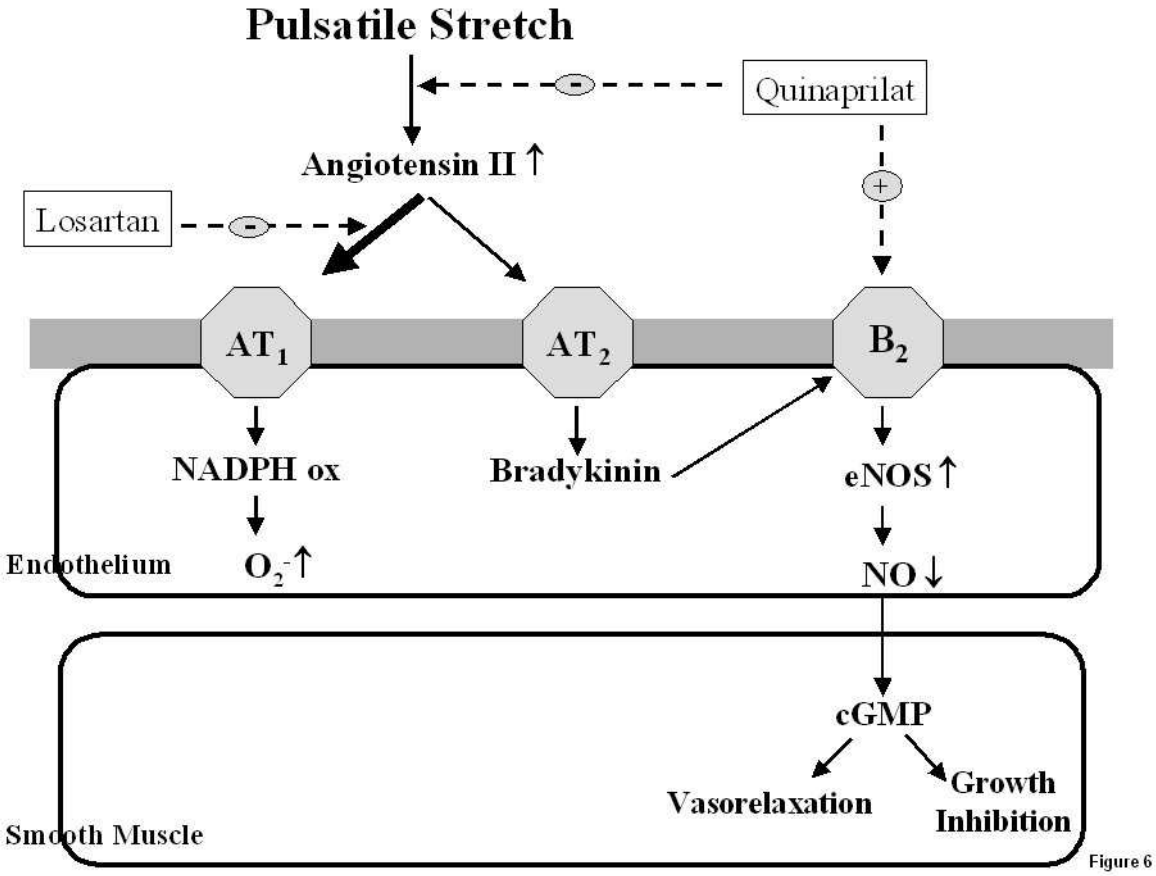

Figure 6. Schematic representation of stretch-induced autocrine release of angiotensin II which in turn unfavourably alters the balance of NO and O_2^-. Please note that activation of bradykinin/NO cascade is the common link to understand the protective effects of ACE inhibition and AT_1 receptor antagonism. AT_1 and AT_2, angiotensin type 1 and type 2 receptor subtypes; B_2, bradykinin receptor; NADPH ox, NADPH oxidase; eNOS, endothelial nitric oxide synthase; cGMP, cyclic guanosine monophosphate.

PART 2. INSIGHTS INTO THE PATHOPHYSIOLOGY OF CORONARY MICROCIRCULATION IN CARDIAC ALLOGRAFT VASCULOPATHY

ORIGINAL DATA

Clinical studies

Determinants of Coronary Flow Reserve in Heart Transplantation: A Study Performed With Contrast-enhanced Echocardiography

Cardiac allograft vasculopathy (CAV) is the main limiting factor of long-term survival in heart transplantation (HT).[1] In CAV, both epicardial coronary vessels and the microvasculature may be affected.[2] Coronary flow reserve (CFR) measurements may provide functional assessment of the microvasculature in patients with CAV.[3,4] We have recently applied a new non-invasive technique based on contrast-enhanced transthoracic echocardiography (CE-TTE) for assessing CFR in the left anterior coronary descending artery (LAD) in HT patients. [3,4] CFR by CE-TTE is a simple, readily available, objective, non-invasive diagnostic tool for the detection of early and severe CAV.[3,4] It has been shown in several studies that CFR is reduced in patients with angiographically advanced vasculopathy.[5,6] Intravascular ultrasound has been used to study the influence of angiographically silent intimal thickening on CFR.[5] Furthermore, the prognostic impact of CFR has been demonstrated.[4] However, few reports have focused on the determinants of CFR in HT.[7] Therefore, the aim of the present study was to identify clinical and functional determinants of CFR in HT patients and, above all, in those without coronary occlusive disease.

METHODS

Study Patients

We studied 119 consecutive HT recipients (97 men, 22 women; median age 55 years at HT, range 9 to 73 years). Median post-HT follow-up at study entry was 8.5 years (range 13 months to 19 years). Our immunosuppression protocol consisted of cyclosporine, azathioprine and steroids (triple therapy), as previously detailed.[2,8] Cytomegalovirus (CMV) serostatus (IgG-positive or IgG-negative) of all donors and recipients was analyzed before HT. The study was approved by the institutional ethics committee, and all patients gave written, informed consent.

Acute Rejection Scores

Acute graft rejection was monitored by endomyocardial biopsy following established protocols.[8] A rejection score was assigned based on a modification of the International Society for Heart and Lung Transplantation (ISHLT) grading system.[2] The following scores were calculated for each patient: rejection score in total follow-up (TRS); rejection score in the first year (RS 1yr); rejection score including only severe grades (≥3A) (sev TRS); and first-year

rejection score including only severe grades (sev RS 1yr). All scores were normalized for the number of biopsies taken in each patient.

Cumulative Immunosuppressive Doses

Cumulative doses (milligrams per killigram) of cyclosporine, azathioprine, prednisone and methylprednisolone at 3, 6 and 12 months, and cumulative total steroid load in the first year were calculated. Cumulative prednisone load for each patient in the first year (PDN 1yr) was calculated (in milligrams per kilogram), as was cumulative methylprednisolone (MethPD 1yr) and total steroid load (TotCORT 1yr = PDN 1yr +MethPD 1yr), following conversion of each methylprednisolone dose to an equivalent prednisone dose (4 mg of methylprednisolone = 5 mg of prednisone).[2]

CMV pp65 Antigen Detection

The CMV pp65 antigenemia immunofluorescence assay was used for the qualitative detection and identification of the lower matrix protein pp65 of CMV in isolated peripheral blood leukocytes. The immediate-early CMV antigen pp65 was investigated in all patients at 1, 6 and 12 months post-HT. Antigen detection was performed at any given time if CMV infection was clinically suspected.

Echocardiography

An echocardiogram was obtained from all patients within 24 hours of coronary angiography. M-mode measurements of the end-diastolic thickness of the interventricular septum and left ventricular posterior wall were taken from the parasternal long-axis view. Left ventricular hypertrophy was defined as diastolic septal or posterior wall thickness >11 mm. Measurements were performed independently by two observers blinded to clinical history and experimental data.

Angiography/Diagnosis of CAV

Cardiac catheterization was performed within 24 hours of CFR evaluation by CE-TTE in all 119 patients. Angiograms were reviewed by a cardiologist who was unaware of clinical and echocardiographic findings. Data were analyzed using the following qualitative grading system: Grade I, normal angiogram; Grade II, luminal irregularities, diameter reduction <30%; Grade III, diameter reduction <50%; Grade IV, diameter reduction ≤50% and/or diffuse narrowing of small vessels.[9] CAV was defined as presence of angiographic changes of Grade II or greater,

and significant CAV as Grade IV changes. Stenosis was considered critical if it reached ≥70%. In an attempt to better quantify the extent of CAV, the following indexes were computed and used as markers of CAV diffusion/severity: total index of stenosis (SDI), and total index of stenosis normalized for the number of diseased segments (SDI/nS), as previously described.[2]

Coronary Flow Velocity Reserve Assessment

We used CE-TTE for coronary flow evaluation before and after adenosine infusion This method has been described in detail in our previous reports.[3,4,10] Briefly, a modified apical 2-chamber view was applied to carefully search for color-coded blood flow as a guide to obtain a pulsed-wave Doppler diastolic flow recording in the distal portion of the LAD, at baseline and after intravenous infusion of adenosine (140 ug/kg/min, for 5 minutes). In most patients, an optimal Doppler signal can be detected even in the case of a sub-optimal color imaging, allowing reliable coronary flow definition. In rare cases, if the Doppler signal is visualized with poor definition, the same procedure can be attempted using Levovist (Schering AG, Berlin, Germany) as a Doppler signal enhancer, infused at a concentration of 300 mg/ml, at a rate of 0.5 to 1 ml/min. Cardiac drugs were not interrupted before testing, although all methylxanthine-containing substances or medications were withheld 48 hours before the study. CFR was determined as the ratio of maximum diastolic hyperemic peak flow velocity to diastolic resting flow velocity, based on studies by an experienced echocardiographer (F.T.) who was blinded to the angiographic and clinical data (Figure 1). Our previous studies demonstrated a high reproducibility for measurement of CFR by TTE.[3,4,10] A cutoff point of >2.5 was selected to define a normal CFR in the present study. This threshold was based on the results of studies that demonstrated a prognostic impact of this value both in HT recipients as well as in patients having undergone successful coronary angioplasty. [11,12]

Statistical Methods

Continuous variables are expressed as mean ± standard deviation. Student's *t*-test for independent samples, chi-square test and Fisher's exact test were used as appropriate. When comparing several groups, 1-way analysis of variance (ANOVA) was followed by the Student–Newman–Keuls post hoc test for statistical significance. Pearson's test was used for bivariate correlations of CFR with clinical conditions. Multiple linear regression analysis was performed between CFR and significant or marginally significant (p <0.1) risk factors or clinical conditions upon univariate analysis. Intra- and inter-observer measurement variability and reproducibility of CFR were evaluated by linear regression analysis. This was expressed by the

correlation coefficient (r) values and standard error of estimates (SEE), and by means of the intraclass correlation coefficients (ICCs), with reproducibility being considered satisfactory if the ICC was between 0.81 and 1.0. Data were analyzed with SPSS software, version 13.0 (SPSS, Inc., Chicago, IL). Statistical significance was assumed if the null hypothesis could be rejected at $p < 0.05$. The investigators had full access to the data and take full responsibility for its integrity.

Results

Baseline Clinical and Diagnostic Features

The baseline features of recipients and donors are shown in Table 1. Echocardiographic regional wall motion abnormalities were not detected. Age and time from HT were comparable in patients with and without abnormal angiography (49 ± 11 vs 51 ± 13 years [p =0.5] and 8 ± 3 vs 7 ± 3 years [p = 0.4], respectively). Ejection fraction was normal in all patients (73 ± 8%). All patients studied were maintained on a cyclosporine (95%) or tacrolimus (5%) and azathioprine (70%) or mycophenolate mofetil–based (30%) immunosuppression protocol. Steroids were withdrawn in 53% of patients at 12 months after transplantation. Eighty-five percent of patients were treated with statins, 63% with aspirin, 10% with ticlopidine, 40% with calcium antagonists, 19% with beta-blockers and 42% with angiotensinconverting enzyme (ACE) inhibitors. Forty-five (38%) angiograms were classified as abnormal, of which 21 (47%) had Grade II lesions, 9 (20%) Grade III lesions and 15 (33%) Grade IV lesions. Ten (22%) patients had LAD critical stenosis and 12 (26%) had diffuse narrowing of small vessels. The left circumflex and right coronary artery were involved in 30 (66%) and 21 (46%) patients, respectively. The mean values for SDI and SDI/nS were 15 ± 13 and 7.2 ± 5, respectively.

CFR Evaluation

CE-TTE studies were always well tolerated and easily performed, with a need for Levovist infusion in only 11 (9%) patients to obtain an optimal Doppler signal. Overall, during adenosine infusion, heart rate increased compared with baseline (92 ± 13 vs 86 ± 11 beats/min, $p < 0.0001$) and systolic blood pressure decreased (126 ± 21 vs 136 ± 19 mm Hg, $p < 0.0001$) as did diastolic blood pressure (80 ± 13 vs 85 ± 12 mm Hg, $p < 0.0001$), whereas peak diastolic velocity in the LAD increased (75 ± 23 vs 28 ± 9 cm/s, $p < 0.0001$). In the entire patient group CFR was 2.79 ± 0.8 (range 1.08 to 4.9).

Relation Between CFR and Clinical Characteristics in Entire Patient Study Group

CFR was lower in men, in patients with CAV and in those with LAD stenosis ≥70%, as well as in patients with ischemic heart disease pre-HT (Figure 2A, top panel). CFR was inversely related to time from HT, SDI, SDI/nS, left ventricular end-diastolic pressure and interventricular septum thickness (Table 2). CFR was directly related to ejection fraction and tended to be related to cumulative cyclosporine doses (Table 2). No relation was found between CFR and rejection scores (Figure 3A, top panel).

Relation Between CFR and Clinical Characteristics in Patients Without CAV

In patients without CAV, CFR was lower in diabetic patients (Figure 2B, bottom panel), inversely related to TRS and sev TRS (Figure 3B, bottom panel), and was marginally significantly related to RS 1yr, sev RS 1yr and total number of rejections (Table 2). TRS and sev TRS were higher in patients with normal coronary angiography and abnormal CFR (Figure 4).

Relation Between CFR and CMV

In all patients, CFR is not significantly altered in CMVnegative HT recipients of CMV-positive hearts ($p = 0.6$) (Figure 5). CFR was also comparable in patients with and without documented CMV infection ($p = 0.8$) (Figure 6). Similar results were found in patients with normal coronary angiograms (data not shown).

Determinants of CFR by Multivariate Analysis

In the multivariate analysis, determinants of CFR were CAV diagnosis, SDI and SDI/nS, interventricular septum thickness and ischemic heart disease pre-HT (Table 3). In patients without angiographic CAV, only sev TRS was independently related to CFR (Table 4). If some variables are forced in the multivariate model because of their well-known documented effect on CFR (i.e., diabetes, hypertension, left ventricular end-diastolic pressure, etc.), then sev TRS remains the only independent determinant of CFR in patients with normal coronary angiography (data not shown).

Intra- and Inter-observer Reproducibility

Intra- and inter-observer reproducibilities of CFR measurements were assessed by repeating the CFR evaluation twice, 1 hour apart, by the same operator (F.T.) in a subgroup of 35 patients and

by another operator (E.O.) in a subgroup of 58 patients, respectively. The intra-observer reproducibility was high (r=0.97, SEE=0.12); ICC was 0.985. The inter-observer reproducibility was also high (r=0.96, SEE=0.14); intraclass correlation coefficient was 0.976.

Discussion

This study demonstrates, for the first time, that rejection score is an independent determinant of CFR in HT patients. In addition, recognized determinants of CFR have been confirmed.[7] CAV is a diffuse process involving the entire coronary circulation, including microvessels.[2] In the present study, CFR impairment in patients with CAV may have been related by hemodynamically significant LAD stenosis. Indeed, it has been shown in several studies that endothelium-dependent and -independent CFR is reduced in patients with CAV.[3,4,13] We found that, although CFR reduction was associated with LAD stenosis of ≥70% according to univariate analysis, a flow-limiting stenosis was not an independent determinant of CFR. A major contribution of non-significant LAD stenosis to overall CFR reduction is unlikely, since epicardial coronary arteries physiologically determine only <10% of the overall coronary vascular resistance.[14] This suggests that CFR reduction may reflect microvascular involvement, even in angiographically visible CAV. Potential explanations for the increased coronary resistance include: a reduced cross-sectional area in resistance vessels as CAV progresses; or an insufficient collateral function, as collateral vessels are not common in HT patients.[15] Vascular lesions are the result of cumulative endothelial injury induced both by alloimmune responses and by non-specific alloimmune-independent insults.[2]

Male gender and ischemic heart disease pre-HT were both CFR determinants. These findings may reflect the influence of recipient pro-ischemic risk factors in CAV progression/modulation.[2] Classic cardiovascular risk factors, such as diabetes, may enhance vascular inflammation by inducing endothelial dysfunction. A novel finding in our study is that severe rejection scores were independently associated with CFR reduction in patients without angiographic CAV. Others investigators failed to identify such a relationship,[11,16] which may have been due to the small number of patients,[11] short follow-up,[16] and lack of quantification of individual rejection burden in terms of rejection score.[16] In addition, multivariate analysis was either not used[16] or applied to inadequate numbers of patients.[11] Our findings show that early graft vascular lesions seem to be confined mostly to small coronary arteries and arterioles. Our novel finding supports the hypothesis that microvasculopathy is an immune-mediated phenomenon, similar to epicardial CAV.[2] CFR reduction seems to have been due to a previous

rejection crisis, which could have induced small areas of fibrotic scars in the myocardium, resulting in an impairment of the capacity of arteriolar vasodilation by extravascular compression, or medial fibrosis or reduction of the number of vessels.

Assessment of microvascular function has been shown to be of predictive value after HT.[4] Predominant allograft microvascular dysfunction is detectable in 15% of patients after HT.[17] The ability to detect and distinguish changes in epicardial and microvascular function may aid in identifying modifiable factors that lead to CAV. Coronary angiography and intravascular ultrasound are not well suited to detect such abnormalities. Conversely, microvascular changes may be easily monitored by CE-TTE. In keeping with our results, Fearon et al recently demonstrated that, in HT recipients without angiographically significant CAV, predominant microcirculatory dysfunction was present, based on normal fractional flow reserve and abnormal CFR.[17] Insults contributing to endothelial injury after HT may include pathogens such as CMV.[1] Our finding that CFR was independent of both CMV serostatus and previous CMV infection is not surprising if we consider that adenosine is an endothelium-independent vasodilator. In support of our findings, other investigators found that endothelium-independent vasomotor function was not significantly altered in CMV-negative HT recipients of CMV-positive hearts. Those same investigators found that CFR was comparable between patients with and without documented CMV infection.[18] However, CMVseronegative recipients of seropositive hearts are of highest risk for development of endothelial dysfunction in small coronary vessels and have more cardiovascularrelated events and death during follow-up.[18] Documented CMV infection episodes are associated with deterioration of epicardial endothelial function, whereas endothelial dysfunction extends to the microcirculation in patients with symptomatic infections.[18] The recruitment of circulating monocytes infected with CMV into allograft coronary vessels is the most likely mechanism by which CMV becomes associated with endothelial dysfunction.

Study Limitations

According to some but not all studies, acute rejection may affect CFR.[19,20] In the present study on stable, long-term HT patients with preserved ejection fraction, no endomyocardial biopsies were taken. The possibility that our CFR findings may be related to undetected acute rejection seems unlikely. Acute rejection frequency is low after the first year, and in none of our patients was acute rejection clinically suspected or diagnosed in the following months. The measurement of coronary flow velocity by CE-TTE is only applicable to the distal part of the LAD, although a recent study reported the feasibility of measuring CFR in the posterior descending coronary

artery.[21] However, CE-TTE–derived CFR measurements relate to microcirculatory function, and thus the choice of the sample vessel would not have influenced the results. Some studies have considered intravascular ultrasound as the "gold standard" for CAV diagnosis[17,22]; however, intravascular ultrasound is often technically difficult or not feasible in advanced disease and is certainly unsuited for long-term follow-up. Moreover, some investigators demonstrated that, in patients without angiographically overt coronary disease, the degree of epicardial intimal thickening as quantified by intravascular ultrasound does not predict the adenosine vasodilator response, when determined by commonly used parameters such as CFR.[23,24] Routine detection of the immediate-early CMV antigen pp65 was performed only during the first 12 months. It is therefore possible that some sub-clinical CMV infection episodes could have been detected with a longer follow-up. In conclusion, the measurement of a lower coronary flow rate has been shown to be a reliable marker for CAV-related major cardiac events.[4,11] The identification of CFR determinants, as shown here, should make it possible to design and test new therapeutic and preventive strategies aimed at modifying the time-dependent CFR reduction post-HT. This may lead to improved outcomes for patients.

References

1. Taylor DO, Edwards LB, Boucek MM, et al. The registry of the International Society for Heart and Lung Transplantation: 24th official adult heart transplant report—2007. J Heart Lung Transplant 2007;26:769–81.

2. Caforio ALP, Tona F, Belloni-Fortina A, et al. Immune and nonimmune predictors of cardiac allograft vasculopathy onset and severity: multivariate risk factor analysis and role of immunosuppression. Am J Transplant 2004;4:962–70.

3. Tona F, Caforio ALP, Montisci R, et al. Coronary flow reserve by contrast-enhanced echocardiography: a new noninvasive diagnostic tool for cardiac allograft vasculopathy. Am J Transplant 2006;6:998–1003.

4. Tona F, Caforio ALP, Montisci R, et al. Coronary flow velocity pattern and coronary flow reserve by contrast-enhanced transthoracic echocardiography predict long-term outcome in heart transplantation. Circulation 2006;114(suppl I):I-49 –55.

5. Heroux AL, Silverman P, Costanzo MR, et al. Intracoronary ultrasound assessment of morphological and functional abnormalities associated with cardiac allograft vasculopathy. Circulation 1994;89:272–7.

6. Shubert S, Abdul-Khaliq H, Wellnhofer E, et al. Coronary flow reserve measurement detects transplant coronary artery disease in pediatric heart transplant patients. J Heart Lung Transplant 2008;27:514–21.

7. Klauss V, Spes C, Rieber J, et al. Predictors of reduced coronary flow reserve in heart transplant recipients without angiographically significant coronary artery disease. Transplantation 1999;68:1477–81.

8. Caforio ALP, Belloni-Fortina A, Piaserico S, et al. Skin cancer in heart transplant recipients: risk factor analysis and relevance of immunosuppressive therapy. Circulation 2000;102(suppl III):III-222–7.

9. Spes CH, Klauss V, Mudra H, et al. Diagnostic and prognostic value of serial dobutamine stress echocardiography for noninvasive assessment of cardiac allograft vasculopathy: a comparison with coronary angiography and intravascular ultrasound. Circulation 1999;100:509–15.

10. Caiati C, Montaldo C, Zedda N, et al. New noninvasive method for coronary flow reserve assessment: contrast-enhanced transthoracic second-harmonic echo Doppler. Circulation 1999;99:771–8.

11. Weis M, Hartmann A, Olbrich HG, et al. Prognostic significance of coronary flow reserve on left ventricular ejection fraction in cardiac transplant recipients. Transplantation 1998;65:103–8.

12. Ruscazio M, Montisci R, Colonna P, et al. Detection of coronary restenosis after coronary angioplasty by contrast-enhanced transthoracic echocardiographic Doppler assessment of coronary flow velocity reserve. J Am Coll Cardiol 2002;40:896–903.

13. Muehling OM, Wilke NM, Panse P, et al. Reduced myocardial perfusion reserve and transmural perfusion gradient in heart transplant arteriopathy assessed by magnetic resonance imaging. J Am Coll Cardiol 2003;42:1054–60.

14. Hoffman JI. Maximal coronary flow and the concept of coronary vascular reserve. Circulation 1984;70:153–9.

15. Marcus ML, Chilian WM, Kanatsuka H, et al. Understanding the coronary circulation through studies at the microvascular level. Circulation 1990;82:1–7.

16. Nitenberg A, Aptecar E, Benvenuti C, et al. Effects of time and previous acute rejection episodes on coronary vascular reserve in human heart transplant recipients. J Am Coll Cardiol 1992;20:1333–8.

17. Fearon WF, Nakamura M, Lee DP, et al. Simultaneous assessment of fractional and coronary flow reserves in cardiac transplant recipients: physiologic investigation for transplant recipients (PITA study). Circulation 2003;108:1605–10.

18. Petracopoulou P, Kubrich M, Pehlivanli S, et al. Citomegalovirus infection in heart transplant recipients is associated with impaired endothelial function. Circulation 2004;110(suppl II):II-207–12.

19. Nitenberg A, Tavolaro O, Loisance D, et al. Severe impairment of coronary flow reserve during rejection in patients with orthotopic heart transplant. Circulation 1989;79:59–65.

20. Wolford TL, Donohue TJ, Bach RJ, et al. Heterogeneity of coronary flow reserve in the examination of multiple individual allograft coronary arteries. Circulation 1999;99:626–32.

21. Voci P, Pizzuto F. Imaging of the posterior descending coronary artery. The last frontier in echocardiography. Ital Heart J 2001;2:418–22.

22. Eisen HJ, Tuzcu EM, Dorent R, et al. RAD B253 Study Group. Everolimus for the prevention of allograft rejection and vasculopathy in cardiac-transplant recipients. N Engl J Med 2003;349:847–58.

23. Caracciolo EA, Wolford TL, Underwood RD, et al. Influence of intimal thickening on coronary blood flow response in orthotopic heart transplant recipients. A combined intravascular Doppler and ultrasound imaging study. Circulation 1995;96(suppl II):II-182–90.

24. Klauss V, Ackermann K, Henneke KH, et al. Epicardial intimal thickening in transplant coronary artery disease and resistance vessel response to adenosine. A combined intravascular ultrasound and Doppler study. Circulation 1997;96(suppl II):II-159–64.

Figure 1

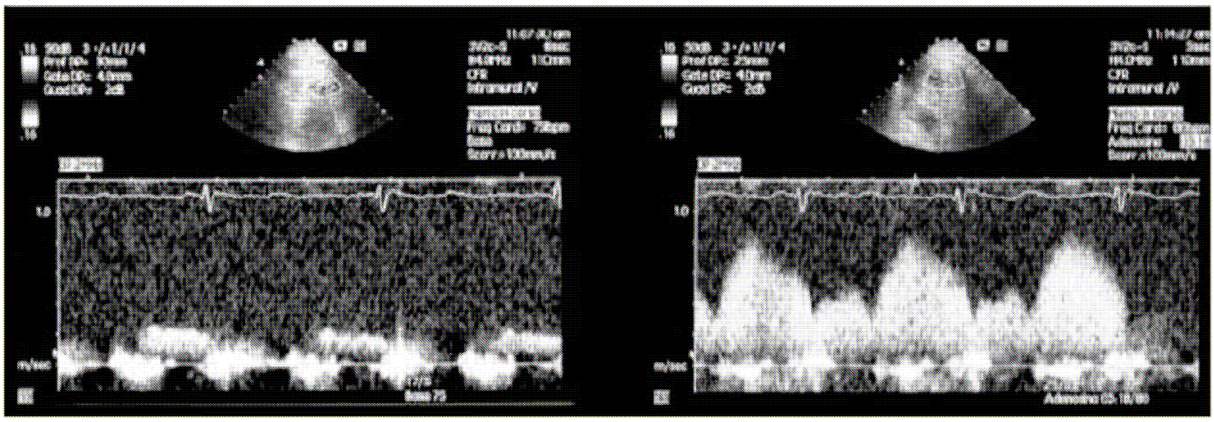

Figure 1: Coronary flow response to adenosine- Coronary flow velocity at rest (left) and during adenosine infusion (right) by transthoracic echocardiography

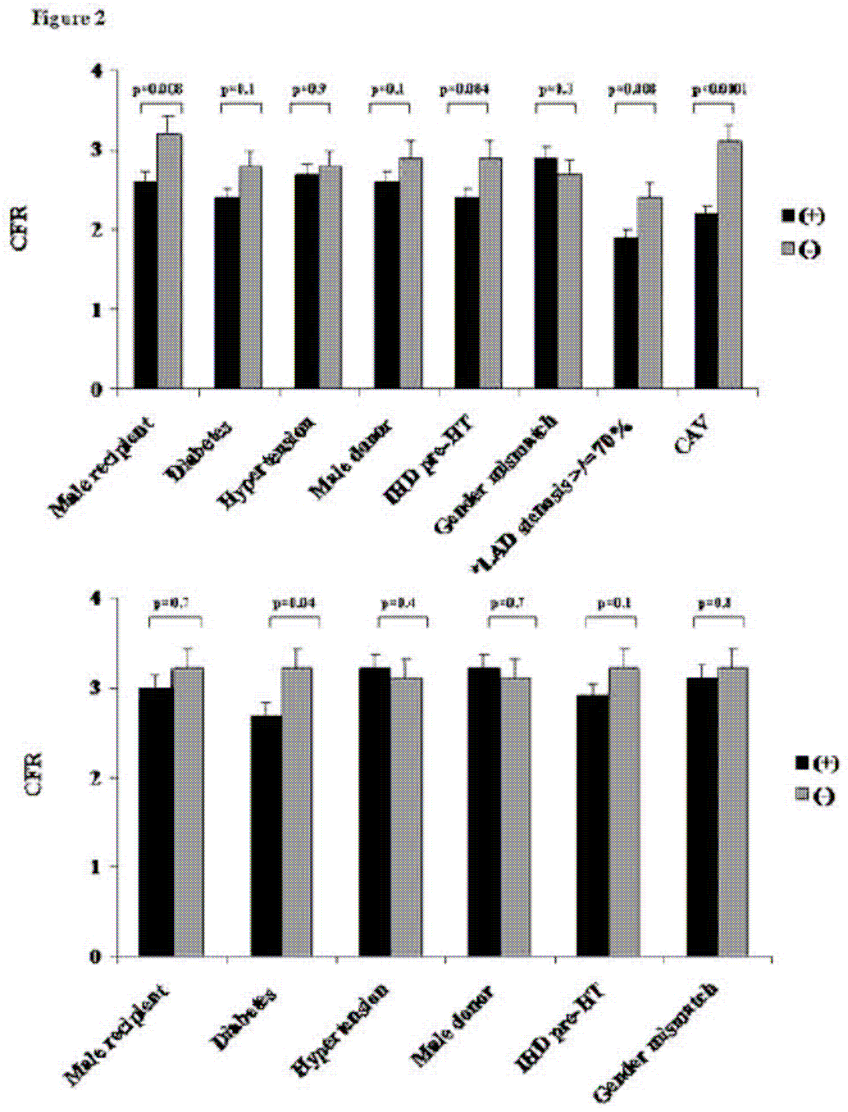

Figure 2: **Relation between CFR and clinical characteristics in the entire patients study group and in patients without CAV**- CFR in the whole patient population (A) and in patients with normal coronary angiography (B) divided according to the presence (+) or the absence (-) of risk factors and clinical conditions considered in the study protocol. *n=45

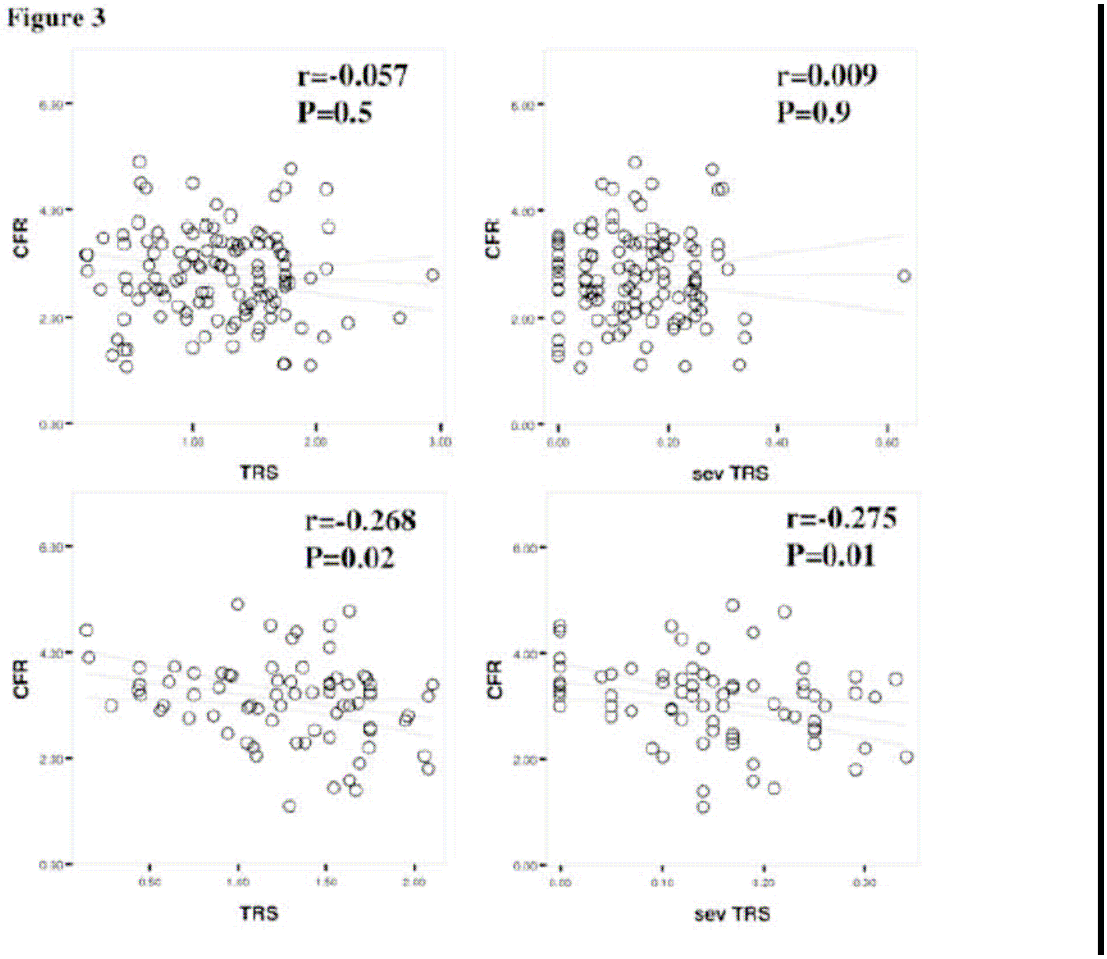

Figure 3: Relation between CFR and rejection scores- Bivariate correlations of CFR with TRS and sev TRS in the whole patient population (A) and in patients with normal coronary angiography (B).

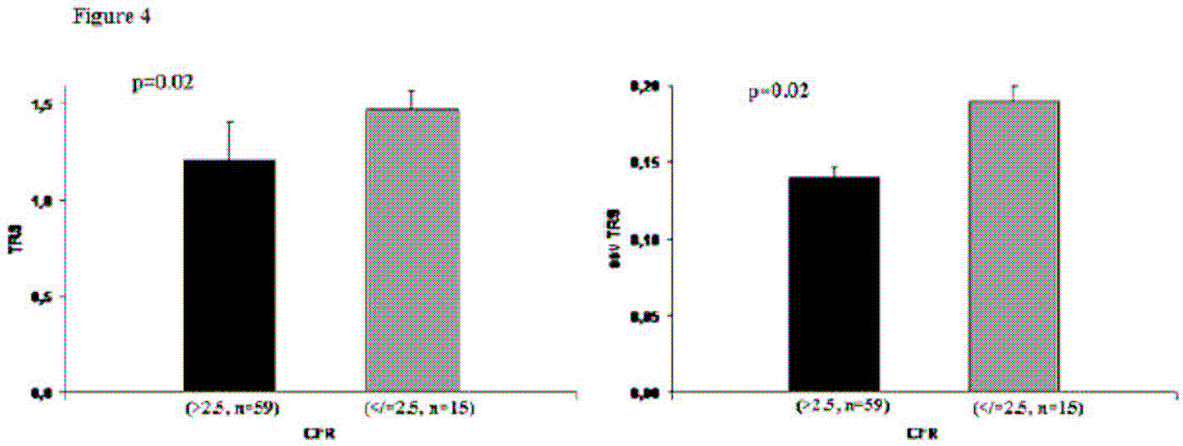

Figure 4: **Rejection scores in patient without CAV and with abnormal CFR-** Levels of TRS and sev TRS in patients without allograft vasculopathy divided according to CFR ≤2.5 or >2.5

Figure 5

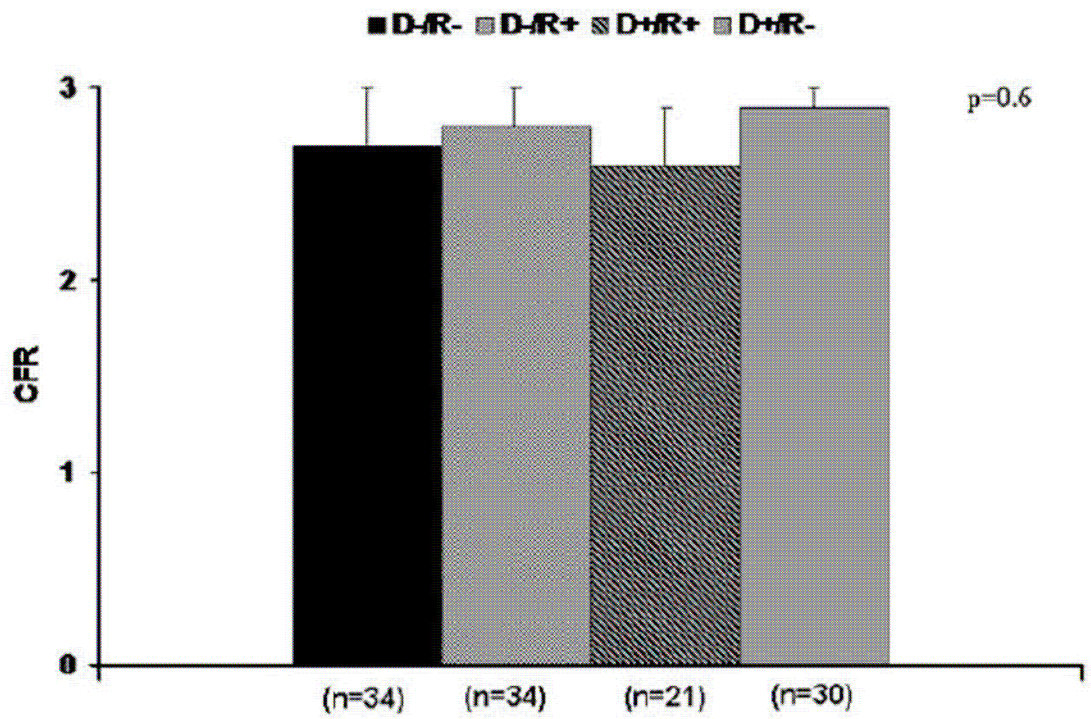

Figure 5: **CFR and CMV serostatus**- CFR is not significantly altered in CMV-negative transplant recipients of CMV-positive hearts.

Figure 6

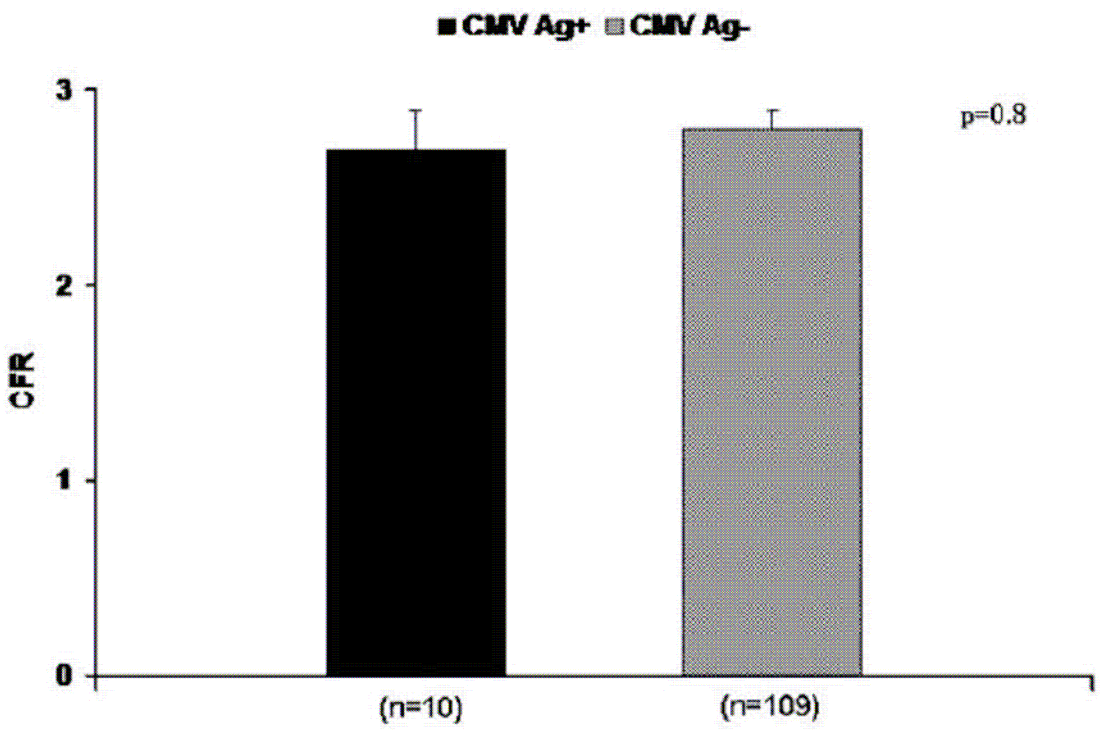

Figure 6: **CFR and previous CMV infection**- CFR was comparable between patients with and without documented CMV infection.

TABLE 1: Recipient and donor characteristics

	All patients (n=119)
Time from HT (yr)	8 ± 5
Ischemic time (min)	179 ± 46
Cholesterol (mmol/L)	5.4 ± 0.9
Triglycerides (mmol/L)	1.76 ± 0.8
Age at HT (yr)	50 ± 12
Male gender (%)	81
Interventricular septum thickness (mm)	12 ± 0.5
Posterior wall thickness (mm)	11 ± 0.8
LVEDP (mm/Hg)	11 ± 4
LVEF (%)	73 ± 8
Diabetes (%)	15
Hypertension (%)	64
Heart rate (beats/min)	86 ± 11
Systolic blood pressure (mm/Hg)	136 ± 19
Diastolic blood pressure (mm/Hg)	85 ± 12
CAV (%)	38
SDI *	15 ± 13
SDI/nS *	7.2 ± 5
TRS	1.21 ± 0.5
RS 1yr	1.3 ± 0.6
sev TRS	0.14 ± 0.1
sev RS 1yr	0.16 ± 0.1
Total number of rejections	3.1 ± 2.5

Rejections in the first year	2.6 ± 2.2
Donor age (yr)	35 ± 12
Donor male gender (%)	62
Gender mismatch (%)	25
IHD pre-HT (%)	33
CsA at 3 months (mg/Kg)	598 ± 207
CsA at 6 months (mg/Kg)	1063 ± 432
CsA at 12 months (mg/Kg)	1970 ± 788
Aza at 3 months (mg/Kg)	143 ± 76
Aza at 6 months (mg/Kg)	266 ± 158
Aza at 12 months (mg/Kg)	524 ± 337
PDN at 3 months (mg/Kg)	14 ± 13
PDN at 6 months (mg/Kg)	25 ± 19
PDN at 12 months (mg/Kg)	40 ± 31
MethPD 1yr (mg/Kg)	72 ± 60
TotCORT 1yr (mg/Kg)	142 ± 92
Donor CMV (-)/Recipient CMV(-) (%)	29
Donor CMV (-)/Recipient CMV(+) (%)	29
Donor CMV (+)/Recipient CMV(-) (%)	25
Donor CMV (+)/Recipient CMV(+) (%)	17
CMV pp65 Ag + (%)	8

* Data in patients with angiographic cardiac allograft vasculopathy (n=45)

Aza= Azathioprine; CsA= Cyclosporine A; IHD= ischemic heart disease; LVEDP= left ventricular end-diastolic pressure; LVEF= left ventricular ejection fraction; PDN= Prednisone. See text for other abbreviation

TABLE 2: Bivariate correlations of CFR with clinical conditions

	All patients (n=119)		Patients without CAV (n=74)	
	r	p	r	p
Time from HT	-0.248	0.01	0.06	0.6
SDI	-0.390	<0.0001	...	...
SDI/nS	-0.366	<0.0001	...	...
LVEDP	-0.291	0.01	-0.001	0.9
LV EF	0.323	0.002	-0.011	0.9
Heart rate	-0.165	0.07	0.072	0.5
Interventricular septum thickness	-0.308	0.007	-0.077	0.6
Posterior wall thickness	0.121	0.2	-0.124	0.4
Age at HT	0.007	0.9	-0.007	0.9
Cholesterol	-0.044	0.7	-0.128	0.3
Triglycerides	-0.134	0.2	0.020	0.8
Donor age	-0.178	0.1	-0.137	0.3
Ischemic time	-0.033	0.7	-0.062	0.6
TRS	-0.057	0.5	-0.269	0.02
RS 1yr	-0.078	0.3	-0.214	0.06
sev TRS	0.009	0.9	-0.275	0.01
sev RS 1yr	-0.034	0.7	-0.203	0.08
Total number of rejections	-0.095	0.3	-0.261	0.05
Rejections in the first year	-0.111	0.2	-0.157	0.2
Systolic blood pressure	-0.120	0.2	-0.156	0.2
Ddiastolic blood pressure	-0.127	0.2	-0.153	0.2
CsA at 3 months	0.200	0.07	0.208	0.1

CsA at 6 months	0.191	0.09	0.267	0.09
CsA at 12 months	0.192	0.09	0.260	0.1
Aza at 3 months	0.072	0.5	0.138	0.3
Aza at 6 months	0.157	0.1	0.271	0.08
Aza at 12 months	0.132	0.2	0.261	0.1
PDN at 3 months	0.035	0.7	0.026	0.8
PDN at 6 months	0.056	0.6	0.114	0.4
PDN at 12 months	0.030	0.7	0.070	0.6
MethPD 1yr	-0.169	0.1	-0.046	0.7
TotCORT 1yr	-0.013	0.9	0.146	0.3

Abbreviations as in table 1 and in the text

TABLE 3: Multiple linear regression analysis between CFR (dependent variable) and risk factors or clinical conditions (independent variables) (n=119)

Variable	B ± SE	β	p
CAV	-0.736 ± 0.20	-0.489	0.001
SDI	-0.054 ± 0.013	-0.855	<0.0001
SDI/nS	0.110 ± 0.035	-0.720	0.003
Time from HT	-0.007 ± 0.017	-0.043	0.6
Male gender	-0.054 ± 0.251	-0.024	0.8
Heart rate	0.003 ± 0.007	0.046	0.6
IHD pre-HT	-0.363 ± 0.154	-0.222	0.02
Interventricular septum thickness	0.167 ± 0.067	0.233	0.01
LVEF	0.007 ± 0.008	0.101	0.3
LVEDP	-0.005 ± 0.016	-0.030	0.7
LAD stenosis ≥ 70%	-0.340 ± 0.251	-0.146	0.2
ANOVA p		<0.0001	
R^2		0.542	

Abbreviations as in table 1 and in the text

TABLE 4: Multiple linear regression analysis between CFR (dependent variable) and risk factors or clinical conditions (independent variables) in patients with normal coronary angiograms (n=74)

Variable	B ± SE	β	p
TRS	-0.101 ± 0.363	-0.057	0.7
RS 1yr	-0.006 ± 0.849	-0.004	0.9
sev TRS	-2.805 ± 1.137	-0.316	0.01
sev RS 1yr	2.811 ± 2.383	0.363	0.2
Total number of rejections	-0.004 ± 0.119	-0.011	0.9
ANOVA p	0.01		
R^2	0.136		

Abbreviations as in the text

Coronary Flow Reserve by Transthoracic Echocardiography Predicts Epicardial Intimal Thickening in Cardiac Allograft Vasculopathy

Cardiac allograft vasculopathy (CAV) is the leading cause of mortality after heart transplantation (HT) [1]. In CAV both epicardial coronary vessels and the microvasculature may be affected [2]. Histopathologically CAV is characterized by discrete intracellular endothelial changes and diffuse concentric intimal thickening [3]. Coronary angiography is the most common tool of screening for CAV; however it is limited in detecting diffuse intimal thickening[4]. Intravascular ultrasound (IVUS) is more sensitive, but it requires some degree of expertise to perform and interpret the images, it is time consuming and expensive, and it only interrogates the epicardial coronary system. Coronary flow reserve (CFR) measurements by intracoronary Doppler flow wire may provide functional assessment of the microvasculature in CAV; however, coronary angiography, IVUS and intracoronary Doppler flow wire are invasive procedures. We have recently applied a new noninvasive technique based on contrast-enhanced transthoracic echocardiography (CE-TTE) for assessing CFR in the left anterior coronary descending artery (LAD) in HT patients [5-6]. CFR by CE-TTE has been shown to correlate with angiographically detectable coronary artery lesion severity as well as intracoronary Doppler flow wire measurements [7], and to stratify the risk of cardiac events in HT patients [6] . We assessed the diagnostic potential of CFR by CE-TTE in CAV detection defined by IVUS and to test whether the extent of intimal thickening affects coronary flow velocity during adenosine infusion in HT recipients with normal coronary angiograms.

Methods

Study Patients

We studied 22 consecutive HT recipients with normal coronary angiogram (20 male, aged 50 ± 7 years at HT, range 36 to 61, mean ischemia time 169 ± 37 minutes), at 6 ± 4 years post-HT. Our immunosuppression protocol consisted of Cyclosporin A, Azathioprine or Mycophenolate mofetil, and steroids (triple therapy) as previously detailed[2, 8]. Twenty-four healthy control subjects, matched for age and gender, were recruited from local community. In the control subjects, the absence of cardiovascular diseases was evaluated by a clinical history and

examination and, when available, echocardiography and coronary angiography. The study was approved by the institutional ethics committee, and all patients gave written, informed consent.

Echocardiography

An echocardiogram was obtained in all patients within 48 hours of coronary angiography. From the parasternal long axis view, M-mode measurements were performed to determine the end-diastolic thickness of the interventricular septum and the left ventricular posterior wall. Left ventricular hypertrophy was defined as a septal plus posterior wall thickness $\geq$ 24 mm [9]. Left ventricular ejection fraction was measured using Simpson's method. CFR was evaluated using CE-TTE before and after adenosine infusion. The method has been previously described in detail [7].

Contrast-Enhanced Transthoracic Doppler Echocardiography

Echocardiography was performed for coronary flow evaluation using CE-TTE before and after adenosine infusion, with an ultrasound system (Sequoia C256, Acuson, Mountain View, California) connected to a broad-band transducer with second harmonic capability (3V2c). All studies were continuously recorded on 0.5-in. (1.27-cm) S-VHS videotape. Briefly, CFR was measured in the distal portion of the LAD, firstly obtaining a modified foreshortened two-chamber view or, if a distal LAD flow recording was not feasible, using a low parasternal short-axis view of the base of the heart [7]. If the angle between color flow and the Doppler beam was $>20^{o}$, angle correction was performed using the software package included in the software unit. Administration of the contrast agent (Levovist, Schering AG, Berlin, Germany) was performed both before and during adenosine intravenous administration [5].

Coronary Flow Velocity Reserve Assessment

All patients had Doppler recordings of the LAD with adenosine infusion at a rate of 0.14 mg/kg per min for 5 min [5]. Cardiac drugs were not interrupted before testing, although all methylxantine-containing substances or medications were withheld 48 h before the study. CFR in the LAD was calculated, as the ratio of hyperemic to basal diastolic flow velocity, by an experienced echocardiographer, blind to angiographic and clinical data. For each variable in the CFR calculation, the highest 3 cycles were averaged [5].

IVUS/Diagnosis of CAV

After anti-coagulation with 5000–10 000 units of heparin and infusion of 200 μg intra-coronary nitroglycerin, standard coronary angiography (evaluating at least six planes of left coronary artery) was performed in order to exclude LAD stenosis, which might contraindicate IVUS performance [10]. IVUS images were obtained using a commercially available 3F IVUS catheter (Volcano Corporation, Rancho Cordova, CA or Atlantis SR Pro 2, Boston Scientific, Natick, Massachusetts, USA) placed under fluoroscopic guidance to the periphery of the LAD. Automatic pullback (1 mm/sec motorized device) was performed and images were stored in a CD-ROM for subsequent analysis off-line by an experienced observer, who was always blinded to the patients' characteristics and echocardiographic findings. External elastic membrane and lumen cross-sectional areas were identified and measured by manual planimetry. Following American College of Cardiology recommendations [11], we measured maximal intimal thickness (MIT); the average MIT was derived by averaging the MIT from the all sites examined. CAV was defined as MIT ≥0.5 mm [11.] The area bounded by the external elastic membrane was considered the external vessel wall area and the difference between the external elastic membrane area and the lumen area was calculated to give the intimal (otherwise known as intima-media) area. An intimal index was calculated as intima area/(intima + lumen area). The luminal, vessel and plaque volumes (in cubic millimeters) of each segment were calculated as cross-sectional areas (lumen area, vessel area and plaque area) x segment length of 2 mm. Total plaque volume was obtained by adding up the measurements of all vascular segments. Since *de novo* graft atherosclerosis often has a diffuse distribution, unlike focal donor-related lesions, we averaged the measurements obtained from serial cross-sectional images taken every 2 mm of proximal 30 mm of LAD to minimize bias in the matching of individual sites in artery wall evaluation [12]. Vascular sites with major side branches or calcifications occupying a vessel circumference of more than 30% were excluded from quantification. To assess the reproducibility of IVUS measurements, we performed two subsequent motorized pullbacks of the IVUS catheter during the same IVUS examination. Mean values of total vessel and lumen areas were calculated on the basis of these two recordings, matching 28 coronary segments. The intra-observer error for vessel and lumen area analysis was 0.46 ± 0.61% and 1.95 ± 1.14%, respectively. The correlation coefficient between the two sets of measurements was 0.95 for vessel wall and 0.92 for lumen areas. The inter-observer error for vessel and lumen analysis was 1.66 ± 1.25% and 3.01 ± 2.2%, respectively. The correlation coefficient between the measurements performed by two different observers was 0.99 for both vessel wall and lumen areas. These reproducibility assessments are in line with previous reports [13].

Fractional Flow Reserve Measurements

Fractional flow reserve (FFR), defined as the mean distal coronary pressure, measured with the pressure wire (Radi Medical Systems), divided by the mean proximal coronary pressure, measured with the guiding catheter, at maximum hyperemia, was measured after administering 48 μg of intracoronary adenosine. The lower limit of the normal range for FFR was below 0.94 [14].

Statistical Analysis

Results are expressed as mean ± standard deviation. CFR distribution was assessed by Shapiro-Wilk test, and it was not significantly different from normality (p=0.142). Student's t test and chi-square test were used as appropriate. Sensitivity, specificity, positive and negative predictive values were determined according to standard definitions. IVUS evidence of CAV was taken as the positive reference standard. Receiver operating characteristics (ROC) curve analysis was generated to test the predictive discrimination of patients with and without CAV. Correlation were sought by use of least-squares regression analysis. Intraobserver and interobserver reproducibilities of CFR were evaluated by linear regression analysis and expressed as correlation of coefficients (r) and standard error of estimates (SEE), and by the intraclass correlation coefficient. Reproducibility is considered satisfactory if the intraclass correlation coefficient is between 0.81 and 1.0. Intraobserver and interobserver reproducibility measurements were calculated in all 22 patients. Probability levels of <0.05 were considered statistically significant. Data were analyzed with SPSS software version 13.0 (Chicago, SPSS, Inc., Chicago, Illinois). The authors had full access to and take full responsibility for the integrity of the data. All authors have read and agree to the manuscript as written.

Results

Baseline Clinical and Diagnostic Features

All patients had normal coronary angiograms. Of the 22 IVUS 10 (45%) were classified as abnormal (MIT ≥0.5 mm) (group A), 12 (55%) had normal coronaries (MIT <0.5 mm) (group B). Time from HT was longer in group A (8 ± 3 vs 6 ± 2 years, p=0.042). Group A was associated with donor male gender (76% vs 46%, p=0.02). Recipient age at HT, male recipient gender, incidence of gender mismatch and donor age were similar in the two groups. Incidences of hypertension, diabetes and hypercholesterolemia after HT were comparable between the two groups. End diastolic dimensions, ejection fraction and mass were similar in the two groups. No

regional wall motion abnormalities were detected. All patients were on aspirin and statins. No differences in immunosuppressive and cardiovascular therapies were observed.

Comparison Between HT Recipients and Control Subjects

CFR in HT recipients was comparable to control subjects (3.1 ± 0.8 vs 3.4 ± 0.7, p=0.3). CFR in HT patients with MIT≥0.5 mm was lower than in controls (2.5 ± 0.6 vs 3.4 ± 0.7, p=0.001). CFR in HT patients without MIT≥0.5 mm was comparable to controls (3.7 ± 0.3 vs 3.4 ± 0.7, p=0.2). The prevalence of CFR≤2.5 was higher in HT patients compared to controls (27.3% vs 4.3%, p=0.04) and CFR is significantly lower in HT patients with CFR≤2.5 compared with the remaining patients' population (2 ± 0.4 vs 3.5 ± 0.4, p<0.0001).

IVUS and FFR Analysis

IVUS was performed successfully in all patients. The mean MIT was 0.7 ± 0.1 mm (range 0.03-1.8 mm) and intimal index was 0.13 ± 0.11 (range 0.05-0.55). MIT was higher in group A (1.16 ± 0.3 mm vs 0.34 ± 0.07 mm, p<0.0001). FFR was successfully measured in all patients. The mean FFR was 0.90 ± 0.05. In 64% of cases, the FFR was less than the normal threshold of 0.94. In only one patient (4.5%), FFR was ≤ 0.80, the upper boundary of the gray zone of the ischemic threshold, and in none the FFR was ≤ 0.75 (15). FFR was inversely related to MIT (r=-0.399, p=0.054).

Noninvasive CFR Evaluation

CE-TTE studies were always well tolerated. Overall, during adenosine infusion heart rate increased compared to baseline (90 ± 13 beats/min vs 83 ± 14 beats/min, p<0.0001), systolic blood pressure decreased (127 ± 18 mmHg vs 135 ± 22 mmHg, p=0.04), as well as diastolic blood pressure (77 ± 13 mmHg vs 82 ± 15 mmHg, p=0.03), whereas peak diastolic velocity in the LAD increased (82 ± 27 cm/s vs 26 ± 7 cm/s, p<0.0001). CFR was 3.1 ± 0.8 in the whole patient group. Adenosine peak diastolic velocity and CFR were lower in group A (68 ± 28 cm/s vs 100 ± 13 cm/s, p=0.01 and 2.5 ± 0.6 vs 3.7 ± 0.3, p<0.0001, respectively) (Figure 1). Figure 2 shows two representative examples.Severe (<2) CFR impairment was found in 3 out of 10 (30%) patients with MIT ≥0.5 mm, but in none of those with MIT <0.5 mm (p=0.04).

Diagnostic Power of CFR by CE-TTE in the Identification of MIT ≥0.5 mm

ROC analysis for separation of the presence or absence of MIT ≥0.5 mm was performed. The area under the ROC curve (AUC) of 0.903 has a SE of 0.022, yielding a 95% confidence interval of 0.941 to 1.026 ($p<0.0001$) (Figure 3). A cutpoint of ≤ 2.9, identified as optimal by ROC analysis, was 100% specific and 80% sensitive (positive predictive value= 100%, negative predictive value= 89%) (OR=8, p=0.007). Accuracy was 91%.

Intra and Interobserver Reproducibility of CFR by CE-TTE

Intraobserver and interobserver reproducibilities of CFR measurements were assessed by repeating CFR evaluation twice, 1 h apart, by the same operator (F.T.) in all patients and by another operator (E.O.) in all patients as well. The intraobserver reproducibility was high (r=0.95, SEE=0.11); intraclass correlation coefficient was 0.976. The interobserver reproducibility was also high (r=0.94, SEE=0.12); intraclass correlation coefficient was 0.968.

Relation Between CFR and Risk Factors for Coronary Allograft Vasculopathy

No relation between CFR and number or severity of previous rejections was observed. Moreover, there was no correlation between CFR and cytomegalovirus status or cytomegalovirus infection after HT. CFR was unrelated to pre-HT risk factors for coronary artery disease, donor/recipient gender, gender mismatch, and donor/recipient age at HT. The time from HT to CE-TTE and IVUS was unrelated to the degree of intimal thickening, resting and hyperaemic coronary flow velocity or CFR, and with FFR.

Relation between CFR by CE-TTE and MIT

CFR was inversely related to MIT ($y=-1.35x + 41$. $r=0.796$; SEE=0.23; $p<0.0001$) (Figure 4), to intimal index ($y=-2.5x + 4$. $r=0.454$; SEE=0.72; p=0.01) (Figure 5) and to plaque volume ($y=-0.009x + 4.2$. $r=0.775$; SEE=0.52; $p<0.0001$ (Figure 6).

To determine whether the intimal hyperplasia of epicardial arteries contributed to the CFR reduction, we separately analyzed patients with normal (≥0.94) FFR. In these patients CFR by CE-TTE was correlated with MIT ($y=-0.91x + 4.0$. $r=-0.814$; SEE=0.26; p=0.01). The correlation between CFR and MIT was no more present in patients with FFR <0.94 (p=0.151). MIT is minor and CFR is higher in patients with a FFR≥0.94 (0.26 ± 0.1 vs 0.81 ± 0.1, p=0.01 and 3.7 ± 0.3 vs 2.7 ± 0.7, p=0.002, respectively).

Relation between CFR by CE-TTE and FFR

CFR by CE-TTE correlated weakly with FFR (r=0.436, p=0.048). In 14% of cases , CFR by CE-TTE was ≤2. CFR and FFR were normal in 8 (36%) patients. FFR was abnormal and CFR normal in 11 (50%), and FFR and CFR were both abnormal in 3 (14%) patients. In one patient FFR was almost normal (0.93) and CFR was severely reduced (1.9), suggesting predominant microcirculatory dysfunction (Figure 7); in this patient MIT was 1 mm.

Discussion

This study demonstrates, for the first time, that CFR by CE-TTE in the LAD is a feasible and accurate noninvasive tool for the detection of MIT ≥0.5 mm identified by IVUS, the gold standard for the diagnosis of CAV in HT [11]. Many authors studied the relation between CFR and angiographic CAV. Some studies, mainly using invasive Doppler flow wire and endothelial-independent vasodilatation, showed that coronary vasodilatatory capacity is preserved in HT patients without angiographic CAV [16-17] and is impaired in patients with mild CAV [5] . Our group demonstrated that CFR by CE-TTE may offer promise as a simple, readily available, objective, noninvasive diagnostic tool for the detection of early and severe CAV [5] , and that a lower CFR is the main independent predictor of poor outcome in long-term clinically stable HT patients [6]. However, to the best of our knowledge, the present study is the first on CFR by CE-TTE and CAV in epicardial arteries defined by IVUS.

Echocardiography for the diagnosis of CAV defined by IVUS

Dobutamine for the assessment of wall motion and left ventricular size and function is the most frequently used technique. Spes et al. analyzed the diagnostic value of dobutamine stress echocardiography for noninvasive assessment of CAV [18]. They found that resting 2D echocardiography detects CAV defined by IVUS with a sensitivity of 57% and a specificity of 88%. Dobutamine stress echocardiography increased the sensitivity to 72%. Moreover, M-mode analysis increased the sensitivity of 2D rest and stress analysis to 85% but reduced the specificity to 82% [18]. In other studies, the sensitivity of stress echocardiography ranged between 15% and 79%, and the specificity ranged between 83% and 85%. In some, but not all studies, the accuracy was comparable to CFR by CE-TTE. However, dobutamine stress echocardiography depends on image quality and cannot be used in all patients. Furthermore, dobutamine echocardiography requires more experience than CFR by CE-TTE [6,18]. CFR by CE-

TTE is also more accurate for predicting cardiac events [6] and for verifying the functional significance of CAV.

Tissue Doppler imaging is another growing practice in the nontransplant population. The limited data in HT showed that there are significant changes for both systolic and diastolic parameters. Compared with patients without CAV, even those with CAV defined by IVUS showed significant differences for all parameters [19] . In particular, sensitivity for systolic and diastolic parameters ranged between 83% and 93%, and the specificity between 92% and 96% [19]. However this methodology have some limitations. All parameters should be corrected to the heart rate and this is time consuming. Moreover, the reproducibility of measurements can be very high for clinical use.

Influence of Intimal Thickening On Coronary Flow Reserve

The relation between CFR and epicardial intimal thickening has been previously studied by other methods [20-21]. CFR was not reduced in our whole patients population and in HT patients without MIT ≥0.5 mm. According with these results, previous studies described a normal endothelium-independent flow response in HT recipients using IVUS, intracoronary Doppler flow wire, or PET [20-21].

In our study, CFR was reduced in patients with CAV defined by IVUS, and average maximal intimal thickness and coronary flow reserve were significantly correlated. By using histology or Doppler flow wire, previous studies investigating whether microvasculopathy occurs in concordance with intimal hyperplasia in epicardial arteries yielded conflicting results [20-22]. However, these studies enrolled patients with either angiographic stenosis or with abnormal epicardial coronary physiology [14, 23]. The inverse correlation between MIT and CFR is evident in our patients with functionally normal epicardial coronary arteries (FFR≥0.94). This correlation may indicate that, in the early stage of CAV, both epicardial arteries and microvasculature are concordantly involved. To the best of our knowledge, this is the first study showing a relation between MIT and CFR by CE-TTE and identifying a CFR cutoff for the diagnosis of CAV defined by IVUS. However, CFR interrogates the entire coronary circulation (25% epicardial function and 75% microvascular system). Therefore, the concordance between CFR and MIT could be because there was little microvascular dysfunction, as evidenced by the fact that there were no patients with normal FFR and abnormal CFR (<2). The only way to distinguish between epicardial and microvascular dysfunction would be to have a simultaneous, invasive and independent assessment of the epicardial artery by measuring FFR and of the microvasculature by calculating the index of microvascular resistance (IMR) with a single

coronary pressure wire, as suggested in the PITA II study [24.] However this independent assessment is, by now, noninvasively impossible.

The combination of FFR and CFR by CE-TTE may provide information about the functional status of the coronary system that would not be available with either each measurement alone or coupled with IVUS. In particular, the combination of FFR and CFR by CE-TTE may identify patients with prevalent microvasculopathy. This finding is clinically relevant because the presence of microvascular dysfunction has been correlated with future development of epicardial allograft vasculopathy and cardiac events [6, 25]. Fearon et al., evaluating a new method for simultaneously measuring FFR and CFR with a single wire, achieved similar results [14.] In this very elegant study Fearon et al. showed that the assessment of FFR and CFR simultaneously help us to distinguish between abnormal epicardial and microvascular physiology and revealed that a different proportion of patients have predominant microvascular dysfunction. They conclude that the ability to detect and distinguish changes in epicardial and microvascular function in HT patients may aid in identifying modifiable factors that lead to transplant arteriopathy. We think that PITA study is a milestone on this topic. However these authors applied, even if very valid, an invasive method to study the coronary circulation. We aimed to identify a noninvasive method that allows us to reduce the number of coronary angiography and IVUS, and at the same time allows us to have information about the function of the coronary circulation. While remaining the undisputed superiority of invasive methods, every cardiac transplant group feels the need for a noninvasive method that can be applied to large populations of patients and at a lower cost compared to costs of invasive procedures and with low risk to the patient. We do not believe that the noninvasive CFR measurement may replace the invasive one, which allows us to have information also on FFR, but certainly it can be very useful in the clinical follow up of HT patients.

Study limitations

The sample size is relatively small, even if similar to previous studies [23-26]. Nevertheless, our study represent the largest CE-TTE and IVUS study after HT reported to date. A recent study suggests that progression of maximal intimal thickening ≥ 0.5 mm in the first year after HT appears to be a reliable marker for subsequent outcome [26]. In the current study, without serial examinations, the progression of intimal thickness and CFR can not be estimated. Therefore a larger study, with serial measurements would provide a better insight into the correlation between macro- and microvasculopathy. Currently, we are following these patients for cardiac events and by repeating IVUS and CFR by CE-TTE. A limitiation of this study is that the 1

mm/sec pull back of the IVUS catheter does not allow as accurate a determination of intimal thickening as 0.5 mm/sec.

CFR was not quantify invasively. Therefore we do not have a comparison of an invasive method of calculating CFR with the noninvasive method. However, CFR by CE-TTE in the LAD has already been validated against Doppler flow wire measurements by our group, thus the validation was beyond the aim of our study [7, 27].

The individual therapeutic protocol might have affected CFR. However, no differences in CFR were detected between patients who were taking calcium antagonists or ACE inhibitors and in patients with different immunosuppressive regimen. Acute rejection may affect CFR. In the current study, on stable long term HT recipients with preserved ejection fraction, no biopsies were taken. The possibility that CFR impairments are related to undetected acute rejection is unlikely. Acute rejection prevalence is low after the first year, and in none of our patients acute rejection was clinically suspected or diagnosed in the following months.

Conclusions

CFR assessment by CE-TTE is a novel noninvasive diagnostic tool in the detection of CAV defined as MIT ≥0.5 mm. The microvascular dysfunction, as assessed by CFR, correlates with intimal hyperplasia measured by IVUS in patients with physiologically normal epicardial coronary arteries, suggesting the possible concordant involvement of both macro- and microvascular system in early CAV. CFR by CE-TTE, coupled with IVUS, may help to detect and distinguish epicardial disease and microvascular dysfunction, emerging as a new noninvasive, useful tool to monitor the course of CAV. Thus, our data provide a rationale for including CFR by CE-TTE in future clinical trials aimed at assessing short-term or long-term pharmacological interventions for CAV prevention or stabilization.

Conflict of interest

None declared

References

1. Taylor DO, Edwards LB, Aurora P, Christie JD, Dobbels F, Kirk R, et al. Registry of the International Society for Heart and Lung Transplantation: twenty-fifth official adult heart transplant report—2008 J Heart Lung Transplant. 2008; 27:943-56.

2. Caforio ALP, Tona F, Belloni-Fortina A, Angelini A, Piaserico S, Gambino A, et al. Immune and nonimmune predictors of cardiac allograft vasculopathy onset and severity:

multivariate risk factor analysis and role of immunosuppression. Am J Transplant 2004; 4: 962-970.

3. Billingham ME. Histopathology of graft coronary disease. J Heart Lung Transplant 1992; 11 (pt 2): S38-S44.

4. Rickenbacher PR, Pinto FJ, Lewis NP, Hunt SA, Gamberg P, Alderman EL, et al. Prognostic importance of intimal thickness as measured by intracoronary ultrasound after cardiac transplantation. Circulation 1995; 92: 3445-3452.

5. Tona F, Caforio ALP, Montisci R, Angelini A, Ruscazio M, Gambino A, et al. Coronary flow reserve by contrast-enhanced echocardiography: a new noninvasive diagnostic tool for cardiac allograft vasculopathy. Am J Transplant 2006; 6: 998-1003.

6. Tona F, Caforio ALP, Montisci R, Gambino A, Angelini A, Ruscazio M, et al. Coronary flow velocity pattern and coronary flow reserve by contrast-enhanced transthoracic echocardiography predict long-term outcome in heart transplantation. Circulation 2006; 114 (suppl I): I-49-I-55.

7. Caiati C, Montaldo C, Zedda N, Bina A, Iliceto S. New noninvasive method for coronary flow reserve assessment: contrast-enhanced transthoracic second-harmonic echo Doppler. Circulation 1999; 99: 771-778.

8. Caforio ALP, Belloni-Fortina A, Piaserico S, Alaibac M, Tona F, Feltrin G, et al. Skin cancer in heart transplant recipients: risk factor analysis and relevance of immunosuppressive therapy. Circulation 2000; 102 [suppl III]:III-222-III-227.

9. Klauss V, Spes CH, Reiber J, Werner F, Stempfle HU, Uberfuhr P, et al. Predictors of reduced coronary flow reserve in heart transplant recipients without angiographically significant coronary artery disease. Transplantation 1999; 68: 1477-1481.

10. Nissen SE, Gurley JC, Booth DC, DeMaria AN. Intravascular ultrasound of the coronary arteries: current applications and future directions. Am J Cardiol 1992; 69: 18H-29H.

11. Mintz G, Nissen SE, Anderson WD, Bailey SR, Erbel R, Fitzgerald PJ, et al. ACC clinical expert consensus document on standards for acquisition, measurement and reporting of intravascular ultrasound sudies: a report of the American College of Cardiology task force on Clinical Expert Consensus Documents (Committee to develop a Clinical Expert Consensus Document on standards for acquisition, measurement and reporting of intravascular ultrasound sudies [IVUS]). J Am Coll Cardiol 2001; 37: 1478-1492.

12. Kobashigawa J, Wener L, Johnson J, Currier JW, Yeatman L, Cassem J, et al. Longitudinal study of vascular remodeling in coronary arteries after heart transplantation. J Heart Lung Transplant 2000; 19: 546-550

13. Bocksch W, Wellnhofer E, Schartl M, Dreysse S, Klimek W, Franke R, et al. Reproducibility of serial intravascular ultrasound measurements in patients with angiographically silent coronary artery disease after heart transplantation. Coron Artery Dis 2000; 11: 555-562.
14. Fearon WF, Nakamura M, Lee DP, Rezaee M, Vagelos RH, Hunt SA, et al. Simultaneous assessment of fractional and coronary flow reserves in cardiac transplant recipients: physiologic investigation for transplant recipients (PITA study). Circulation 2003; 108: 1605-1610.
15. Pijls NH. Is it time to measure fractional flow reserve in all patients? J Am Coll Cardiol 2003; 41: 1122-1124.
16. Jackson PA, Akosah KO, Kirckberg DJ, Mohanty PK, Minisi AJ. Relationship dobutamine-induced regional wall motion abnormalities and coronary flow reserve in heart transplant patients without angiographic coronary artery disease. J Heart Lung Transplant 2002; 21: 1080-1089.
17. Nitemberg A, Tavolaro O, Loisance D, Foult JM, Benhaiem N, Cachera JP. Severe impairment of coronary reserve during rejection in patients with orthotopic heart transplant. Circulation 1989; 79: 59-65.
18. Spes CH, Klauss V, Mudra H, Schnaack SD, Tammen AR, Rieber J, et al. Diagnostic and prognostic value of serial dobutamine stress echocardiography for noninvasive assessment of cardiac allograft vasculopathy: a comparison with coronary angiography and intravascular ultrasound. Circulation 1999; 100: 509-515.
19. Dandel M, Hummel M, Muller J, Wellnhofer E, Meyer R, Solowjowa N, et al. Reliability of tissue Doppler wall motion monitoring after heart transplantation for replacement of invasive routine screenings by optimally timed cardiac biopsies and catheterizations. Circulation 2001; 104 (suppl I): I-184-I-191.
20. Kofoed KF, Czernin J, Johnson J, Kobashigawa J, Phelps ME, Laks H, et al. Effects of cardiac allograft vasculopathy on myocardial blood flow, vasodilatory capacity, and coronary vasomotion. Circulation 1997; 95: 600-606
21. Caracciolo EA, Wolford TL, Underwood RD, Donohue TJ, Bach RG, Miller LW, et al. Influence of intimal thickening on coronary blood flow responses in orthotopic heart transplant recipients. A combined intravascular Doppler and ultrasound imaging study. Circulation 1995; 92 (suppl II): II-182-II-190.
22. Clausell N, Butany J, Molossi S, Lonn E, Gladstone P, Rabinovitch M, et al. Abnormalities in intramyocardial arteries detected in cardiac transplant biopsy specimens and lack of

correlation with abnormal intracoronary ultrasound or endothelial dysfunction in large epicardial coronary arteries. J Am Coll Cardiol 1995; 26: 110-119.
23. Klauss V, Ackermann K, Henneke KH, Spes C, Zeitlmann T, Werner F, et al. Epicardial intimal thickening in transplant coronary artery disease and resistance vessel response to adenosine: a combined intravascular ultrasound and Doppler study. Circulation 1997; 96 (suppl II): II-159-II-164.
24. Fearon WF, Hirohata A, Nakamura M, Luikart H, Lee DP, Vagelos RH, et al. Discordant changes in epicardial and microvascular coronary physiology after cardiac transplantation: physiologic investigation for transplant arteriopathy II (PITA II) study. J Heart Lung Transplant 2006; 25: 765-771.
25. Hiemann NE, Wellnhofer E, Knosalla C, Lehmkuhl HB, Stein J, Hetzer R, et al. Prognostic impact of microvasculopathy on survival after heart transplantation: evidence from 9713 endomyocardial biopsies. Circulation 2007; 116:1274-1282.
26. Kobashigawa JA, Tobis JM, Starling RC, Tuzcu EM, Smith AL, Valantine HA, et al. Multicenter intravascular ultrasound validation study among heart transplant recipients. Outcomes after five years. J Am Coll Cardiol 2005; 45: 1532-1537.
27. Caiati C, Montaldo C, Zedda N, Montisci R, Ruscazio M, Lai G, et al. Validation of a new noninvasive method (contrast-enhanced transthoracic second harmonic echo Doppler) for the evaluation of coronary flow reserve: comparison with intracoronary Doppler flow wire. J Am Coll Cardiol 1999; 34:1193-1200.

Figures

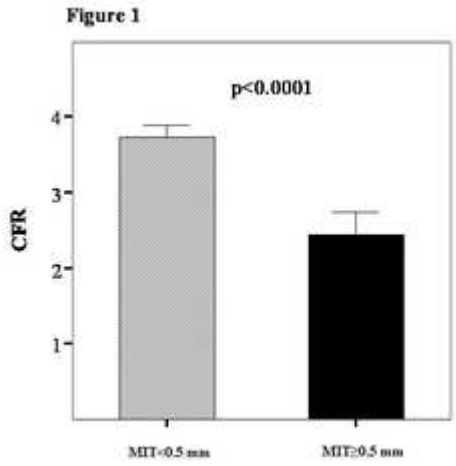

Figure 1: Coronary flow velocity reserve by CE-TTE in patients with and without MIT≥0.5 mm.

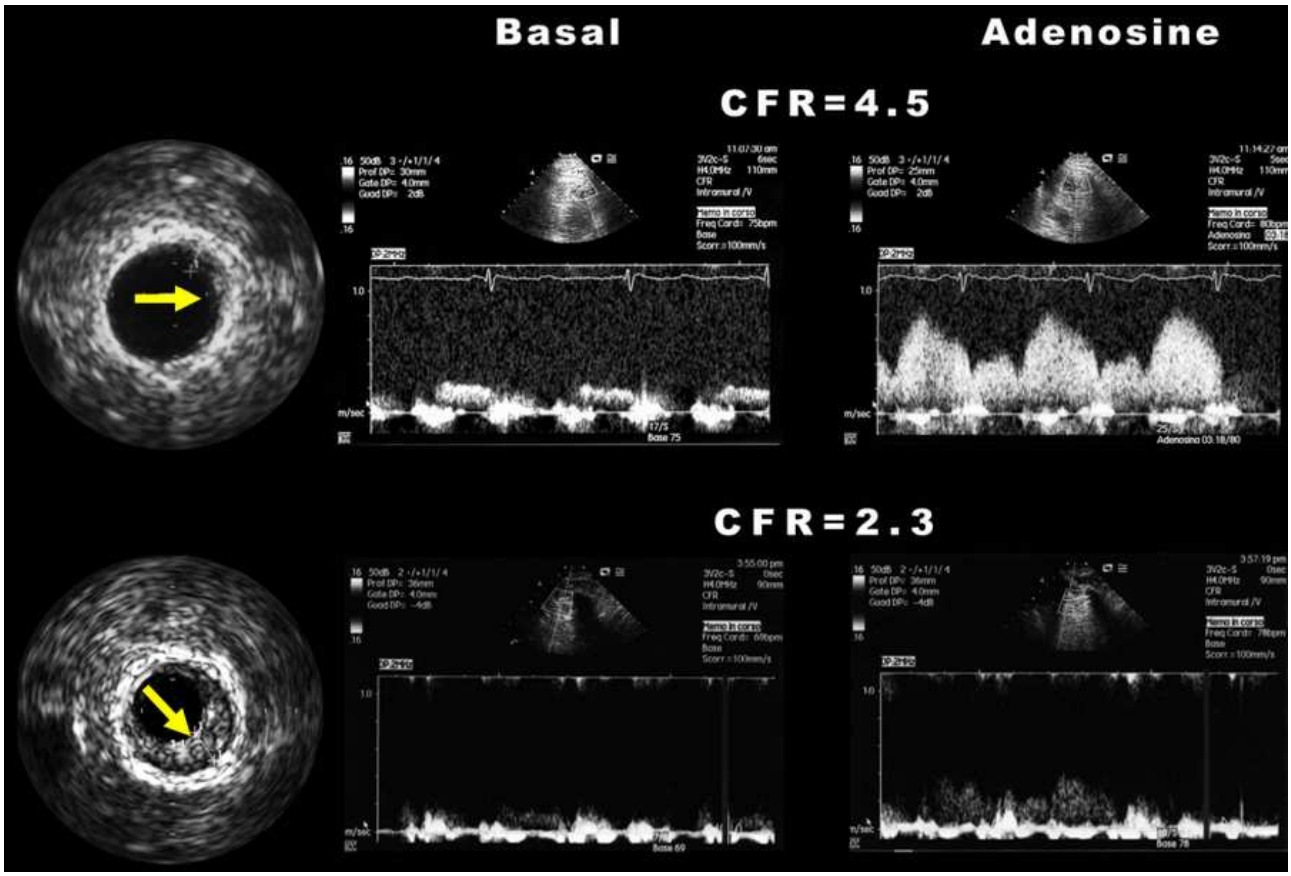

Figure 2: (A) MIT <0.5 mm (upper left panel). Coronary flow velocity assessed by CE-TTE on the same day of IVUS increased from baseline (upper middle panel) to post-adenosine administration (upper right panel), with a calculated CFR of 4.5. (B) MIT >0.5 mm (lower left panel). Coronary flow velocity assessed by CE-TTE on the same day of IVUS increased from baseline (lower middle panel) to post-adenosine administration (lower right panel), with a calculated CFR of 2.3.

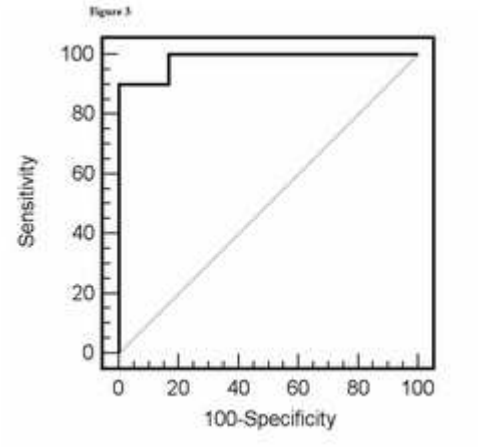

Figure 3: ROC analysis for separation of the presence or absence of CAV. True-positive rate (sensitivity) in the ordinate is plotted against false-positive rate (100-specificity) on the abscissa. The AUC of 0.903 has a SE of 0.022, yelding a 95% confidence interval of 0.941 to 1.026, indicating that this area is significantly different from the area of 0.500 under the diagonal identity line ($p<0.0001$).

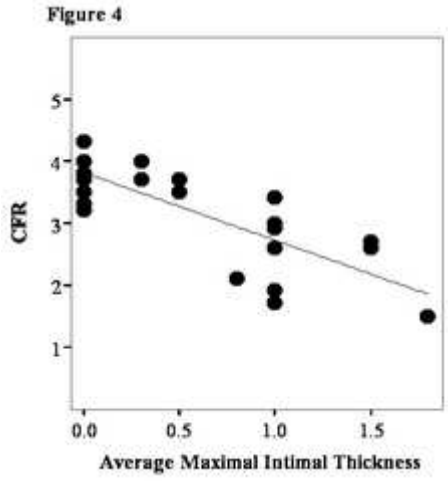

Figure 4: CFR by CE-TTE (y axis) as a function of average maximal intimal thickness (x axis) in the territory of the LAD. Increases in intimal thickness were associated with decreases in CFR. The relation was $y=-1.35x + 41$. $r=0.796$; $SEE=0.23$; $p<0.0001$.

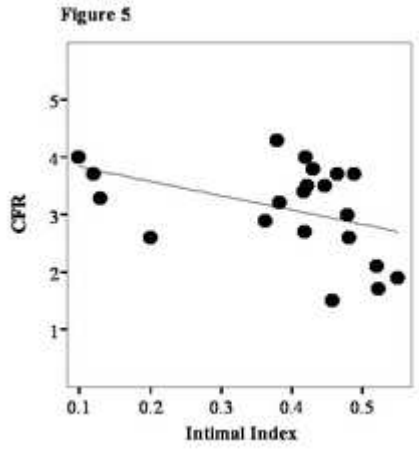

Figure 5: CFR by CE-TTE (y axis) as a function of intimal index (x axis) in the territory of the LAD. Increases in intimal index were associated with decreases in CFR. The relation was y=-2.5x + 4. r=0.454; SEE=0.72; p=0.01.

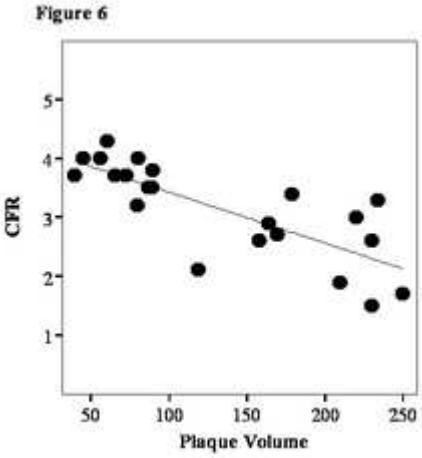

Figure 6: CFR by CE-TTE (y axis) as a function of plaque volume (x axis) in the territory of the LAD. Increases in plaque volume were associated with decreases in CFR. The relation was y=-0.009x + 4.2. r=0.775; SEE=0.52; p<0.0001.

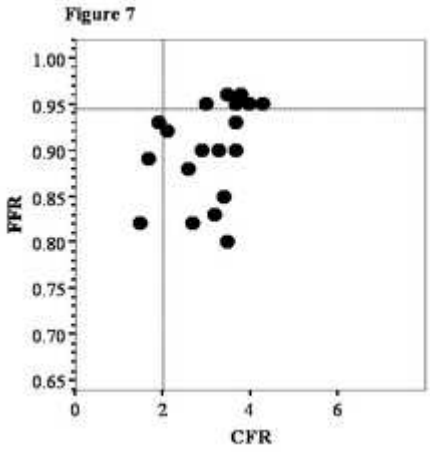

Figure 7: Scatterplot of FFR and CFR by CE-TTE values in each patient. Dashed lines represent FFR and CFR normal cutoff values.

Table 1: Recipient and Donor Characteristics

	Group A (MIT≥0.5 mm) (n=12)	Group B (MIT<0.5 mm) (n=10)	p
Age at HT, years	48 ± 6	51 ± 7	0.6
Male gender, n (%)	11 (92)	9 (90)	0.8
Ischemic time, min	170 ± 37	183 ± 30	0.5
Time from HT, years	8 ± 3	6 ± 2	0.04
Hypertension, n (%)	8 (66)	8 (80)	0.2
Diabetes, n (%)	2 (16)	2 (20)	0.7
Hypercholesterolemia, n (%)	4 (33)	3 (30)	0.6
Donor age, years	35 ± 12	37 ± 10	0.5
Donor male gender, n (%)	9 (75)	4(40)	0.02
Gender mismatch, n (%)	3 (25)	3 (30)	0.5
End-diastolic diameter, mm	46 ± 6	48 ± 5	0.9
End-systolic diameter, mm	25 ± 3	27 ± 2	0.7
LVEF (%)	68 ± 5	66 ± 3	0.7
Interventricular septum thickness, mm	12 ± 0.5	12 ± 0.3	0.8
Posterior wall thickness, mm	11 ± 0.4	11 ± 0.3	0.9
IHD pre-HT, n (%)	4 (33)	3 (30)	0.6
Total numbers of rejections	3.1 ± 2.5	3 ± 2	0.5

Unless specified otherwise, the values are means ± SD

HT = heart transplantation; IHD = ischemic heart disease; LVEF = left ventricular ejection fraction

Endothelial Progenitor Cells Are Decreased In Blood and in The Graft of Heart Transplant Patients With Microvasculopathy

Cardiac allograft vasculopathy (CAV) is the main limiting factor of long-term survival in heart transplantation (HT) [1]. In CAV both epicardial coronary vessels and the microvasculature may be affected [2], but in about 15% of patients only microvasculopathy can be detected [3]. Coronary flow reserve (CFR) by contrast-enhanced transthoracic echocardiography (CE-TTE) may provide functional assessment of the microvasculature in HT patients [4,5]. Nowadays, the pathogenesis of CAV remains poorly understood, although alloimmune-dependent and–independent factors have been recognized to play an important role [2]. Emerging evidence indicates that bone marrow-derived endothelial progenitor cells (EPCs) take part in postnatal neovascularization [6]. The EPCs co-express surface markers of both hematopoietic stem cells (CD34 and CD133) and endothelial cells (VEGF-R2, also known as KDR) [7,8]. There is increasing evidence of reduced availability and impaired EPCs function in the presence of both cardiovascular disease and associated risk factors [9]. A previous small study suggested that angiographically evidenced CAV is associated with reduction in EPCs (10). However, to the best of our knowledge, no data about the relationship between EPCs and microvascular function in patients with normal angiograms have been reported. Thus, we investigated the relationship between EPCs, their incorporation into allografts and coronary microvascular damage in HT.

Methods

Study Patients, Blood Sampling and Endomyocardial Biopsy

We studied 29 consecutive HT recipients with normal coronary angiogram (24 male, age at HT 50 ± 12 years) at 5 ± 2 years from HT. Angiographic evidence of CAV was defined as >20% stenosis in a main, branch epicardial, or intramyocardial coronary artery [10]. No evidence of CAV was defined as normal-appearing coronary artery anatomy. CFR by CE-TTE to evaluate coronary microvascular function was performed in all patients within 24 hours from catheterization. The immunosuppression protocol consisted of cyclosporine, azathioprine , mycophenolate mofetil or everolimus, and steroids as previously detailed [2,11]. Fresh blood was collected by venipuncture and anticoagulated in citrate phosphate dextrose solution (CPD) (Baxter). Biopsies of the first year, at 2 different time points, were examined in each patient. Immunohistochemistry for the stem cells marker c-Kit and the EPC markers, CD34 and KDR

was performed in serial sections in all biopsies. Cells positive for each marker were counted in all biopsy area-section and the number obtained was corrected by area-section. HT patients were compared with 40 healthy subjects, matched for age and gender, recruited from the local community. In control subjects, the absence of type 2 diabetes mellitus and impaired glucose tolerance was documented by means of fasting glucose and 2-h glucose determination or oral glucose tolerance test. The absence of cardiovascular diseases was evaluated by a clinical history and examination, carotid ultrasonography, and, when available, echocardiography and coronary angiography. The study was approved by the institutional ethics committee, and all patients gave written, informed consent.

Quantification of Circulating Progenitor Cells

Human progenitor cells were analyzed for the expression of surface antigens with direct three color flow cytometry as previously described [12] using fluorescein isothiocyanate (FITC)-conjugated anti-CD34, PE-conjugated anti-KDR, and activated protein C (APC)-conjugated anti-CD133 mAbs. Cells within the mononuclear morphological gate were first assayed for CD34 and CD 133 expression and then for KDR expression. 5x105 events were always acquired. EPCs were defined as CD34+KDR+ cells, according to recent population-based studies [13,14]. CD133+KDR+ and CD34+CD133+KDR+ were also considered as putative EPC phenotypes. Total CD34+, CD133+ cells as well as CD34+CD133+ cells were considered generic circulating progenitor cells (CPCs). The same trained operator (I.B.), who was blinded to the subjects'characteristics, performed all of the tests throughout the study.

EPC Immunohistochemistry

The antibody clones, used alone or in combination to identify EPCs in the biopsy sections, were the same to the direct flow cytometry ones. EPCs markers were CD34 (Immunotech, Marseilles, France) and VEGFR2/KDR (Santa Cruz, UK). Briefly, slides were treated with 0.3% hydrogen peroxide in methanol to block endogenous peroxidase activity, washed with phosphate-buffered saline, and incubate in buffered normal horse serum to prevent unspecific antibody binding. Sections were incubated with the primary antibodies for 1 hour at room temperature. After washing, a biotin-labelled secondary antibody was applied, followed by an avidin-peroxidase conjugate. As chromogen DAB was used. Slides were counterstaining with haematoxylin. Immunostaining on serial section was performed with antibodies against KDR and CD34.

Interphase Fluorescent In Situ Hybridization

We prepared 5-μm sections from formalin-fixed, paraffin-embedded tissue blocks from biopsy specimens and subjected them to immunohistochemical staining and in situ hybridisation techniques as previously described. [15] Immunohistochemical analyses were performed to discriminate EPC phenotypes. The Y chromosome was detected by fluorescence in situ hybridization in nuclei in interphase by use of combined CEP X /CEP Y (alpha) SO DNA probes (Vysis Inc, Downers Grove, IL) consisting of two different probes specific for the centromeric region of the X (orange) and Y (green) chromosomes, respectively. A human Y chromosome centromeric-painting biotin conjugate probe (Star*FISH, Cambio, Cambridge, UK) was also used to confirm the in situ hybridization by optical microscope analysis. After overnight hybridization and stringent washes, the probe was visualized with a peroxidase-conjugated avidin-biotin complex using DAB (Dakocytomation).

Tissue Analysis

Morphologic evaluation of the hematoxylin and eosin and immunostained sections was done under the light microscope. The fluorescent hybridized sections were analyzed with a confocal Leica TCS SL microscope (Leica Microsystems, Wetzlar, Germany). Sections were scanned under identical imaging parameters. For conventional bright-field microscopy, rigorous criteria were used to determine whether a Y-chromosome signal was indeed within the nucleus of the cell and whether that nucleus resided within a labelled cell population. Staining for Y chromosome was regarded as positive if a punctate, dark-brown signal was present within a given blue-stained nucleus and in the same focal plane.

Cell Counting

Each antibody was analyzed separately in all the sections. The count of positive cells was performed with the same criteria employed for in situ hybridization analyses. For each antibody cells positive count was done on the entire biopsy area. Cells number for each antibody was normalized for the total area and expressed as cells/mm2.

Transthoracic Doppler Echocardiography

An echocardiogram was obtained in all patients within 48 hours of coronary angiography. From the parasternal long axis view, M-mode measurements were performed to determine the end-diastolic thickness of the interventricular septum and the left ventricular posterior wall. Left ventricular hypertrophy was defined as a septal plus posterior wall thickness $\geq$ 24 mm [16]. Left ventricular ejection fraction was measured using Simpson's method. Once the routine echo

Doppler examination was completed, the CFR was evaluated using CE-TTE before and after adenosine infusion. The method has been previously described in detail [17].

Coronary Flow Velocity Reserve Assessment

All patients had Doppler recordings of the left anterior descending coronary artery with adenosine infusion at a rate of 0.14 mg/kg per min for 5 min [4]. Cardiac drugs were not interrupted before testing, although all methylxantine-containing substances or medications were withheld 48 h before the study. CFR in the left anterior descending coronary artery was calculated, as the ratio of hyperemic to basal diastolic flow velocity, by an experienced echocardiographer, blind to angiographic and clinical data. For each variable in the CFR calculation, the highest 3 cycles were averaged [4].

Statistical Analysis

Data are expressed as mean ± SEM. Results from flow cytometry are expressed as cells per 106 cytometric events. Comparison between 2 groups was performed with a 2-tailed Student's *t* test. Correlations between 2 variables were assessed by Pearson's coefficient (r). The variables included in the multiple linear regression analysis for the determinants of CFR were CPCs, EPCs, time from HT, diabetes, hypertension and hypertrophy. Statistical significance was accepted if the null hypothesis could be rejected at $p<0.05$. Data were analyzed with SPSS software version 13.0 (Chicago, SPSS, Inc., Chicago, Illinois). The authors had full access to and take full responsibility for the integrity of the data. All authors have read and agree to the manuscript as written.

Results

Circulating Progenitor Cells in Patients vs Controls

Flow cytometry was used to determine the number of circulating peripheral blood progenitor cells (CD133+ and CD34+) and EPCs (CD34+KDR+, CD133+KDR+, and CD34+CD133+KDR+). Because only 0.02% to 0.07% of white blood cells were CD34+, EPCs and CPCs counts were expressed for one million cytometric events. CD133+ and CD34+ progenitor cells were reduced in HT recipients ($p<0.05$). In parallel, EPCs were profoundly reduced in HT patients ($p<0.05$) (Figure 1).

Circulating EPCs in Patients With Microvasculopathy

CFR was abnormal (<2) in 6 patients (group A) and normal in 23 patients (group B). Patients characteristics are presented in the Table. Briefly, all study subjects were nonsmokers, were

treated with statins at equivalent dosages and had similar systolic and diastolic blood pressure. Subjects were well matched for all other risk factors and for other determinants of CFR, including recipient age, donor age, gender mismatch and number of previous rejection episodes. There was no statistically significant difference between the two groups in any of the clinical or laboratory parameters studied. There was also no significant difference between groups in the time interval between initial transplantation and CFR measurement with EPCs isolation. CFR was lower in group A (1.5 ± 0.1 vs 3.3 ± 0.8, $p<0.0001$). CD34+KDR+, CD133+KDR+, and CD34+CD133+KDR+ cell count were lower in group A ($p<0.05$) (Figure 2). At multivariable analysis, adjusted for time from HT, diabetes, hypertension and hypertrophy, only CD34+-CPCs were independently related to CFR ($\beta=-0.773$, $p=0.006$).

Endothelial Progenitor Cells in Endomyocardial Biopsies

The number of CD34+KDR+ EPCs in biopsy sections tended to be lower in group A ($p=0.06$) and were correlated with circulating CD133+KDR+, and CD34+CD133+KDR+ counts ($r=0.752$, $p=0.003$ and $r=0.513$, $p=0.05$, respectively) (Figure 3).

Detection of Recipient EPC in Gender-Mismatched Heart Transplantation Recipients

Four subjects who had undergone gender-mismatched heart transplantation were studied using combined endothelial marker immunohistochemistry and FISH. The biopsy specimens from nontransplanted female subjects (used to test the sensitivity of the probes) showed 59.29 ± 5.9% of cells with the X-chromosome and no orange fluorescent signals indicative of the Y-chromosome, whereas the biopsies of non-transplanted male subjects (positive male controls) showed a high percentage of cells with the Y-chromosome (69.71 ± 4.47%). No evidence of opposite-sex chimerism was detected in same-gender HT recipients (data not shown). To further characterize the potential angioblastic lineage of recipient endothelial cells in donor vessels, combined FISH for Y chromosome and CD34, and KDR staining was performed. Recipient male endothelial cells within female donor microvessels were positive for each of these markers (Figure 4).

Discussion

Our study demonstrates, for the first time, that human EPCs in the circulation and in the graft are significantly decreased in HT recipients with normal angiogram and microvasculopathy, defined as a severe impairment of CFR. We also show that CPCs and EPCs are reduced in HT

patients compared with healthy subjects, matched for age and gender. The reduction of circulating CPCs and EPCs in HT patients as compared to controls can be explained by the effect of immunosuppressive therapy. Immunosuppression in the setting of heart transplantation causes a severe reduction in progenitor cells capable of differentiating into endothelial and smooth muscle cells [18] which can be explained by the inhibitory effect of cyclosporine. Cyclosporine alters the proliferation, migration and differentiation capacity of endogenous vascular progenitors with consequences for allograft endothelial biology [18]. Cyclosporine was seen to affect a range of vascular progenitor biologic functions. Cyclosporine has previously been shown to inhibit endothelial cell proliferation in the context of increased interleukin-6 protein and mRNA expression[19] and decreased nitric oxide production[19]. Other immunosuppressive drugs, such as mTOR inhibitors, can have a potent inhibitory effect on circulating vascular progenitor cells as well[20]. The in vivo effect of sirolimus has been also evaluating in a model of neointimal hyperplasia with bone marrow chimeric mice. Results suggest that sirolimus has a potent inhibitory effect on both smooth muscle progenitor cell and endothelial progenitor cell incorporation at the sites of vascular lesions [20]. It was also observed, in the clinical setting of stent implantation, that oral administration of everolimus, a macrolide of the same family of sirolimus, results in delayed endothelial coverage over the stent surface with loose endothelial cell junction, although in-stent neointimal growth was suppressed [21]. The immunosuppressive protocol we used in these patients also included a dose of steroids, which could have also altered progenitor cells number [18]. To the best of our knowledge, we present the first data showing differential levels of circulating EPCs in subjects who have developed transplant microvasculopathy and a different engraftment of recipient endothelial cells into the donor microvasculature. It is possible that EPCs are mobilized from bone marrow of the recipient and engrafted into the donor coronary microcirculation during immunologic myocardial injury over time [15]. Previous animal [22] and human data [10] support such an endothelial recruitment from the recipient circulation. In keeping with our findings, Simper et al. [10] provided evidence that circulating EPCs are decreased in patients with angiographic allograft vasculopathy compared with matched transplantation subjects without evidence of disease and that these cells are of recipient origin. In contrast, these authors also showed a significant seeding of recipient endothelial cells in large-vessel lumen and adventitial microvessel lumen of arteriopathic vessels. This result is not in contrast with our study maybe because the authors studied circulating and tissue EPC in patients with angiographic evidence of CAV. Although the study of chemokine and chemokine receptors is beyond our aim, a possible explanation for the EPCs reduction in patients with microvasculopathy may involve humoral factors that influence

mobilization, migration and cell survival as may happen in the context of chronic low grade rejection [15]. Recently, it has been demonstrated that apoA-I transfer increases the number of EPCs in hypercholesterolemic apoE-/- mice, enhances the incorporation of bone marrow-derived EPCs into transplanted arteries in apoE-/- mice, promotes endothelial regeneration, and attenuates neointima formation in a murine model of allograft vasculopathy [23.]. Soluble Kit-ligand induces the release of stromal cell-derived factor (SDF)-1 from platelets, enhancing neovascularization through mobilization of CXCR4+ progenitors [24]. Using a mouse aortic transplantation model, some authors showed that SDF-1 is a critical molecular target for the progenitor homing. In support of a functional role for these molecules, in vivo neutralization of SDF-1 inhibited stem cell homing [24]. This confirms that bone marrow is the main source of stem cells participating in endothelial repair after alloimmune-induced endothelial loss in grafted vessels. However, it was also reported that a large proportion of EPCs in circulating blood is of non-bone marrow origin. For example, the spleen, some parenchymatous organs and the blood vessels themselves are particularly rich in EPCs [24]. It has been recognized that EPCs number may be a surrogate marker of vascular function. Some authors showed an inverse correlation between the circulating EPCs and endothelial dysfunction or cardiovascular risk [9]. Our findings showing EPCs number reduction in HT patients with microvascular dysfunction are consistent with these data and extend to allograft vasculopathy the concept of abnormal EPCs mobilization and homing in the presence of microvascular disease.

Study limitations

This study has certain limitations. First, there is a lack of consensus in the field of EPCs research regarding the precise definition of this cells. We accordingly quantified cells with phenotypes which have been frequently used to define EPCs in clinical cardiovascular studies. However this study shares with existing literature a lack of mechanistic certainty regarding the identity of the most important specific cell type involved in vascular repair. It therefore remains possible that there are other cell populations with EPC properties which were not identified using our immunophenotyping techniques. Another limitation is that biopsies and blood samples for EPCs counts were not simultaneous. However, we can speculate that EPCs present in the biopsies of the first year could also be found in the next years of follow up. In support of this concept, it has been demonstrated by our and other groups that the recruitment of EPCs to sites of endothelial injury or dysfunction in the transplanted heart is an ongoing process [10,15]. It is conceivable that EPCs are recruited early and late. We can specualate that EPCs may be

continuously engrafted to areas of donor endothelial dysfunction in a cycle of continuous repair and in the context of ongoing alloimmune interactions.

Conclusions

EPCs are decreased in the circulation and in the graft of HT patients with microvasculopathy. Cells mobilization and engrafting after HT seem to preserve microvascular function. Our findings may be crucial in understanding the pathogenesis of allograft vasculopathy and in establishing new strategies for therapeutic intervention. If we could learn to control chimerism, it might be possible to delay or prevent this disease, which is the most common cause for failure of transplanted hearts. However, further studies are warranted to elucidate the nature and mechanism of circulating EPCs participation in CAV pathophisiology.

Conflict of interest

None declared

References

1. Taylor DO, Edwards LB, Aurora P, Christie JD, Dobbels F, Kirk R, et al. Registry of the International Society for Heart and Lung Transplantation: twenty-fifth official adult heart transplant report--2008. J Heart Lung Transplant 2008; 27:943-56.

2. Caforio ALP, Tona F, Belloni-Fortina A, Angelini A, Piaserico S, Gambino A, et al. Immune and nonimmune predictors of cardiac allograft vasculopathy onset and severity: multivariate risk factor analysis and role of immunosuppression. Am J Transplant 2004;4:962-70.

3. Fearon WF, Nakamura M, Lee DP, Rezaee M, Vagelos RH, Hunt SA, et al. Simultaneous assessment of fractional and coronary flow reserves in cardiac transplant recipients: Physiologic Investigation for Transplant Arteriopathy (PITA Study). Circulation 2003;108:1605-10.

4. Tona F, Caforio ALP, Montisci R, Angelini A, Ruscazio M, Gambino A, et al. Coronary flow reserve by contrast-enhanced echocardiography: a new noninvasive diagnostic tool for cardiac allograft vasculopathy. Am J Transplant 2006;6:998-1003.

5. Tona F, Caforio ALP, Montisci R, Gambino A, Angelini A, Ruscazio M, et al. Coronary flow velocity pattern and coronary flow reserve by contrast-enhanced transthoracic echocardiography predict long-term outcome in heart transplantation. Circulation 2006;114:I49-55.

6. Asahara T, Murohara T, Sullivan A, Silver M, van der Zee R, Li T, et al. Isolation of putative progenitor endothelial cells for angiogenesis. Science 1997;275:964-7.

7. Hristov M, Erl W, Weber PC. Endothelial progenitor cells: isolation and characterization. Trends Cardiovasc Med 2003;13:201-6.
8. Salven P, Mustjoki S, Alitalo R, Alitalo K, Rafii S. VEGFR-3 and CD133 identify a population of CD34+ lymphatic/vascular endothelial precursor cells. Blood 2003;101:168-72.
9. Hill JM, Zalos G, Halcox JP, Schenke WH, Waclawiw MA, Quyyumi AA, et al. Circulating endothelial progenitor cells, vascular function, and cardiovascular risk. N Engl J Med 2003;348:593-600.
10. Simper D, Wang S, Deb A, Holmes D, McGregor C, Frantz R, et al. Endothelial progenitor cells are decreased in blood of cardiac allograft patients with vasculopathy and endothelial cells of noncardiac origin are enriched in transplant atherosclerosis. Circulation 2003;108:143-9.
11. Caforio ALP, Belloni-Fortina A, Piaserico S, Alaibac M, Tona F, Feltrin G, et al. Skin cancer in heart transplant recipients: risk factor analysis and relevance of immunosuppressive therapy. Circulation 2000;102:III222-7.
12. Fadini GP, de Kreutzenberg SV, Coracina A, Baesso I, Agostini C, Tiengo A, et al. Circulating CD34+ cells, metabolic syndrome, and cardiovascular risk. Eur Heart J 2006;27:2247-55.
13. Werner N, Kosiol S, Schiegl T, Ahlers P, Walenta K, Link A, et al. Circulating endothelial progenitor cells and cardiovascular outcomes. N Engl J Med 2005;353:999-1007.
14. Schmidt-Lucke C, Rossing L, Fichtlscherer S, Vasa M, Britten M, Kamper U, et al. Reduced number of circulating endothelial progenitor cells predicts future cardiovascular events: proof of concept for the clinical importance of endogenous vascular repair. Circulation 2005;111:2981-7.
15. Angelini A, Castellani C, Tona F, Gambino A, Caforio A, Feltrin G, et al. Continuous engraftment and differentiation of male recipient Y-chromosome-positive cardiomyocytes in donor female human heart transplants. J Heart Lung Transplant 2007;26:1110-8.
16. Klauss V, Spes CH, Reiber J, Siebert U, Werner F, Stempfle HU, et al. Predictors of reduced coronary flow reserve in heart transplant recipients without angiographically significant coronary artery disease. Transplantation 1999;68:1477-81.
17. Caiati C, Montaldo C, Zedda N, Bina A, Iliceto S. New noninvasive method for coronary flow reserve assessment: contrast-enhanced transthoracic second harmonic echo Doppler. Circulation 1999;99:771-8.
18. Davies WR, Wang S, Oi K, Bailey KR, Tazelaar HD, Caplice NM, et al. Cyclosporine decreases vascular progenitor cell numbers after cardiac transplantation and attenuates progenitor cell growth in vitro. J Heart Lung Transplant 2005;24:1868-77.

19. Storogenko M, Pech-Amsellem MA, Kerdine S, Rousselet F, Pallardy M. Cyclosporin-A inhibits human endothelial cells proliferation through interleukin-6-dependent mechanisms. Life Sci 1997;60:1487-96.
20. Fukuda D, Sata M, Tanaka K, Nagai R. Potent inhibitory effect of sirolimus on circulating vascular progenitor cells. Circulation 2005;111:926-31.
21. Farb A, John M, Acampado E, Kolodgie FD, Prescott MF, Virmani R. Oral everolimus inhibits in-stent neointimal growth. Circulation 2002;106:2379-84.
22. Xu Q. Stem cells and transplant arteriosclerosis. Circ Res 2008;102:1011-24.
23. Feng Y, Jacobs F, Van Craeyveld E, Brunaud C, Snoyes J, Tjwa M, et al. Human ApoA-I transfer attenuates transplant arteriosclerosis via enhanced incorporation of bone marrowderived endothelial progenitor cells. Arterioscler Thromb Vasc Biol 2008;28:278-83.
24. Belperio JA, Ardehali A. Chemokines and transplant vasculopathy. Circ Res 2008;103:454-66.

Table and Figures

TABLE 1: Baseline Clinical and Laboratory Characteristics of Endothelial Progenitor Study Patients

Characteristics	CFR≥2 (n=23)	CFR<2 (n=6)	p
Age, y	50 ± 10	49 ± 9	0.8
Male sex, No. (%) of patients	19 (83)	5 (83)	0.9
Time from transplantation, y	5 ± 1	6 ± 1	0.7
Systolic blood pressure, mmHg	145 ± 13	135 ± 14	0.6
Diastolic blood pressure, mmHg	85 ± 5	78 ± 4	0.7
Echo ejection fraction, %	63 ± 6	62 ± 7	0.8
Interventricular septum thickness, mm	12 ± 1	12 ± 1	0.7
Posterior wall thickness, mm	11 ± 0.9	11 ± 0.8	0.7
Total cholesterol, mg/dL	160 ± 8	165 ± 9	0.6
LDL cholesterol, mg/dL	83 ± 10	78 ± 5	0.6
HDL cholesterol, mg/dL	44.7 ± 3.1	39 ± 1.5	0.4
Triglycerides, mg/dL	150 ± 18.3	235 ± 53.7	0.3
Haemoglobin, mg/dL	14 ± 1	14 ± 1	0.9
Diabetes mellitus, No. (%) of patients	0	1 (17)	0.2
Smokers, No. (%) of patients	0	0	0.9
Donor heart age, y	40 ± 10	43 ± 8	0.7
Gender mismatch, No. (%) patients	6 (26)	2 (33)	0.4
Ischemic time, min	175 ± 44	169 ± 28	0.5
Number of rejections in the 1st year	2.64 ± 0.2	2.53 ± 0.6	0.8
Total number of rejections	3.19 ± 0.2	3.07 ± 0.7	0.8

Figure 1

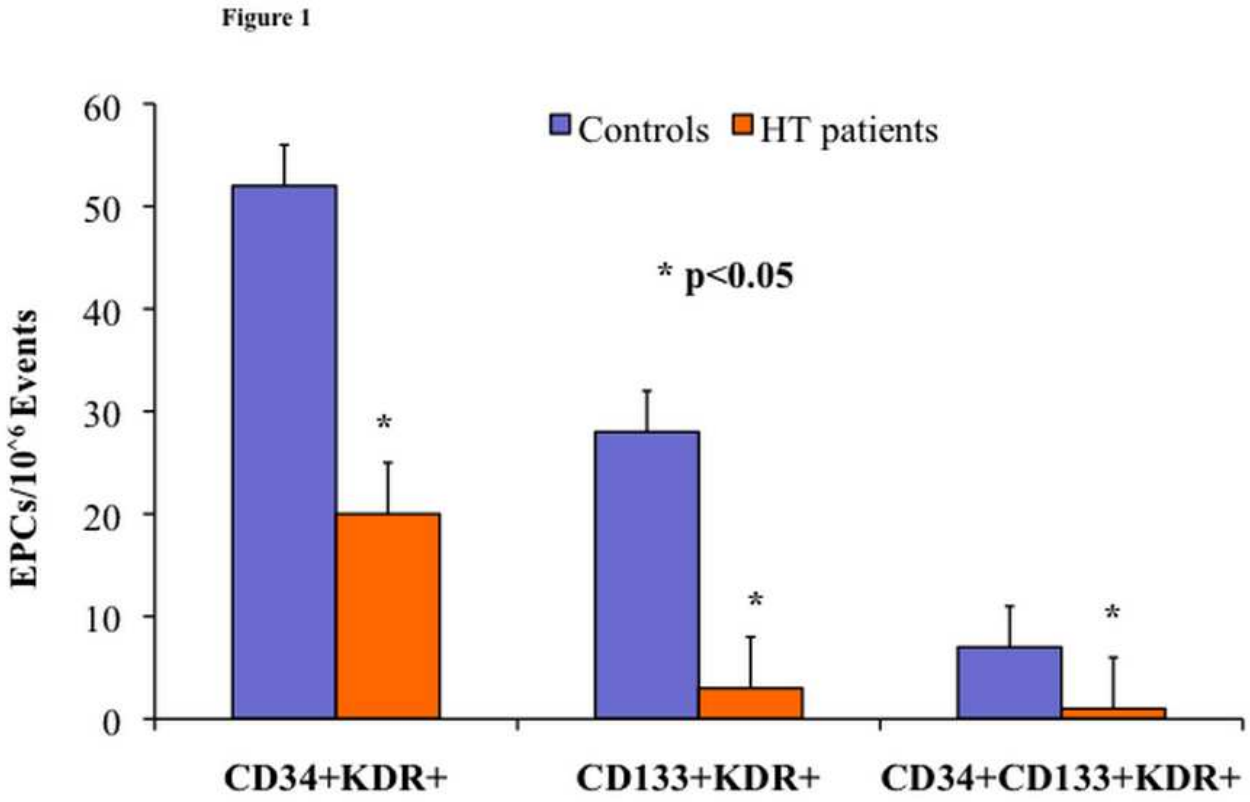

Figure 1: **EPCs in HT recipients and controls**. Heart transplant patients have lower levels of circulating endothelial progenitor cells when compared to control subjects.

Figure 2

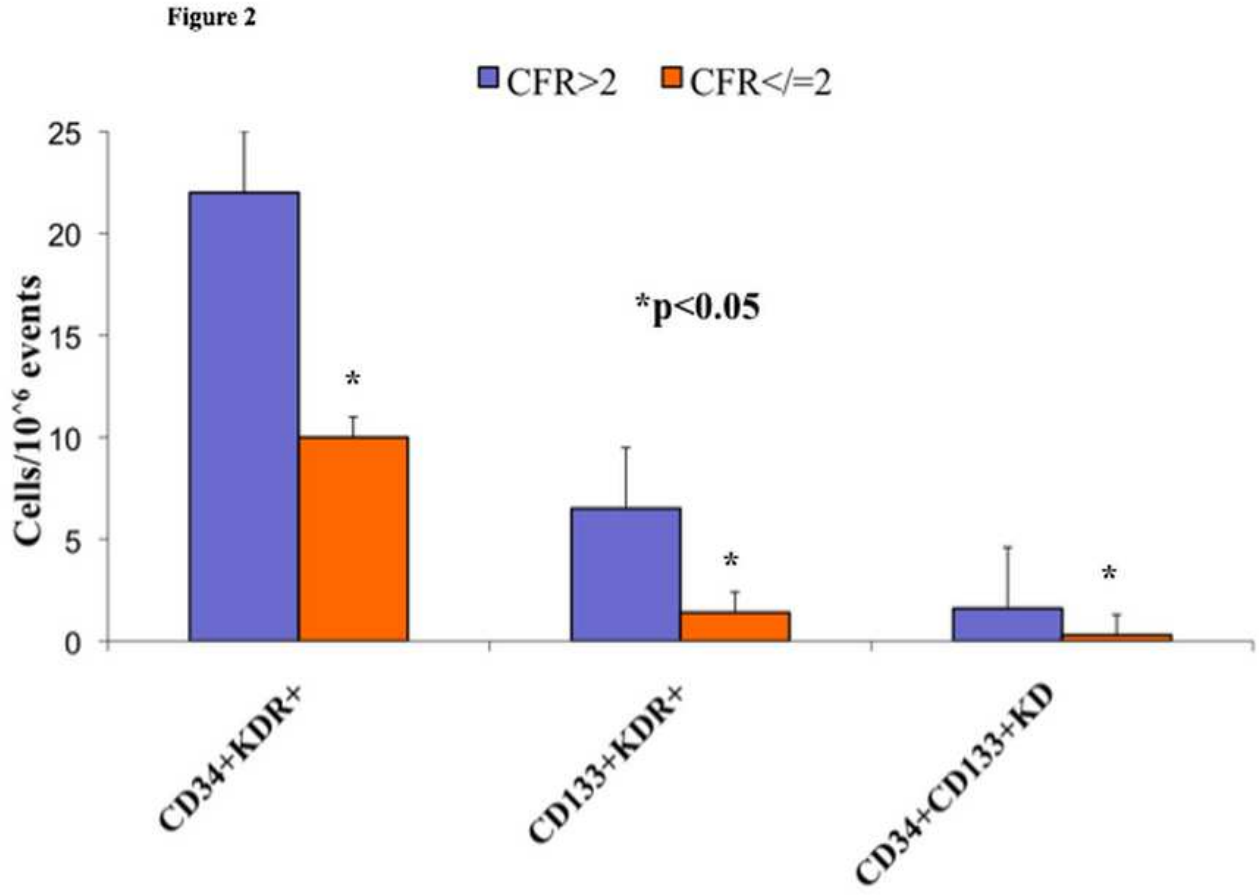

Figure 2: **EPCs in HT patients**. Levels of endothelial progenitor cells in heart transplant patients divided according to CFR with cutoff of normality (CFR<2).

Figure 3

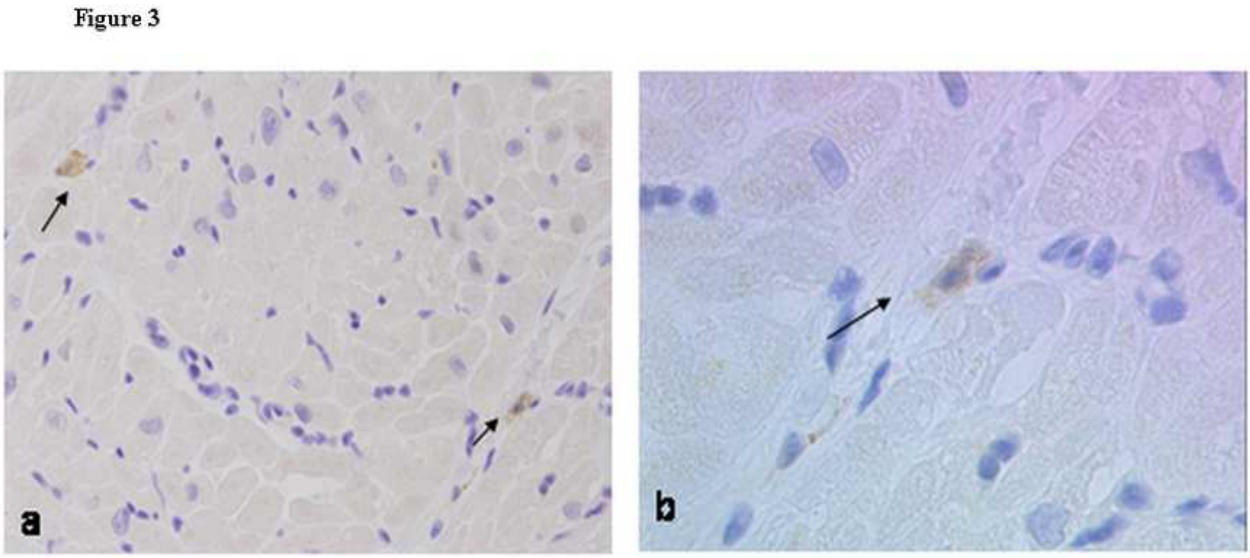

Figure 3: **KDR positive cells on monitoring endomyocardial biopsies**. Brightfield micrographs representing: a)Circulating KDR+ endothelial progenitor cells in the myocardium interstitium (black arrows). Original magnification 320X; b) close up view of KDR+ endothelial progenitor cells (black arrow). Original magnification 600X.

Figure 4

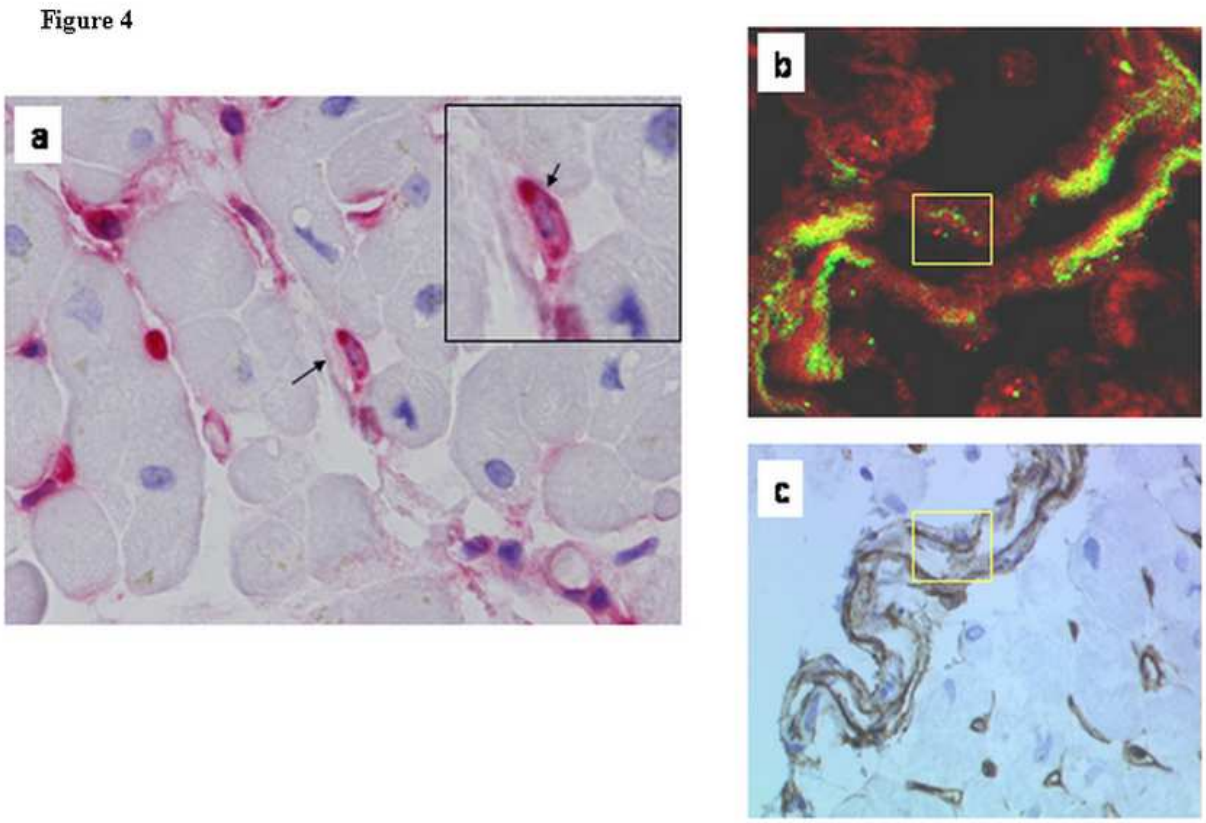

Figure 4: **Recipient endothelial progenitor cells**. a) Brightfield micrograph chromogenic in situ hybridization for Y-chromosome. Recipient male endothelial cell (black arrow) within endomyocardial biopsy tissue showing Y-chromosome (brown punctate dot in the blue nuclei) and positive for endothelial progenitor marker CD34 staining (red cytoplasm). Original magnification 64X. The inlet represent a close up view of Y-chromosome positive cell; b) Confocal photomicrograph depicting fluorescence in situ hybridization (FISH) for X/Y chromosome showing the presence of two male progenitor endothelial cells (yellow square) in the endomyocardial biopsy vessel. Cells has one Y-chromosome (red dot) and one X-chromosome (green dot). Original magnification 40X;c) CD34 staining on the same biopsy. Note as the male progenitor Ychromosome positive cells (yellow square) are CD34 positive. Original magnification 40X.

Conclusion

The body of evidence collected up to date, clearly indicates that an impairment of endothelial function has profound and independent prognostic implications associated with cardiovascular events [84-86]. Nevertheless, it has to be noted that at present, there is still a void in a prospective randomized trial, which demonstrates that improvement of endothelial function is associated with a reduction in cardiovascular events and attenuation of the disease process. The ongoing prospective studies analyzing the additive value of standardized endothelial function measurements to predict cardiovascular risk, such as the PREVENT-it study, should provide important insights [87].

Currently there is also no gold standard treatment for endothelial dysfunction, however several pharmacological and non pharmacological approaches have been proved to be effective like statin, ACE inhibitors, physical exercise and so on. Endothelial dysfunction can be regarded as a syndrome that exhibits various systemic manifestations associated with significant morbidity and mortality rather than a localized vascular disorder. The concept of endothelial dysfunction should be extended beyond the conduit vessels into the vascular wall and even to the bone marrow and the progenitor endothelial cells. The clinical correlation between certain markers of inflammation and an increased rate of cardiovascular events represents an intriguing confirmation of the inflammation-derived endothelial injury framework. This concept has been nicely illustrated by a recent study in patients with chronic periodontitis. Indeed, after intense treatment of periodontitis associated with chronic inflammation, endothelial dysfunction was substantially improved, strongly suggesting that chronic inflammation promotes endothelial dysfunction [88]. These findings have further stimulated interest in investigating mechanisms that underlie endothelial dysfunction and, more specifically, reduced NO availability [89].

Current molecular data link aging, diabetes, endothelial dysfunction, inflammation, traditional atherosclerosis but also cardiac allograft vasculopathy. Indeed, common mechanisms underlying these conditions have been described suggesting a detrimental role of ROS.

Vascular biology successfully brought together basic and clinical sciences unmasking the key unifying role of oxidative stress in endothelial dysfunction and vascular inflammation. We believe that future efforts should be finalized to translate our current knowledge into the development of new therapeutic strategies to prevent, diagnose and cure atherosclerotic cardiovascular disease and the allograft vasculopathy of transplanted hearts.

With this motivation I have been working on my PhD for the past 3 years

Future perspectives

All forms of cardiovascular disease show higher frequency with age, even in the absence of cardiovascular risk factors [90-92]. These observations prompted research efforts to focus on the vascular biology of aging to define mechanisms that may underlie the increased risk conferred by aging per se. Recently, in view of its reported role in determining the redox state of the cells and their responses to free radicals, we investigated the age-related endothelial dysfunction in a JunD deleted mouse model.

There are quite common diseases, such as psoriasis and primary hyperparathyroidism, proven to be at increased risk for cardiovascular mortality, however poorly understood on a cardiovascular point of view. As a consequence these diseases still have inappropriate screening and diagnosis of associated cardiovascular complications as well as risk factors assessment, inadequate patient counselling and follow-up protocols.

We though to evaluate coronary microcirculatory function in psoriasis and primary hyperparathyroidism to investigate the earliest steps involved in the pathophysiology of cardiovascular diseases associated to such diseases.

The following are preliminary data collected so far regarding the above mentioned ongoing projects.

Enhanced age-related endothelial dysfunction in genetic deletion of JunD

Background: JunD is a transcription factor that regulates genes involved in antioxidant defense. This study aimed to investigate whether JunD deficient mice (*JunD*$^{-/-}$) are more prone to age-related, oxidative stress-mediated endothelial dysfunction in comparison to age-matched wild type (WT) mice**.**

Methods. Thoracic aortic rings from young (3 months old), middle aged (6 months old) and old (22 months old) male *JunD*$^{-/-}$ and WT mice were suspended for isometric tension recording. Endothelium-dependent relaxation to acetylcholine (Ach, 10^{-9}-10^{-6}mol/L) was assessed after submaximal contraction with norepinephrine (10^{-6}mol/L). Calcium ionophore stimulated nitric oxide (NO), superoxide anion (O_2^-) and peroxynitrite ($ONOO^-$) were measured with electrochemical nanosensors placed near the surface (5±2 μm) of a single endothelial cell.

Results. The age-associated impairment of endothelium-dependent relaxations to Ach (Ach, 10^{-9}-10^{-6} mol/L) was significantly enhanced in *JunD*$^{-/-}$ as compared to age-matched WT. Maximal relaxations were 55±5 vs 78±4% at 6 months and 39±3 vs 50±2% at 22 months for JunD-/- and WT mice, respectively (n=6-8, $p<0.05$ vs age-matched group). Endothelium-independent relaxations to sodium nitroprusside (10^{-10}-10^{-5} mol/L) did not differ in *JunD*$^{-/-}$ and WT of different age groups (n=6-8, p<NS). Age-induced decrease of NO production was higher in *JunD*$^{-/-}$ as compared with WT (475±32 vs 350±28 nmol/L and 358±26 vs 220±23 nmol/L for 6 and 22 months old WT and *JunD*$^{-/-}$, respectively; n=3-5, $p<0.05$ vs age-matched group) (Figure1). O_2^- and $ONOO^-$ generation increased with age in WT and more significantly in *JunD*$^{-/-}$ mice (O_2^-, 67±6 vs 103±8 nmol/L and 116±9 vs 210 ±16 nmol/L (Figure2).; $ONOO^-$, 224±17 vs 319±22 nmol/L and 313±21 vs 492±29 nmol/L for 6 and 22 months old WT and *JunD*$^{-/-}$,

respectively; n= 3-5, p<0.05 vs age-matched group. eNOS and MnSOD protein expression was downregulated in *JunD*$^{-/-}$ mice as compared with WT controls (n=3-5, p<0.05 vs age-matched group). Relaxations to Ach in *JunD*$^{-/-}$ mice were restored by free radical scavengers superoxide dismutase (SOD) (150 U/ml) and catalase (1200 U/ml).

Conclusion. Our results indicate that JunD protects against vascular oxidative stress providing new insights into the pathophysiology of age-associated endothelial dysfunction.

Figure1

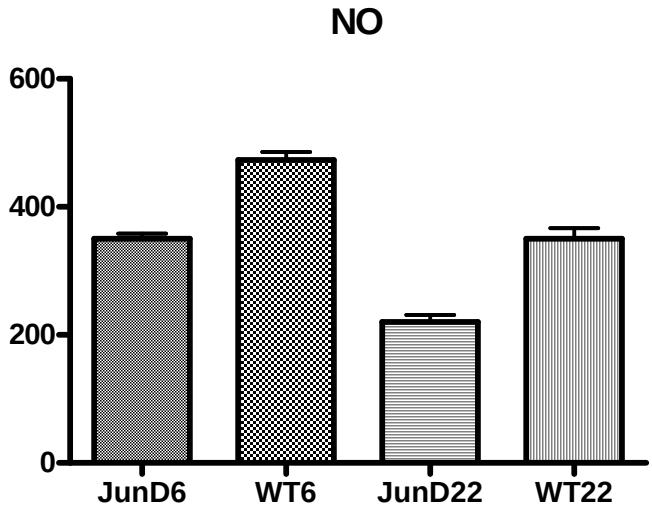

Figure2

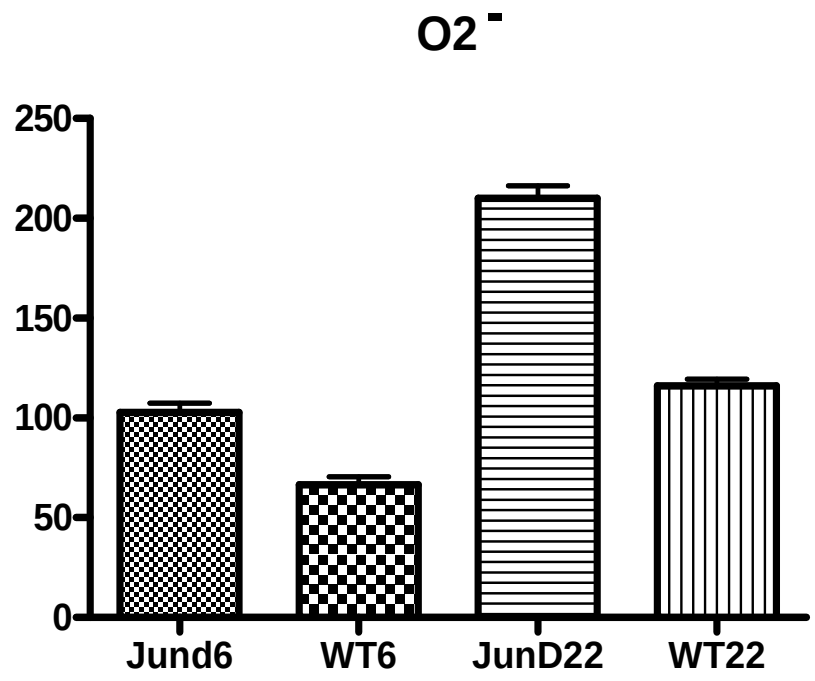

Coronary microvascular dysfunction in Primary Hyperparathyroidism patients: a hint for their increased cardiovascular risk.

Background: Primary hyperparathyroidism (pHPT) increases the risk for myocardial infarction (MI). We evaluated coronary flow reserve (CFR) by transthoracic Doppler echocardiography (TDE), as an index of coronary microvascular function, in pHPT.

Methods: 100 pHPT patients (pts) (80 F, aged 58±12 years) without clinical evidence of heart disease, and 50 controls matched for age and gender were studied. Coronary flow velocity in the left anterior descending coronary artery was detected by TDE at rest and during adenosine infusion. CFR was the ratio of hyperaemic diastolic flow velocity (DFV) to resting DFV. A CFR ≤2.5 was considered abnormal. The median time from pHPT diagnosis was 6 months (range 1-109).

Results: In pHPT pts, CFR was lower than in controls (3.0±0.8 vs 3.6±0.7, p<0.0001) (Figure A). CFR was ≤2.5 in 27 (27%) pts compared with controls (4%) (p<0.0001). CFR was inversely related to parathyroid hormone (PTH) levels (Figure B). In pts with CFR ≤2.5, PTH was higher (410 ±95 vs 207±16 ng/L, p=0.01) while calcium levels were similar (2.7±0.2 vs 2.9±1 mmol/L, p=0.7). At multivariable linear regression analysis adjusted for age, gender and cardiovascular risk factors, PHT and age were the only determinants of CFR (PHT β=-0.230, p=0.03; age β=-0.272, p=0.01 respectively). At multiple logistic regression analysis only PHT increased the probability of CFR ≤2.5 (OR 2.5, p=0.03). Out of 27 pHPT pts with pre-operative CFR ≤2.5, 9 pts were evaluated 6months after parathyroidectomy and all surprisingly showed a complete CFR normalization (CFR 2±0.4 vs 3.2±0.9 p<0.0001, respectively).

Conclusions: Coronary microvascular function is impaired by pHPT and quickly restored after parathyroidectomy. PTH independently correlates with abnormal CFR, suggesting a negative effect on coronary microcirculation that may contribute to the increased cardiovascular risk of pHPT.

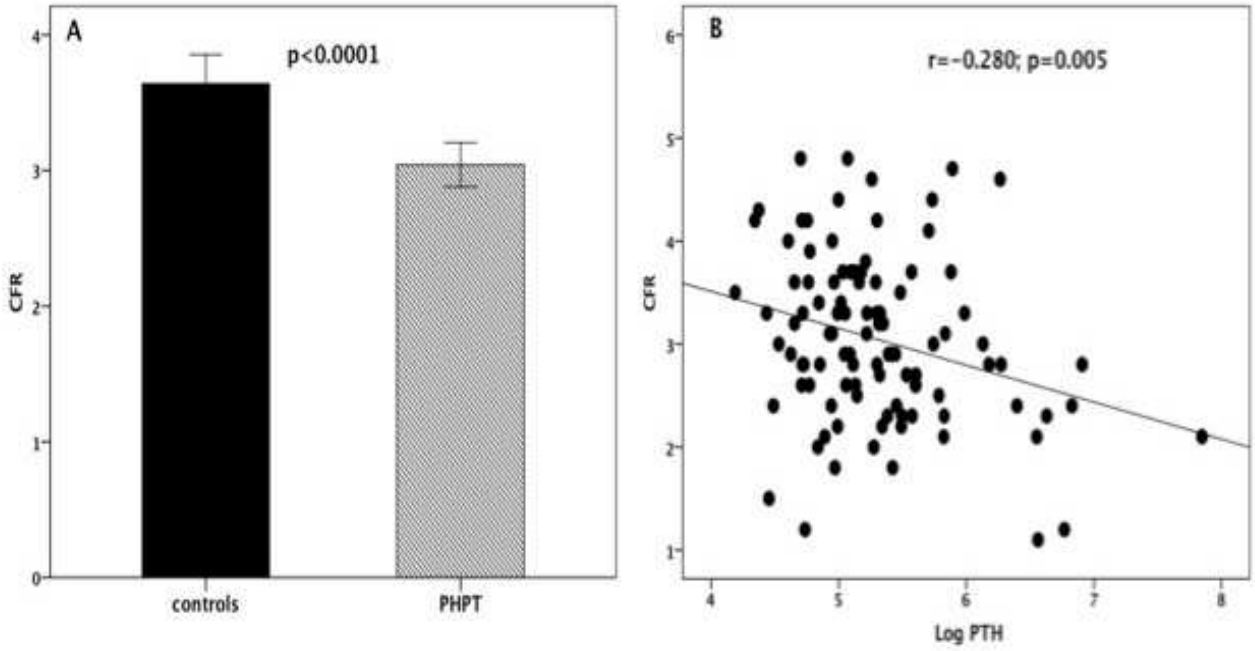

Psoriasis Impairs Coronary Flow Reserve: new Insights into the Clinical Value of Early Coronary Microvascular Dysfunction

Background: Psoriasis (Ps) is a recently recognized independent determinant for myocardial infarction (MI), associated with cardiovascular risk factors.We investigated whether coronary flow reserve (CFR), an index of coronary microvascular function, was impaired in young patients with Ps and the relationship between clinical markers of Ps activity and coronary blood flow abnormalities.

Methods: 56 patients (pts) with Ps (42 M, aged 37±7 years) without clinical evidence of heart diseases, and 48 controls matched for age and sex were studied. Coronary flow velocity in the left anterior descending coronary artery was detected by transthoracic Doppler echocardiography at rest and during adenosine infusion. CFR was the ratio of hyperaemic diastolic flow velocity (DFV) to resting DFV. A CFR ≤2.5 was considered abnormal. Mean time from diagnosis of Ps was 17±7 years.

Results: In pts with Ps, CFR was lower than in controls (3.2±0.9 vs 3.7±0.7, p=0.02). (Figure1A) CFR was abnormal (≤2.5) in 12 pts with Ps (22% vs 0% controls, OR 1.27, p<0.0001). Moreover, in CFR ≤2.5 pts Psoriasis Area Severity Index (PASI), a clinical grade of Ps severity, was higher (11±6 vs 7±3, p=0.006) and duration of the disease was longer (13±6 vs 9±5 years, p=0.03). (Figure1B) The highest probability for patients with psoriasis to have a CFR <2.5 occurred in those patients with higher PASI (Figure2) At multivariable analysis adjusted for age, smoke, hypertension and gender, PASI was the only determinant of CFR ≤2.5 (p=0.03).

Conclusions: CFR is often reduced in pts with Ps, suggesting a preclinical coronary microvascular impairment. This microvascular dysfunction seems to be related to the severity,

extension and duration of Ps. Our findings may explain the increased risk of MI conferred by Ps.

Figure 1

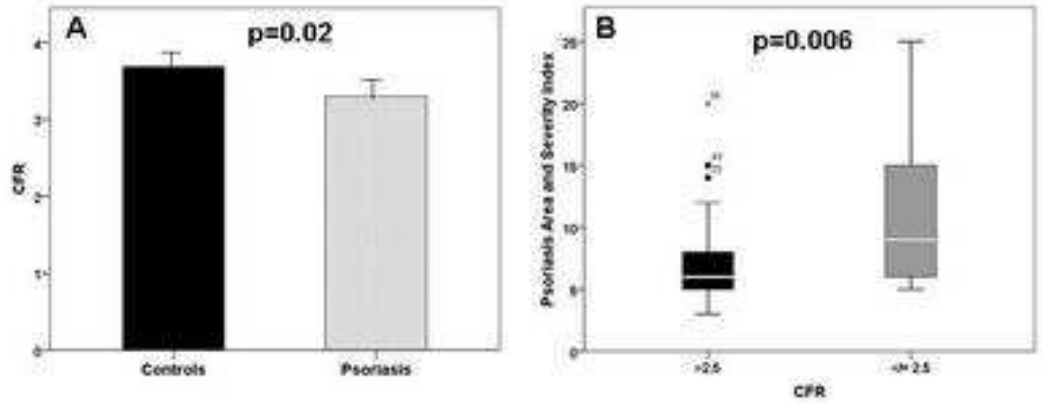

Figure 2

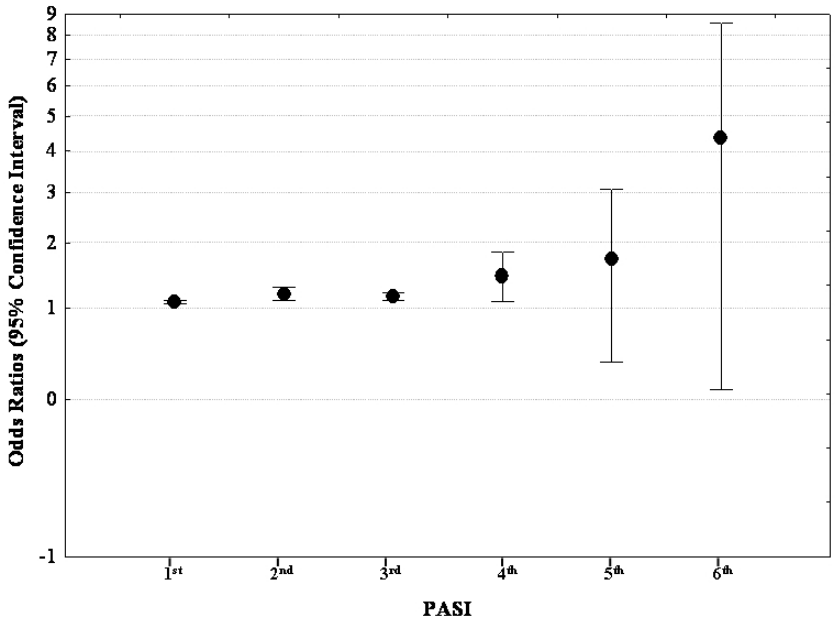

Adjusted OR for CFR< 2.5 based on PASI

References to introduction,conclusion and future perspectives

1. Opie L. *The Heart: Physiology, from Cell to Circulation* Lippincott Williams & Wilkins 1998.

2. Starling EH, Visscher MB. The regulation of the energy output of the heart. *J Physiol.* Jan 12 1927;62(3):243-261.

3. Panza J. *Endothelium,nitric oxide,and atherosclerosis*; 1999.

4. Kannel WB, Dawber TR, Kagan A, Revotskie N, Stokes J, 3rd. Factors of risk in the development of coronary heart disease--six year follow-up experience. The Framingham Study. *Ann Intern Med.* Jul 1961;55:33-50.

5. Gibbons GH, Dzau VJ. Molecular therapies for vascular diseases. *Science.* May 3 1996;272(5262):689-693.

6. Furchgott RF, Zawadzki JV. The obligatory role of endothelial cells in the relaxation of arterial smooth muscle by acetylcholine. *Nature.* Nov 27 1980;288(5789):373-376.

7. Moncada S. The 1991 Ulf von Euler Lecture. The L-arginine: nitric oxide pathway. *Acta Physiol Scand.* Jul 1992;145(3):201-227.

8. Cosentino F, Luscher TF. Maintenance of vascular integrity: role of nitric oxide and other bradykinin mediators. *Eur Heart J.* Nov 1995;16 Suppl K:4-12.

9. Fisslthaler B, Popp R, Kiss L, Potente M, Harder DR, Fleming I, Busse R. Cytochrome P450 2C is an EDHF synthase in coronary arteries. *Nature.* Sep 30 1999;401(6752):493-497.

10. Kinlay S, Libby P, Ganz P. Endothelial function and coronary artery disease. *Curr Opin Lipidol.* Aug 2001;12(4):383-389.

11. Moncada S, Higgs A. The L-arginine-nitric oxide pathway. *N Engl J Med.* Dec 30 1993;329(27):2002-2012.

12. Sarkar R, Meinberg EG, Stanley JC, Gordon D, Webb RC. Nitric oxide reversibly inhibits the migration of cultured vascular smooth muscle cells. *Circulation research.* Feb 1996;78(2):225-230.

13. Kubes P, Suzuki M, Granger DN. Nitric oxide: an endogenous modulator of leukocyte adhesion. *Proc Natl Acad Sci U S A.* Jun 1 1991;88(11):4651-4655.

14. Loscalzo J. Nitric oxide insufficiency, platelet activation, and arterial thrombosis. *Circulation research.* Apr 27 2001;88(8):756-762.

15. Luscher TF, Barton M. Biology of the endothelium. *Clin Cardiol.* Nov 1997;20(11 Suppl 2):II-3-10.

16. Asahara T, Murohara T, Sullivan A, Silver M, van der Zee R, Li T, Witzenbichler B, Schatteman G, Isner JM. Isolation of putative progenitor endothelial cells for angiogenesis. *Science.* Feb 14 1997;275(5302):964-967.

17. Carmeliet P. Angiogenesis in health and disease. *Nat Med.* Jun 2003;9(6):653-660.

18. Kawamoto A, Gwon HC, Iwaguro H, Yamaguchi JI, Uchida S, Masuda H, Silver M, Ma H, Kearney M, Isner JM, Asahara T. Therapeutic potential of ex vivo expanded endothelial progenitor cells for myocardial ischemia. *Circulation.* Feb 6 2001;103(5):634-637.

19. Wassmann S, Werner N, Czech T, Nickenig G. Improvement of endothelial function by systemic transfusion of vascular progenitor cells. *Circulation research.* Oct 13 2006;99(8):e74-83.

20. Feletou M, Vanhoutte PM. Endothelial dysfunction: a multifaceted disorder (The Wiggers Award Lecture). *Am J Physiol Heart Circ Physiol.* Sep 2006;291(3):H985-1002.

21. Ludmer PL, Selwyn AP, Shook TL, Wayne RR, Mudge GH, Alexander RW, Ganz P. Paradoxical vasoconstriction induced by acetylcholine in atherosclerotic coronary arteries. *N Engl J Med.* Oct 23 1986;315(17):1046-1051.

22. Quyyumi AA, Dakak N, Andrews NP, Husain S, Arora S, Gilligan DM, Panza JA, Cannon RO, 3rd. Nitric oxide activity in the human coronary circulation. Impact of risk factors for coronary atherosclerosis. *J Clin Invest.* Apr 1995;95(4):1747-1755.
23. Bonetti PO, Lerman LO, Lerman A. Endothelial dysfunction: a marker of atherosclerotic risk. *Arteriosclerosis, thrombosis, and vascular biology.* Feb 1 2003;23(2):168-175.
24. Heistad DD, Armstrong ML. Sick vessel syndrome. Can atherosclerotic arteries recover? *Circulation.* May 1994;89(5):2447-2450.
25. Packard RR, Libby P. Inflammation in atherosclerosis: from vascular biology to biomarker discovery and risk prediction. *Clin Chem.* Jan 2008;54(1):24-38.
26. Libby P. Inflammation in atherosclerosis. *Nature.* Dec 19-26 2002;420(6917):868-874.
27. Hansson GK. Inflammation, atherosclerosis, and coronary artery disease. *N Engl J Med.* Apr 21 2005;352(16):1685-1695.
28. Steinbrecher UP, Parthasarathy S, Leake DS, Witztum JL, Steinberg D. Modification of low density lipoprotein by endothelial cells involves lipid peroxidation and degradation of low density lipoprotein phospholipids. *Proc Natl Acad Sci U S A.* Jun 1984;81(12):3883-3887.
29. Kita T, Kume N, Minami M, Hayashida K, Murayama T, Sano H, Moriwaki H, Kataoka H, Nishi E, Horiuchi H, Arai H, Yokode M. Role of oxidized LDL in atherosclerosis. *Ann N Y Acad Sci.* Dec 2001;947:199-205; discussion 205-196.
30. Steffen Y, Jung T, Klotz LO, Schewe T, Grune T, Sies H. Protein modification elicited by oxidized low-density lipoprotein (LDL) in endothelial cells: protection by (-)-epicatechin. *Free radical biology & medicine.* Apr 1 2007;42(7):955-970.
31. Cooke JP. Asymmetrical dimethylarginine: the Uber marker? *Circulation.* Apr 20 2004;109(15):1813-1818.
32. Quyyumi AA, Mulcahy D, Andrews NP, Husain S, Panza JA, Cannon RO, 3rd. Coronary vascular nitric oxide activity in hypertension and hypercholesterolemia. Comparison of acetylcholine and substance P. *Circulation.* Jan 7 1997;95(1):104-110.
33. Masumoto A, Hirooka Y, Hironaga K, Eshima K, Setoguchi S, Egashira K, Takeshita A. Effect of pravastatin on endothelial function in patients with coronary artery disease (cholesterol-independent effect of pravastatin). *The American journal of cardiology.* Dec 1 2001;88(11):1291-1294.
34. Gilligan DM, Guetta V, Panza JA, Garcia CE, Quyyumi AA, Cannon RO, 3rd. Selective loss of microvascular endothelial function in human hypercholesterolemia. *Circulation.* Jul 1994;90(1):35-41.
35. Rodriguez C, Slevin M, Rodriguez-Calvo R, Kumar S, Krupinski J, Tejerina T, Martinez-Gonzalez J. Modulation of endothelium and endothelial progenitor cell function by low-density lipoproteins: implication for vascular repair, angiogenesis and vasculogenesis. *Pathobiology.* 2009;76(1):11-22.
36. Taylor DO, Edwards LB, Aurora P, Christie JD, Dobbels F, Kirk R, Rahmel AO, Kucheryavaya AY, Hertz MI. Registry of the International Society for Heart and Lung Transplantation: twenty-fifth official adult heart transplant report--2008. *J Heart Lung Transplant.* Sep 2008;27(9):943-956.
37. Aranda JM, Jr., Hill J. Cardiac transplant vasculopathy. *Chest.* Dec 2000;118(6):1792-1800.
38. Ramzy D, Rao V, Brahm J, Miriuka S, Delgado D, Ross HJ. Cardiac allograft vasculopathy: a review. *Canadian journal of surgery.* Aug 2005;48(4):319-327.
39. Hayry P, Aavik E, Palgi M, Petrov L, Savolainen H, Luoto NM, Loubtchenkov M, Frosen J. Molecular biology of transplant arteriosclerosis and sites of therapeutic intervention. *Transplantation proceedings.* Feb-Mar 2001;33(1-2):293-294.
40. Hayry P. New targets for the prevention of transplant vascular disease. *Transplantation proceedings.* May 2001;33(3):2332-2333.
41. Tufveson G, Johnsson C. Chronic allograft dysfunction--chronic rejection revisited. *Transplantation.* Aug 15 2000;70(3):411-412.

42. Rahmani M, Cruz RP, Granville DJ, McManus BM. Allograft vasculopathy versus atherosclerosis. *Circulation research.* Oct 13 2006;99(8):801-815.
43. Valantine HA. Cardiac allograft vasculopathy: central role of endothelial injury leading to transplant "atheroma". *Transplantation.* Sep 27 2003;76(6):891-899.
44. Koskinen PK, Kallio EA, Tikkanen JM, Sihvola RK, Hayry PJ, Lemstrom KB. Cytomegalovirus infection and cardiac allograft vasculopathy. *Transpl Infect Dis.* Jun 1999;1(2):115-126.
45. Pearson PJ, Schaff HV, Vanhoutte PM. Long-term impairment of endothelium-dependent relaxations to aggregating platelets after reperfusion injury in canine coronary arteries. *Circulation.* Jun 1990;81(6):1921-1927.
46. Labarrere CA, Deng MC. Microvascular prothrombogenicity and transplant coronary artery disease. *Transplant immunology.* May 2002;9(2-4):243-249.
47. Wever RM, Luscher TF, Cosentino F, Rabelink TJ. Atherosclerosis and the two faces of endothelial nitric oxide synthase. *Circulation.* Jan 6-13 1998;97(1):108-112.
48. Weis M, Cooke JP. Cardiac allograft vasculopathy and dysregulation of the NO synthase pathway. *Arteriosclerosis, thrombosis, and vascular biology.* Apr 1 2003;23(4):567-575.
49. Trapp A, Weis M. The impact of immunosuppression on endothelial function. *Journal of cardiovascular pharmacology.* Jan 2005;45(1):81-87.
50. Schmauss D, Weis M. Cardiac allograft vasculopathy: recent developments. *Circulation.* Apr 22 2008;117(16):2131-2141.
51. Celermajer DS, Sorensen KE, Gooch VM, Spiegelhalter DJ, Miller OI, Sullivan ID, Lloyd JK, Deanfield JE. Non-invasive detection of endothelial dysfunction in children and adults at risk of atherosclerosis. *Lancet.* Nov 7 1992;340(8828):1111-1115.
52. Joannides R, Haefeli WE, Linder L, Richard V, Bakkali EH, Thuillez C, Luscher TF. Nitric oxide is responsible for flow-dependent dilatation of human peripheral conduit arteries in vivo. *Circulation.* Mar 1 1995;91(5):1314-1319.
53. Celermajer DS, Sorensen KE, Bull C, Robinson J, Deanfield JE. Endothelium-dependent dilation in the systemic arteries of asymptomatic subjects relates to coronary risk factors and their interaction. *Journal of the American College of Cardiology.* Nov 15 1994;24(6):1468-1474.
54. Corretti MC, Plotnick GD, Vogel RA. Correlation of cold pressor and flow-mediated brachial artery diameter responses with the presence of coronary artery disease. *The American journal of cardiology.* Apr 15 1995;75(12):783-787.
55. Anderson TJ, Uehata A, Gerhard MD, Meredith IT, Knab S, Delagrange D, Lieberman EH, Ganz P, Creager MA, Yeung AC, et al. Close relation of endothelial function in the human coronary and peripheral circulations. *Journal of the American College of Cardiology.* Nov 1 1995;26(5):1235-1241.
56. Takase B, Hamabe A, Satomura K, Akima T, Uehata A, Matsui T, Ohsuzu F, Ishihara M, Kurita A. Comparable prognostic value of vasodilator response to acetylcholine in brachial and coronary arteries for predicting long-term cardiovascular events in suspected coronary artery disease. *Circ J.* Jan 2006;70(1):49-56.
57. Wu WC, Sharma SC, Choudhary G, Coulter L, Coccio E, Eaton CB. Flow-mediated vasodilation predicts the presence and extent of coronary artery disease assessed by stress thallium imaging. *J Nucl Cardiol.* Sep-Oct 2005;12(5):538-544.
58. Eskurza I, Seals DR, DeSouza CA, Tanaka H. Pharmacologic versus flow-mediated assessments of peripheral vascular endothelial vasodilatory function in humans. *The American journal of cardiology.* Nov 1 2001;88(9):1067-1069.
59. Moens AL, Goovaerts I, Claeys MJ, Vrints CJ. Flow-mediated vasodilation: a diagnostic instrument, or an experimental tool? *Chest.* Jun 2005;127(6):2254-2263.
60. Weis M, von Scheidt W. Cardiac allograft vasculopathy: a review. *Circulation.* Sep 16 1997;96(6):2069-2077.

61. Schwaiblmair M, von Scheidt W, Uberfuhr P, Ziegler S, Schwaiger M, Reichart B, Vogelmeier C. Functional significance of cardiac reinnervation in heart transplant recipients. *J Heart Lung Transplant.* Sep 1999;18(9):838-845.
62. Spes CH, Klauss V, Mudra H, Schnaack SD, Tammen AR, Rieber J, Siebert U, Henneke KH, Uberfuhr P, Reichart B, Theisen K, Angermann CE. Diagnostic and prognostic value of serial dobutamine stress echocardiography for noninvasive assessment of cardiac allograft vasculopathy: a comparison with coronary angiography and intravascular ultrasound. *Circulation.* Aug 3 1999;100(5):509-515.
63. Romeo G, Houyel L, Angel CY, Brenot P, Riou JY, Paul JF. Coronary stenosis detection by 16-slice computed tomography in heart transplant patients: comparison with conventional angiography and impact on clinical management. *Journal of the American College of Cardiology.* Jun 7 2005;45(11):1826-1831.
64. Caus T, Kober F, Marin P, Mouly-Bandini A, Quilici J, Metras D, Cozzone PJ, Bernard M. Non-invasive diagnostic of cardiac allograft vasculopathy by 31P magnetic resonance chemical shift imaging. *Eur J Cardiothorac Surg.* Jan 2006;29(1):45-49.
65. Kass M, Allan R, Haddad H. Diagnosis of graft coronary artery disease. *Current opinion in cardiology.* Mar 2007;22(2):139-145.
66. Weis M, von Scheidt W. Coronary artery disease in the transplanted heart. *Annual review of medicine.* 2000;51:81-100.
67. Kobashigawa JA, Tobis JM, Starling RC, Tuzcu EM, Smith AL, Valantine HA, Yeung AC, Mehra MR, Anzai H, Oeser BT, Abeywickrama KH, Murphy J, Cretin N. Multicenter intravascular ultrasound validation study among heart transplant recipients: outcomes after five years. *Journal of the American College of Cardiology.* May 3 2005;45(9):1532-1537.
68. Yeung AC, Davis SF, Hauptman PJ, Kobashigawa JA, Miller LW, Valantine HA, Ventura HO, Wiedermann J, Wilensky R. Incidence and progression of transplant coronary artery disease over 1 year: results of a multicenter trial with use of intravascular ultrasound. Multicenter Intravascular Ultrasound Transplant Study Group. *J Heart Lung Transplant.* Nov-Dec 1995;14(6 Pt 2):S215-220.
69. Rickenbacher PR, Pinto FJ, Chenzbraun A, Botas J, Lewis NP, Alderman EL, Valantine HA, Hunt SA, Schroeder JS, Popp RL, et al. Incidence and severity of transplant coronary artery disease early and up to 15 years after transplantation as detected by intravascular ultrasound. *Journal of the American College of Cardiology.* Jan 1995;25(1):171-177.
70. Costanzo MR, Naftel DC, Pritzker MR, Heilman JK, 3rd, Boehmer JP, Brozena SC, Dec GW, Ventura HO, Kirklin JK, Bourge RC, Miller LW. Heart transplant coronary artery disease detected by coronary angiography: a multiinstitutional study of preoperative donor and recipient risk factors. Cardiac Transplant Research Database. *J Heart Lung Transplant.* Aug 1998;17(8):744-753.
71. Kapadia SR, Ziada KM, L'Allier PL, Crowe TD, Rincon G, Hobbs RE, Bott-Silverman C, Young JB, Nissen SE, Tuzcu EM. Intravascular ultrasound imaging after cardiac transplantation: advantage of multi-vessel imaging. *J Heart Lung Transplant.* Feb 2000;19(2):167-172.
72. Hollenberg SM, Klein LW, Parrillo JE, Scherer M, Burns D, Tamburro P, Oberoi M, Johnson MR, Costanzo MR. Coronary endothelial dysfunction after heart transplantation predicts allograft vasculopathy and cardiac death. *Circulation.* Dec 18 2001;104(25):3091-3096.
73. Davis SF, Yeung AC, Meredith IT, Charbonneau F, Ganz P, Selwyn AP, Anderson TJ. Early endothelial dysfunction predicts the development of transplant coronary artery disease at 1 year posttransplant. *Circulation.* Feb 1 1996;93(3):457-462.
74. Schachinger V, Britten MB, Zeiher AM. Prognostic impact of coronary vasodilator dysfunction on adverse long-term outcome of coronary heart disease. *Circulation.* Apr 25 2000;101(16):1899-1906.

75. Potluri SP, Mehra MR, Uber PA, Park MH, Scott RL, Ventura HO. Relationship among epicardial coronary disease, tissue myocardial perfusion, and survival in heart transplantation. *J Heart Lung Transplant.* Aug 2005;24(8):1019-1025.
76. Weis M, Peter-Wolf W, Mazzilli N, Olbrich HG, Schacherer C, Wiemer J, Burger W, Hartmann A. Variations of segmental endothelium-dependent and endothelium-independent vasomotor tone after cardiac transplantation (qualitative changes in endothelial function). *American heart journal.* Aug 1997;134(2 Pt 1):306-315.
77. Fearon WF, Nakamura M, Lee DP, Rezaee M, Vagelos RH, Hunt SA, Fitzgerald PJ, Yock PG, Yeung AC. Simultaneous assessment of fractional and coronary flow reserves in cardiac transplant recipients: Physiologic Investigation for Transplant Arteriopathy (PITA Study). *Circulation.* Sep 30 2003;108(13):1605-1610.
78. Hiemann NE, Wellnhofer E, Knosalla C, Lehmkuhl HB, Stein J, Hetzer R, Meyer R. Prognostic impact of microvasculopathy on survival after heart transplantation: evidence from 9713 endomyocardial biopsies. *Circulation.* Sep 11 2007;116(11):1274-1282.
79. Konig A, Spes CH, Schiele TM, Rieber J, Stempfle HU, Meiser B, Theisen K, Mudra H, Reichart B, Klauss V. Coronary Doppler measurements do not predict progression of cardiac allograft vasculopathy: analysis by serial intracoronary Doppler, dobutamine stress echocardiography, and intracoronary ultrasound. *J Heart Lung Transplant.* Aug 2002;21(8):902-905.
80. Caiati C, Montaldo C, Zedda N, Bina A, Iliceto S. New noninvasive method for coronary flow reserve assessment: contrast-enhanced transthoracic second harmonic echo Doppler. *Circulation.* Feb 16 1999;99(6):771-778.
81. Caiati C, Montaldo C, Zedda N, Montisci R, Ruscazio M, Lai G, Cadeddu M, Meloni L, Iliceto S. Validation of a new noninvasive method (contrast-enhanced transthoracic second harmonic echo Doppler) for the evaluation of coronary flow reserve: comparison with intracoronary Doppler flow wire. *Journal of the American College of Cardiology.* Oct 1999;34(4):1193-1200.
82. Tona F, Caforio AL, Montisci R, Angelini A, Ruscazio M, Gambino A, Ramondo A, Thiene G, Gerosa G, Iliceto S. Coronary flow reserve by contrast-enhanced echocardiography: a new noninvasive diagnostic tool for cardiac allograft vasculopathy. *Am J Transplant.* May 2006;6(5 Pt 1):998-1003.
83. Tona F, Caforio AL, Montisci R, Gambino A, Angelini A, Ruscazio M, Toscano G, Feltrin G, Ramondo A, Gerosa G, Iliceto S. Coronary flow velocity pattern and coronary flow reserve by contrast-enhanced transthoracic echocardiography predict long-term outcome in heart transplantation. *Circulation.* Jul 4 2006;114(1 Suppl):I49-55.
84. Golino P, Piscione F, Willerson JT, Cappelli-Bigazzi M, Focaccio A, Villari B, Indolfi C, Russolillo E, Condorelli M, Chiariello M. Divergent effects of serotonin on coronary-artery dimensions and blood flow in patients with coronary atherosclerosis and control patients. *N Engl J Med.* Mar 7 1991;324(10):641-648.
85. Ganz P, Vita JA. Testing endothelial vasomotor function: nitric oxide, a multipotent molecule. *Circulation.* Oct 28 2003;108(17):2049-2053.
86. Lerman A, Zeiher AM. Endothelial function: cardiac events. *Circulation.* Jan 25 2005;111(3):363-368.
87. Munzel T, Sinning C, Post F, Warnholtz A, Schulz E. Pathophysiology, diagnosis and prognostic implications of endothelial dysfunction. *Ann Med.* 2008;40(3):180-196.
88. Tonetti MS, D'Aiuto F, Nibali L, Donald A, Storry C, Parkar M, Suvan J, Hingorani AD, Vallance P, Deanfield J. Treatment of periodontitis and endothelial function. *N Engl J Med.* Mar 1 2007;356(9):911-920.
89. Landmesser U, Hornig B, Drexler H. Endothelial function: a critical determinant in atherosclerosis? *Circulation.* Jun 1 2004;109(21 Suppl 1):II27-33.

90. Yusuf S, Reddy S, Ounpuu S, Anand S. Global burden of cardiovascular diseases: part I: general considerations, the epidemiologic transition, risk factors, and impact of urbanization. *Circulation.* Nov 27 2001;104(22):2746-2753.
91. Lakatta EG, Levy D. Arterial and cardiac aging: major shareholders in cardiovascular disease enterprises: Part II: the aging heart in health: links to heart disease. *Circulation.* Jan 21 2003;107(2):346-354.
92. Lakatta EG. Arterial and cardiac aging: major shareholders in cardiovascular disease enterprises: Part III: cellular and molecular clues to heart and arterial aging. *Circulation.* Jan 28 2003;107(3):490-497.

Publications

Peer reviewed:

1. **Osto E**, Coppolino G, Cosentino F. Restoring the dysfunctional endothelium. *Curr Pharm Des.* 2007;13:1053-68. **(I.F. 4.39)**
2. Cosentino F, **Osto E.** Aging and Endothelial dysfunction. *Clin Hemorheol Microcirc.* 2007;37:143-7.
3. Delli Gatti C, **Osto E**, Kouroedov A, Eto M, Shaw S, Volpe M, Lüscher TF, Cosentino F. Pulsatile stretch induces release of angiotensin II and oxidative stress in human endothelial cells: effects of ACE inhibition and AT1 receptor antagonism. *Clin Exp Hypertens.* 2008;30:616-27. **(I.F. 1.079)**
4. **Osto E**, Matter CM, Kouroedov A, Malinski T, Bachschmid M, Camici GG, Kilic U, Stallmach T, Boren J, Iliceto S, Lüscher TF, Cosentino F. c-Jun N-terminal kinase 2 deficiency protects against hypercholesterolemia-induced endothelial dysfunction and oxidative stress. *Circulation.* 2008;118:2073-80. **(I.F. 14.595)**
5. **Osto E**, Kouroedov A, Mocharla P, Akhmedov A, Besler C, Rohrer L, von Eckardstein A, Iliceto S, Volpe M, Lüscher TF, Cosentino F. Inhibition of Protein Kinase C{beta} Prevents Foam Cell Formation by Reducing Scavenger Receptor A Expression in Human Macrophages. *Circulation.* 2008;118:2174-82. **(I.F. 14.595)**
6. **Osto E,** Tona F, Angelini A, Montisci R, Vinci A, Bortolami A, Napodano M, Tarantini G, Thiene G, Gerosa G, Caforio ALP, Iliceto S. Clinical and Functional Determinants of Coronary Flow Reserve in Heart Transplantation: a Contrast-Enhanced Echocardiographic Study. *Journal Heart Lung Transplantation.* 2009,28:453-60. **(I.F. 3.323)**
7. **Osto E,** Tona F, De Bon E, Iliceto S, Cella G. Endothelial Dysfunction in Cardiac Allograft Vasculopathy. Potential Pharmacological Interventions. *Curr Vasc Pharmacol. 2010 Jan 1. In press.* **(I.F. 3.582)**
8. Tona F, **Osto E**, Tarantini G, Napodano M, Gambino A, Ramondo A, Montisci R, Gerosa G, Caforio ALP, Iliceto S. Coronary Flow Velocity Reserve by Contrast-Enhanced Transthoracic Echocardiography Predicts Maximal Epicardial Intimal Thickening in Cardiac Allograft Vasculopathy. *American Journal of Transplantation. Accepted for publication.*
9. **Osto E,** Tona F, Castellani C, Angelini A, Fadini G, Baesso I, Gambino A, Agostini A, Avogaro A, Caforio ALP, Gerosa G, Thiene G, Iliceto S. Endothelial Progenitor Cells Are

Decreased In Blood and in The Graft of Heart Transplant Patients With Microvasculopathy. *American Journal of Transplantation Submitted*

10. **Osto E**, Cosentino F. The role of oxidative stress in endothelial dysfunction and vascular inflammation. In *Nitric Oxide, second edition edited by Louis Ignarro*. Academic press. Published November 2009 ISBN-13: 978-0-12-373866-0. *ISBN-10: 0-12-373866-0*
11. G. Tarantini, M. Napodano, N. Gasparetto, E. Favaretto, M. Perazzolo Marra, L. Cacciavillani, C. Bilato, **E. Osto,** F. Cademartiri, G. Musumeci, F. Corbetti, R. Razzolini, S. Iliceto. Impact of multivessel coronary artery disease on early ischemic injury, late clinical outcome, and remodeling in patients with acute myocardial infarction treated by primary coronary angioplasty. *Coronary Artery Disease. Accepted for publication* **(I.F. 1.254)**

Abstracts

1. Kuroedov A, **Osto E**, Mocharla P, Volpe M, Luscher TF, Cosentino F. Nebivolol reduces VCAM-1 and MCP-1 expression in human endothelial cells and prevents foam cells formation via inhibition of protein kinase C beta. *European Heart Journal 2007 28 (Abstract Supplement), 108.* European Society of Cardiology congress, Wien, Austria, 1-5 September 2007.

2. Cucchini U, Pegoraro C, **Osto E**, Marzot F, Iliceto S, pengo V. Prevention of stroke in elderly patients with atrial fibrillation: effectiveness of low-intensity anticoagulant treatment. *European heart Journal (2007) 28 (Abstract Supplement), 215*. European Society of Cardiology congress, Wien, Austria, 1-5 September 2007.

3. **Osto E,** Matter CM; Kuroedov A, Camici G; Malinski T; Bachschmid M; Stallmach T; Boren J; Iliceto S; Luscher TF, Cosentino F. Deletion of *JNK2* Prevents Hypercholesterolemia-Induced Oxidative Stress and Endothelial Dysfunction. American Heart Association congress, Orlando, FL, USA 4-7 November 2007. *Circulation. 2007;116:II_180.*

4. **Osto E**, Kuroedov A, Mocharla P, Volpe M, Luscher TF, Cosentino F "Dual role of inducile NO synthase in foam cell formation. 68° Congresso Nazionale della Società Italiana di Cardiologia, Roma, Italia, 15-18 Dicembre 2007. *G Ital Cardiol 2007;vol 8 Suppl I-12*

5. **Osto E**, Kuroedov A, Mocharla P, Volpe M, Luscher TF, Cosentino F. Nebivolol decreases VCAM-1 and MCP-1 expression in human endothelial cells and prevents foam cells formation via inhibition of protein kinase C beta. 68° Congresso Nazionale della Società Italiana di Cardiologia, Roma, Italia, 15-18 Dicembre 2007. *G Ital Cardiol 2007;vol 8 Suppl I-12*

6. **Osto E**, Tona F, Caforio ALP, Napodano M, Bortolami A, Angelini A, Gerosa G, Iliceto S. Coronary flow reserve by contrast-enhanced transthoracic echocardiography predicts cardiac allograft vasculopathy onset in heart transplant

patients with normal coronary angiogram. *Journal of Heart and LungTransplantation. 2008;27, 2S, S95 101*.

7. Tona F, **Osto E**, G Tarantini, Caforio, ALP, Angelini, A, Gerosa, G, Iliceto S. Coronary flow reserve by contrast-enhanced transthoracic Echocardiography predicts maximal epicardial intimal thickness in heart transplant patients with normal coronary angiogram. *Journal of Heart and Lung Transplantation 2008;27, 2S, S170-306.*

8. **Osto E**, Tona F, Bortolami A, Caforio ALP, Angelini, A, Ramondo A, Gerosa, G, Iliceto S.Strain and Strain Rate by Velocity Vector Imaging in Diagnosing Acute Rejection after Heart Transplantation. *Journal of Heart and Lung Transplantation. 2008;27, 2S, S115-153.*

9. **Osto E**, Tona F, Bortolami A, Ramondo A, Angelini, A, Gerosa, G, Iliceto S. Velocity Vector Imaging To Quantify Regional Left Ventricular Function in Heart Transplantation. *Journal of Heart and Lung Transplantation. 2008;27, 2S, S148-244.*

10. **Osto E**, Tona F, Castellani C, Caforio ALP, Ramondo A, Gerosa G, Iliceto S, Angelini A. Impaired Coronary Flow Reserve in Heart Transplant Patients with Normal Coronary Angiograms: Predictive Role of Interstitial Fibrosis and Medial Thickening of Intramyocardial Coronary Arteries. *Journal of Heart and Lung Transplantation. 2008;27, 2S, S171-307.*

11. **Osto E**, Tona F, Fadini,G, Basso I, Caforio ALP, Agostini C, Tarantini G, Avogaro A, Angelini A, Gerosa G, Iliceto S. Potential Role of Circulating Progenitor Cells in Coronary Microvascular Dysfunction of Heart Transplant Patients with Normal Coronary Angiograms. *Journal of Heart and Lung Transplantation 2008;27, 2S, S195-373.*

12. **Osto E**, Tona F, Tarantini G, Napodano M, Montisci R, Gambino A, Ramondo A, Gerosa G, Caforio ALP, Iliceto S. Coronary flow reserve by contrast-enhanced transthoracic echocardiography predicts maximal epicardial intimal thickening in transplant coronary artery disease. International Academy of Cardiology 14th World Congress on Heart Disease Annual Scientific Session Toronto, Canada, July 26-29, 2008. *The journal of Heart Disease 2008;6:1 abstracts ISSN 1556-7451*

13. **Osto E**, Tona F, Caforio ALP, Napodano M, Bortolami A, Angelini A, Gerosa G, Iliceto S Coronary flow reserve by contrast-enhanced transthoracic echocardiography predicts cardiac allograft vasculopathy onset in heart transplant patients with normal coronary angiogram. International Academy of Cardiology 14th World Congress on Heart Disease Annual Scientific Session Toronto, Canada, July 26-29, 2008. *The journal of Heart Disease 2008;6:1 abstracts ISSN 1556-7451*

14. **Osto E**, Tona F, Castellani C, Caforio ALP, Gambino A, Tarantini G, Gerosa G, Thiene G, Angelini A, Iliceto S. Everolimus prevents the development of microvasculopaty after heart transplantation. International Academy of Cardiology 14th World Congress on Heart Disease Annual Scientific Session Toronto, Canada, July 26-29, 2008. *The journal of Heart Disease 2008;6:1 abstracts ISSN 1556-7451.*

15. **Osto E**, Tona F, Castellani C, Caforio ALP, Ramondo A, Gerosa G, Iliceto S, Angelini A. Impaired coronary flow reserve in heart transplant patients with normal coronary angiograms: predictive role of interstitial fibrosis and medial thickening of intramyocardial coronary arteries. International Academy of Cardiology 14th World Congress on Heart Disease Annual Scientific Session Toronto, Canada, July 26-29, 2008. *The journal of Heart Disease 2008;6:1 abstracts ISSN 1556-7451*

16. **Osto E**, Tona F, Fadini,G, Basso I, Caforio ALP, Agostini C, Tarantini G, Avogaro A, Angelini A, Gerosa G, Iliceto S. Potential role of circulating progenitor cells in coronary microvascular dysfunction of heart transplant patients with normal coronary angiograms. International Academy of Cardiology 14th World Congress on Heart Disease Annual Scientific Session Toronto, Canada, July 26-29, 2008. *The journal of Heart Disease 2008;6:1 abstracts ISSN 1556-7451*.

17. **Osto E**, Tona F, Tarantini G, Napodano M, Montisci R, Gambino A, Ramondo A, Gerosa G, Caforio ALP, Iliceto S. Coronary flow reserve by contrast-enhanced transthoracic echocardiography predicts maximal epicardial intimal thickening in transplant coronary artery disease. ESC Congress 2008. 30 August -03 September 2008 Munich, Germany. *European Heart Journal 2008, 29,334*

18. **Osto E**, Tona F, Castellani C, Caforio ALP, Gambino A, Tarantini G, Gerosa G, Thiene G, Angelini A, Iliceto S. Everolimus prevents the development of microvasculopaty after heart transplantation. ESC Congress 2008. 30 August -03 September 2008 Munich, Germany. *European Heart Journal 2008, 29,52*.

19. **Osto E**, Tona F, Fadini G, Castellani C, Baesso I, Gambino A, Agostini C, Tarantini G, Vinci A, Avogaro A, Caforio ALP, Gerosa G, Thiene G, Angelini A, Iliceto S. Endothelial Progenitor Cells Are Decreased In the Blood And In The Graft Of Heart Transplant Patients With Microvasculopathy. *Circulation, 2008; 118: S-707.*

20. Tona F, **Osto E**, Tarantini G, Napodano M, Gambino A, Vinci A, Vecchiati A, Ramondo A, Montisci R, Gerosa G, Caforio ALP, Iliceto S. Coronary Flow Velocity Reserve by Contrast-Enhanced Transthoracic Echocardiography Predicts Maximal Epicardial Intimal Thickening in Cardiac Allograft Vasculopathy. *Circulation, 2008; 118: S-708 – S-709.*

21. **Osto E**, Tona F, Fadini G, Castellani C, Baesso I, Gambino A, Agostini C, Tarantini G., Napodano M., Vinci A, Avogaro A, A. Ramondo, Caforio ALP, Gerosa G, Thiene G, Angelini A, Iliceto S. Endothelial Progenitor Cells are decreased In Blood of cardiac allograft patients with Microvasculopathy. 69° Congresso Nazionale della Società Italiana di Cardiologia, Roma, Italia, 13-16 Dicembre 2008. *G Ital Cardiol 2008;vol 9 Suppl I-12.*

22. **Osto E,** Tona F, Tarantini G, Napodano M, Gambino A, Vinci A, Vecchiati A, Ruscazio M, Ramondo A, Montisci R, Gerosa G, Caforio ALP, Iliceto S. Coronary Flow Velocity Reserve by Contrast-Enhanced Transthoracic Echocardiography Predicts Maximal Epicardial Intimal Thickening in Cardiac Allograft Vasculopathy. 69° Congresso Nazionale della Società Italiana di Cardiologia, Roma, Italia, 13-16 Dicembre 2008. *G Ital Cardiol 2008;vol 9 Suppl I-12.*

23. **Osto E**, Tona F, Castellani C, Gambino A, Tarantini G, Vinci A, Napodano M, Thiene G,Ramando A, Caforio ALP, Gerosa G, Angelini A, Iliceto S. Everolimus prevents the development of microvasculopaty after heart transplantation. 69° Congresso Nazionale della Società Italiana di Cardiologia, Roma, Italia, 13-16 Dicembre 2008. *G Ital Cardiol 2008;vol 9 Suppl I-12.*

24. **E. Osto**, F. Tona, G. Tarantini, M. Napodano, A. Gambino, A. Vinci, Bodo S, Ruscazio M, Montisci R, A. Ramondo, G. Gerosa, ALP. Caforio, S. Iliceto. Microvasculopathy Preceeds Epicardial Coronary Stenosis in Heart Transplant Patients with Cardiac Allograft Vasculopathy. 69° Congresso Nazionale della Società Italiana di Cardiologia, Roma, Italia, 13-16 Dicembre 2008. *G Ital Cardiol 2008;vol 9 Suppl I-12.*

25. **Osto E**, Kouroedov A, Mocharla P, Akhmedov A, Besler C, Rohrer L, von Eckardstein A, Iliceto S, Volpe M, Lüscher TF, Cosentino F. Inhibition of Protein Kinase C{beta} Prevents Foam Cell Formation by Reducing Scavenger Receptor A Expression in Human Macrophages. 69° Congresso Nazionale della Società Italiana di Cardiologia, Roma, Italia, 13-16 Dicembre 2008. *G Ital Cardiol 2008;vol 9 Suppl I-12.*

26. A. Kouroedov, **E. Osto,** P. Mocharla, T.F. Lüscher, F. Cosentino. Dual Role of Inducible NO Synthase in Foam Cell Formation. Cardiology Update 2009. February 15-20, 2009. Davos, Switzerland. *Hospitalis 2009 Supplementum.*

27. A. Kouroedov, **E. Osto,** P. Mocharla, T.F. Lüscher, F. Cosentino. Nebivolol protects against atherosclerosis reducing adhesion molecule expression and foam cells formation via inhibition of protein kinase Cbeta intracellular signaling. Cardiology Update 2009. February 15-20, 2009. Davos, Switzerland. *Hospitalis 2009 Supplementum*.

28. Tona F, **Osto E**, Tarantini G., Napodano M., Gambino A, Vinci A, Vecchiati A., Ramondo A, Gerosa G, Caforio ALP, Iliceto S. Coronary Flow Velocity Reserve by Contrast-Enhanced Transthoracic Echocardiography Predicts Maximal Epicardial Intimal Thickening in Cardiac Allograft Vasculopathy. *Journal of Heart and Lung Transplantation. 2009;28, S166.*

29. **E. Osto**, F. Tona, C. Castellani, A. Gambino, G. Tarantini, A. Vinci, M. Napodano, A. Ramondo, A.L.P. Caforio, G. Thiene, G. Gerosa, A. Angelini, S. Iliceto. Everolimus Prevents Allograft Microvasculopathy after Heart Transplantation. *Journal of Heart and Lung Transplantation*. 2009;28, S177.

30. **E. Osto,** F. Tona, C. Castellani, G. Fadini, I. Baesso, A. Gambino, A. Vinci, A. Avogaro, A. Ramondo, A.L.P. Caforio, G. Gerosa, G. Thiene, A. Angelini, S. Iliceto. Endothelial Progenitor Cells Are Decreased in the Blood and in the Graft of Heart Transplant Patients with Microvasculopathy. *Journal of Heart and Lung Transplantation. 2009;28, S91.*

31. F. Tona, **E. Osto**, G. Tarantini, M. Napodano, A. Gambino, A. Vinci, A. Ramondo, G. Gerosa, A.L.P. Caforio, S. Iliceto. Microvasculopathy Preceeds Epicardial Coronary Stenosis in Heart Transplant Patients with Cardiac Allograft Vasculopathy. *Journal of Heart and Lung Transplantation* 2009;28, S228.

32. **Osto E**, Tona F, Castellani C, Angelini A, Fadini G, Baesso I, Gambino A, Agostini C, Avogaro A, Caforio ALP, Gerosa G, Thiene G, Iliceto S.Reduced Endothelial Progenitor Cells In Blood and in The Graft are associated with Coronary Microvascular dysfunction of Heart Transplant patients. Arteriosclerosis, Thrombosis and Vascular Biology Annual Conference, Washington DC, April 29-May 1 2009. *Arterioscler Thromb Vasc Biol 2009;29:e9-e130.*

33. A. Kuroedov, **E. Osto**, P. Mocharla, T.F. Lüscher, F. Cosentino. Nebivolol protects against atherosclerosis reducing adhesion molecule expression and foam cells formation via inhibition of protein kinase C-beta intracellular signaling. Assemblée Annuelle commune Société Suisse de Cardiologie. Société Suisse de Chirurgie Thoracique et Cardio-vasculaire. Lausanne 10-12 june 2009. *Médecine Cardiovasculaire Supplementum 17 2009;12(5).Oral communication.*

34. **E. Osto**, F. Vianello, F. Tona, F. Cozzi, H. Marotta, G. Saggiorato, O. Iqbal, J. Fareed, G. Cella. Plasma markers of endothelial cells activation in patients with secondary pulmonary hypertension related to connective tissue diseases: effect of bosentan" *22° International Society on Thrombosis and haemostasis Congress Boston, MA USA. July 11-16, 2009. Thrombosis and Haemostasis 7 (Suppl. 2) (2009) 1–1204*

35. Tarantini G, Gasparetto N, Napodano M, Cacciavillani L, Favaretto E, Perazzolo Marra M, Fraccaro C, **Osto E**, Facchin M, Razzolini R, Musumeci R, Iliceto S, Ramondo A. Impact of Multivessel Coronary Artery Disease on Early Ischemic Injury, Late Clinical Outcome and Remodeling in Patients With Acute Myocardial Infarction Treated by Primary Coronary Angioplasty. *American Journal of Cardiology 2009;104,6A,123D.*

36. **Osto E**, Tona F, Gambino A, Maddalozzo A, Caforio ALP, mentisci R, Ramondo A, Gerosa G, Iliceto S. Microvascular dysfunction preceeds epicardial coronary stenosis in heart transplant patients with cardiac allograft vasculopathy. Europeans Society of cardiology. ESC congress 2009. Barcelona 29 Aug-2sept 2009. *EHJ 2009, 30 abstract supplement.*

37. **E. Osto**, G. Coppolino, B Mateescu, A. Akhmedov, T. Malinski, R. Kubant, F. Mechta-Grigoriou, C. Matter, TF. Lüscher, F. Cosentino. Genetic deletion of JunD enhances age-related endothelial dysfunction. European Society of Cardiology. ESC congress 2009. Barcelona 29 Aug-2sept 2009. *EHJ 2009, 30 abstract supplement*.

38. **Osto E**, F. Tona, L. Furian, C. Crepaldi, F. Marchini, P, A. Gloria, C. Silvestre, R. Montisci, Rigotti, S. Iliceto. Evaluation of Coronary Microvascular Function in Renal-Pancreas Allograft Recipients.ESC congress 2009. Barcelona 29 Aug-2sept 2009. *EHJ 2009, 30 abstract supplement.*

39. L. Furian, F. Tona, F. Marchini, C Crepaldi, **Osto E**, P. Rigotti, S. Iliceto. Evaluation of Coronary Microvascular Function by coronary flow reserve measurements in simultaneous Pancreas and kidney transplantation Allograft Recipients. *Transplant International 2009;22:332. Suppl.*

40. L. Furian, F. Tona, F. Marchini, C Crepaldi, **Osto E**, P. Rigotti, S. Iliceto. Evaluation of Coronary Microvascular Function by coronary flow reserve measurements in simultaneous Pancreas and kidney transplantation Allograft Recipients. *Xenotransplantation 2009;16:311.*

41. Tarantini G, Gasparetto N, Napodano M, Cacciavillani L, Favaretto E, Perazzolo Marra M, Fraccaro C, **Osto E**, Facchin M, Razzolini R, Musumeci R, Iliceto S, Ramondo A. Impact of Multivessel Coronary Artery Disease on Early Ischemic Injury, Late Clinical Outcome and Remodeling in Patients With Acute Myocardial Infarction Treated by Primary Coronary Angioplasty. American Heart Association congress, Orlando, FL, USA 14-18 November 2009. *Circulation, Nov 2009; 120: S984.*

42. **Osto E,** Coppolino G, Mateescu B, Akhmedov A, Malinski T, Perna E, Kubant R, Mechta-Grigoriou F, Matter CM, Luescher TF, Cosentino F. Enhanced age-related endothelial dysfunction in genetic deletion of JunD**.** American Heart Association congress, Orlando, FL, USA 14-18 November 2009. *Circulation, Nov 2009; 120**:** S1108.*

43. **Osto E,** Piaserico S, Maddalozzo A, Forchetti G, Schiesari L, Montisci R, Peserico A, Iliceto S, Tona F Coronary Microvascular Dysfunction in Patients With Psoriasis: a Study Performed With Transthoracic Doppler Echocardiography.. 70° Congresso Nazionale della Società Italiana di Cardiologia, Roma, Italia, 12-15 Dicembre 2009. *G Ital Cardiol 2009;vol 10 Suppl I-11-12.*

44. **Osto E**, Fallo F, Maddalozzo A, Sorgato N, Montisci R, Pellizzo MR, Iliceto S, Tona F. Coronary Microvascular Dysfunction in Primary Hyperparathyroidism: a Study Performed With Transthoracic Doppler Echocardiography. 70° Congresso Nazionale della Società Italiana di Cardiologia, Roma, Italia, 12-15 Dicembre 2009. *G Ital Cardiol 2009;vol 10 Suppl I-11-12.*

45. **Osto E,** Maddalozzo A, Gambino A, Tarantini G, Ramondo A, Feltrin G, Gerosa G, Iliceto S, Tona F. Microvasculopathy Preceeds Epicardial Coronary Stenosis in Heart Transplant Patients With Cardiac Allograft Vasculopathy. 70° Congresso Nazionale della Società Italiana di Cardiologia, Roma, Italia, 12-15 Dicembre 2009. *G Ital Cardiol 2009;vol 10 Suppl I-11-12.*

46. **Osto E,** Furian L, Marchini F, Crepaldi C, Montisci R, Gloria A, Rigotti P, Iliceto S, Tona F. Impairment of Coronary Flow Reserve Assessed by Transthoracic Echocardiography in Simultaneous Pancreas and Kidney Transplant Recipients. 70° Congresso Nazionale della Società Italiana di Cardiologia, Roma, Italia, 12-15 Dicembre 2009. *G Ital Cardiol 2009;vol 10 Suppl I-11-12.*

47. **Osto E,** Coppolino G, Mateescu B, Akhmedov A, Malinski T, Perna E, Kubant R, Mechta-Grigoriou F, Matter CM, Luescher TF, Cosentino F. Enhanced age-related endothelial dysfunction in genetic deletion of JunD**.** 70° Congresso Nazionale della Società Italiana di Cardiologia, Roma, Italia, 12-15 Dicembre 2009. *G Ital Cardiol 2009; vol 10 Suppl I-11-12.*

48. **Osto E,** Piaserico S, Maddalozzo A, Forchetti G, Montisci R, Peserico A, Iliceto S, Tona F. Psoriasis early impairs coronary flow reserve: new insights into

inflammation and coronary microvascular dysfunction. American College of Cardiology 59° Annual scientific session, March 14-16, 2010 Atlanta, Georgia, USA. *Accepted for Poster presentation.*

49. **Osto E**, Pellizzo MR, Fallo F, Maddalozzo A, Sorgato N, Montisci R, Iliceto S, Tona F. Coronary Microvascular Dysfunction in Primary Hyperparathyroidism patients: a hint for their increased cardiovascular risk. American College of Cardiology 59° Annual scientific session, March 14-16, 2010 Atlanta, Georgia, USA. *Accepted for Oral presentation.*

50. Enhanced age-related endothelial dysfunction and increased oxidative stress in genetic deletion of JunD. **E. Osto**, F. Paneni, G. Coppolino, B. Mateescu, A. Akhmedov, T. Malinski, E.Perna, F. Mechta-Grigoriou, T. Lüscher, F. Cosentino. Assemblée Annuelle commune Société Suisse de Cardiologie. Société Suisse de Chirurgie Thoracique et Cardio-vasculaire. St Gallen 9-11 june 2010. *Submitted*

Acknowledgments

I would like to thank:

my parents and my sister Melania for their love and support.

Professor Sabino Iliceto (Cardiovascular Unit, University of Padova School of Medicine) for giving me the nice opportunity to go abroad and to participate to an international PhD programme but also for the absolute freedom and trust he always gave me during my research.

Professor Gaetano Thiene (Cardiovascular Pathology, University of Padova School of Medicine) PhD program Supervisor, for his such enthusiastic and open-minded but accurate approach to science.

Prof. Dr. med. Thomas F. Lüscher and Prof. Dr med Francesco Cosentino for giving me the opportunity to work in their group, for their guidance and support throughout the years of my thesis; for helpful discussions and advice concerning my projects;
Dr med Francesco Tona, for all his scientific support, patience and encouragement throughout my PhD programme.

Professor John Pernow and and Professor Jan A. Staessen for their kind external reviewing of my thesis;

Dr med Alexey Kouroedov for his friendship, generosity in providing technical support as well as constructive discussions regarding the molecular projects.

The members of my thesis committee,

I am grateful to all the people who contributed with their work and expertise to the completion of my thesis .

List of abbreviations

nitric oxide (NO)

superoxide anion (O2-)

reactive oxygen species (ROS)

cardiac allograft vasculopathy (CAV)

heart transplantation (HT)

coronary artery disease (CAD)

diabetes mellitus (DM)

cardiovascular diseases (CVD)

vascular smooth muscle cell (VSMC)

acetylcholine (Ach)

endothelium derived relaxing factor (EDRF)

endothelial cells (ECs)

prostacyclin (PGI2)

endothelium derived hyperpolarizing factors (EDHF)

angiotensin II (AT II),

endothelin-1 (ET-1)

prostaglandin H2 (PGH2

endothelial NO synthase (eNOS, NOSIII)

tetrahydrobiopterin (BH4)

cyclic guanosine monophosphate (cGMP)

cyclooxygenase 2 (COX-2)

endothelial progenitor cells (EPCs)

low density lipoprotein (LDL)

oxidized low density lipoproteins (OxLDL)

asymmetric dimethylarginine (ADMA)

intravascular ultrasonography (IVUS)

flow mediated dilation (FMD)

coronary flow reserve (CFR)

intracoronary Doppler flow wire (IDFW)

contrast-enhanced transthoracic echocardiography (CE-TTE)

left anterior descending artery (LAD)